Optimizing Cooperative Spectrum Sensing in Cognitive Radio Networks using Interference Alignment and Space-Time Coding

Idris A. Yusuf

A thesis submitted to the University of Hertfordshire in partial fulfilment of the requirements for the degree of Doctor of Philosophy

The programme of research was carried out in the Science and Technology Research Institute (STRI), University of Hertfordshire, United Kingdom.

Supervisor: Prof Yichuang Sun

April, 2017

In loving memory of my late mother, Amina Kangmi with whom we started this journey together but she never saw its finish.

Acknowledgments

I would firstly like to thank the Almighty Allah for the grace and guidance He has granted me up till this point, and for making this distant dream a reality.

My sincere gratitude goes to my supervisor Prof Yichuang Sun for his guidance and continuous motivation. His technical advice and method of instruction have been exceedingly valuable and have helped to create a wonderful learning experience. His expertise, perceptiveness, and encouragement have helped me reach many academic milestones, and have helped to develop a solid foundation for my future endeavours.

I would like to thank my second supervisor Dr. David Lauder as well as my fellow research colleagues for taking time out of their busy schedule to assist me with some significant aspects of my work. I also want to thank my dear friends for their kindness and encouragement.

I cannot express enough gratitude to my entire family, especially my wife Asmau and our children for the love, affection, and support they have shown me all through this research period. They have stood by me all the way and have been there for me at all times, their affection means more than words can express.

Abstract

In this thesis, the process of optimizing Cooperative Spectrum Sensing in Cognitive Radio has been investigated in fast-fading environments where simulation results have shown that its performance is limited by the Probability of Reporting Errors. By proposing a transmit diversity scheme using Differential space-time block codes (D-STBC) where channel state information (CSI) is not required and regarding multiple pairs of Cognitive Radios (CR's) with single antennas as a virtual MIMO antenna arrays in multiple clusters, Differential space-time coding is applied for the purpose of decision reporting over Rayleigh channels. Both Hard and Soft combination schemes were investigated at the fusion center to reveal performance advantages for Hard combination schemes due to their minimal bandwidth requirements and simplistic implementation. The simulations results show that this optimization process achieves full transmit diversity, albeit with slight performance degradation in terms of power with improvements in performance when compared to conventional Cooperative Spectrum Sensing over non-ideal reporting channels.

Further research carried out in this thesis shows performance deficits of Cooperative Spectrum Sensing due to interference on sensing channels of Cognitive Radio. Interference Alignment (IA) being a revolutionary wireless transmission strategy that reduces the impact of interference seems well suited as a strategy that can be used to optimize the performance of Cooperative Spectrum Sensing. The idea of IA is to coordinate multiple transmitters so that their mutual interference aligns at their receivers, facilitating simple interference cancellation techniques. Since its inception, research efforts have primarily been focused on verifying IA's ability to achieve the maximum degrees of freedom (an approximation of sum capacity), developing algorithms for determining alignment solutions and designing transmission strategies that relax the need for perfect alignment but yield better performance.

With the increased deployment of wireless services, CR's ability to opportunistically sense and access the unused licensed frequency spectrum, without causing harmful interference to the licensed users becomes increasingly diminished, making the concept of introducing IA in CR a very attractive proposition.

For a multiuser multiple-input–multiple-output (MIMO) overlay CR network, a space-time opportunistic IA (ST-OIA) technique has been proposed that allows spectrum sharing between a single primary user (PU) and multiple secondary users (SU) while ensuring zero interference to the PUs. With local CSI available at both the transmitters and receivers of SUs, the PU employs a space-time WF (STWF) algorithm to optimize its transmission and in the process, frees up unused eigenmodes that can be exploited by the SU. STWF achieves higher performance than other WF algorithms at low to moderate signal-to-noise ratio (SNR) regimes, which makes it ideal for implementation in CR networks. The SUs align their transmitted signals in such a way their interference impairs only the PU's unused eigenmodes. For the multiple SUs to further exploit the benefits of Cooperative Spectrum Sensing, it was shown in this thesis that IA would only work when a set of conditions were met. The first condition ensures that the SUs satisfy a zero interference constraint at the PU's receiver by designing their post-processing matrices such that they are orthogonal to the received signal from the PU link. The second condition ensures a zero interference constraint at both the PU and SUs receivers i.e. the constraint ensures that no interference from the SU transmitters is present at the output of the post-processing matrices of its unintended receivers. The third condition caters for the multiple SUs scenario to ensure interference from multiple SUs are aligned along unused eigenmodes. The SU system is assumed to employ a time division multiple access (TDMA) system such that the Principle of Reciprocity is employed towards optimizing the SUs transmission rates.

Since aligning multiple SU transmissions at the PU is always limited by availability of spatial dimensions as well as typical user loads, the third condition proposes a user selection algorithm by the fusion centre (FC), where the SUs are grouped into clusters based on their numbers (i.e. two SUs per cluster) and their proximity to the FC, so that they can be aligned at each PU-Rx. This converts the cognitive IA problem into an unconstrained standard IA problem for a general cognitive system.

Given the fact that the optimal power allocation algorithms used to optimize the SUs transmission rates turns out to be an optimal beamformer with multiple eigenbeams, this work initially proposes combining the diversity gain property of STBC, the zero-forcing function of IA and beamforming to optimize the SUs transmission rates. However, this solution requires availability of CSI, and to eliminate the need for this, this work then combines the D-STBC scheme with optimal IA precoders (consisting of beamforming and zero-forcing) to maximize the SUs data rates.

Table of Contents

List of Figures

List of Acronyms

AF: amplify and forward

BPSK: binary phase shift keying

BER: bit error rate

CSI: channel state information

CP: cyclic prefix

DPSK: differential phase shift keying

DSA: dynamic spectrum access

DSFC: distributed space frequency codes

DSTBC: distributed space time block codes

DSTBC-OFDM: DSTBC orthogonal frequency division multiplexing

DSTFC: distributed space time frequency codes

FFT: fast Fourier transform

FSA: fixed spectrum access

IA: interference alignment

ML: maximum likelihood

MIMO: multiple input multiple output

MISO: multiple input single output

PEP: pairwise error probability

PSK: phase shift keying

OFDM: orthogonal frequency division multiplexing

QAM: quadrature amplitude modulation

QPSK: quadrature phase shift keying

SNR: signal-to-noise ratio

SISO: single input single output

ST: space time

STBC: space time block codes

Declaration

The following papers have been published and parts of their material are included in this thesis:

Published Manuscripts

Y. I. Abdulkadir, N. Nwanekezie, O. Simpson and Y. Sun, "A Differential Space-Time Coding Scheme for Cooperative Spectrum Sensing in Cognitive Radio Networks", *IEEE International Symposium on Personal, Indoor and Mobile Radio Communication* – (PIMRC), Hong Kong, September 2015.

N. Nwanekezie, O. Simpson, Y. I. Abdulkadir and Y. Sun, "Optimizing Diversity Gain for Non-Coherent Wireless Multimedia Sensor Networks", *IEEE International Workshop on Selected Topics in Mobile and Wireless Computing* – (WIMob), Abu Dhabi, October 2015.

O. Simpson, Y. I. Abdulkadir. N. Nwanekezi and Y. Sun, "Relay-Based Cooperative Spectrum Sensing with Improved Energy Detection in Cognitive Radio", *International Conference on Broadband and Wireless Computing, Communications and Applications* – (BWCCA), Poland, November 2015.

Y. I. Abdulkadir, O. Simpson, N. Nwanekezie and Y. Sun, "Space-Time Opportunistic Interference Alignment in Cognitive Radio Networks" *IEEE Wireless Communications and Networking Conference* – (WCNC), Qatar, April 2016.

Manuscripts Submitted for Publication

Y. I. Abdulkadir, O. Simpson, N. Nwanekezie and Y. Sun, "Opportunistic Interference Alignment in Cognitive Radio Networks with Space-Time Coding", submitted to *IEEE Transactions on Cognitive Communications and Networking*, 2016

Y. I. Abdulkadir and Y. Sun, “Interference Alignment in Cognitive Radio Networks: An Overview”, submitted to *IEEE Transactions on Communications,* 2016

1. Introduction

1.1.Wireless and Mobile Communications

Increasing interest and demand in wireless applications has led to the continuous development of wireless technologies, none more so than in the last two decades, which have seen this development, grow at a geometric rate. Users of wireless applications are now more and more dependent on wireless devices that provide mobile data usage, real-time information processing, and multi-media sharing. This trend [1], [2] has led to a significant increase in demand and utilization of the spectrum resources and thus, an increased scarcity of the radio frequency spectrum [1], [3]. As a consequence, there have been marked changes in research and spectrum access policies aimed at ensuring that wireless resources meet the expectations and demands of wireless technologies. The current *fixed spectrum access* (FSA) policy is still very much based on the notion that the wireless radio spectrum is a limited resource that must be apportioned among licensed users and services. This FSA policy is based on a static allocation of the spectrum resources, where the radio spectrum is partitioned into frequency bands that are licenced to operators for certain periods of time, giving them exclusive rights of usage [4]. Interestingly, the FSA policy has been observed as the major factor in the current spectrum drought because those frequency bands are only active when the licensed users are active. This leaves several portions of the licenced spectrum unused/underutilized when the licensed users are idle, proving that indeed spectrum scarcity is a direct consequence of spectrum underutilization [5]. It is therefore clear that the scarcity of the frequency spectrum is not exclusively as a direct result of physical scarcity of spectrum resources, but rather as a result of the inefficiency of the FSA policy. As a consequence, there has been a growing demand for more efficient utilization of spectral resources, leading to the development of an alternative spectrum policy called *dynamic spectrum access* (DSA) [5].

1.1.1. Dynamic Spectrum Access and Cognitive Radio

Recent regulatory considerations of dynamic radio spectrum access as encapsulated in [6], [7] create the potential for more intensive use of the spectrum in order to boost opportunities for technologically innovative and economically efficient solutions use with much greater robustness than in the past. To this end, the DSA policy is much more flexible and market-oriented regulatory model. With DSA, the spectrum resources are still allocated to the licensed users, but its usage is not exclusively granted. Unlicensed users, referred to as SUs, can also access the spectrum resources. To support DSA, SUs are required to have cognition capabilities in order to sense the radio frequency spectrum environment, and SUs with such capabilities are referred to as *cognitive radios* (CR) [8], [9]. The CR unique technology which allows a cognitive wireless terminal to dynamically access the unused spectrum (otherwise known as *spectrum holes*) has enabled its emergence as one of the technologies for meeting the ever increasing growth of wireless communication services [8] – [10].

A CR, as defined in [9], [10] is "a radio that is aware of its operational environment and can dynamically and independently adjust its radio operating parameters accordingly". A more generalized definition was given in [6] as a radio that senses its electromagnetic environment and adjusts its operating parameters with the aim of maximizing throughput, mitigating interference as well as facilitating interoperability. Unlike traditional radios, a CR has two distinguishing features namely the *cognition capability* and the *reconfigurability* as shown in the *cognition cycle* of Figure 1.1 which aptly illustrates how these unique features of a CR continuously interact with the radio environment.

1.1.2. Cognition Capability of a CR

This refers to the CRs ability to observe and analyze the radio spectrum and make a decision about which spectrum band to make use as well as adopting an optimal transmission strategy.

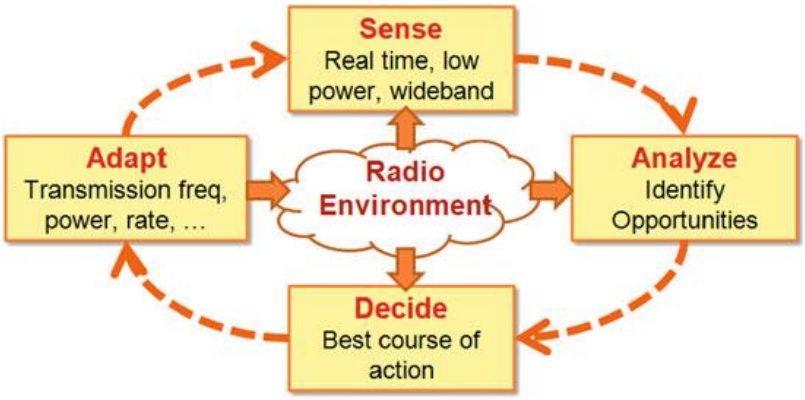

Fig. 1.1 Cognition cycle of a Cognitive Radio [9]

The cognition cycle follows three main components as follows:

- Spectrum Sensing: This refers to the ability of a CR to measure spectrum usage (based on parameters such as cumulative power levels, user activities, etc.) over different spectrum bands in order to capture the existence of licensed users. Spectrum sensing is one of the most critical functions of a CR as it must make real-time decisions about exploiting dimensions of frequency, space and time [8], [11].
- Spectrum Analysis: This is defined based on the sensed radio environment, as the existence of spectral opportunities in the surrounding radio environment. A spectral opportunity refers to "a band of frequencies that are not being used by the licensed user at a particular time in a particular geographic area" based on the three dimensions of the spectrum space [12]. In more recent times, other dimensions of the spectrum space such as coding, beamforming and the use of Multiple-Input Multiple-Output (MIMO) at the physical layer, can present opportunities to be exploited [12].
- Spectrum Access or Spectrum Decision: This is the last step of the cognition cycle that decides the set of actions to be taken based on the outcomes of the first two components of the cognition cycle. More specifically, a CR utilizes the information gathered regarding the spectrum bands identified as available spectral transmit

opportunities (TO) to define the radio transceiver's parameters for the upcoming transmission(s) over such frequency bands.

1.1.3. Reconfigurability of a Cognitive Radio

The second key feature of a CR is its ability to re-tune its transceiver parameters based on its assessment of the surrounding radio environment. While traditional radios have considerable flexibility with their ability to reconfigure some of their transmission parameters, they are mostly designed to operate over specific frequency band(s). A CR on the other hand, is designed to be more flexible in order to exploit spectral holes over a wider frequency range. For instance, a CR must be able to configure its transmission bandwidth to adapt to transmit opportunities (TO) of different sizes be able to determine the appropriate communication protocol to be used over different spectral opportunities. CRs were originally referred to as software radios with extended self-awareness capabilities [13], given that software-defined radios were designated as the ideal implementation environment of radios with seamless configuration capabilities [9].

1.2. Spectrum Sensing in Cognitive Radio

The cognition cycle earlier defined in *1.1.2* implies a wide range of hard research problems for CR. Therefore the scope of this research work will be limited to the "Spectrum Sensing" component of the cognition cycle. As stated under the Spectrum Sensing component of the cognition cycle, the most crucial task of each CR user is to detect whether the PUs are present or absent. This the CRs can do by sensing for the spectrum holes, gaining access and making use of these spectrum holes in an opportunistic manner, when the PU are absent/idle thus avoiding causing harmful interference to the PUs. Alternatively, the CR can make use of the licensed spectrum concurrently with the PU provided the CR can limit its interference to the

PUs to a predefined level [8]. Detection performance in spectrum sensing is therefore very crucial to the performance of both PU and CR networks and can be determined on the basis of two metrics: *probability of false alarm*, which denotes the probability of a CR user declaring that a PU is present when the spectrum is actually free, and *probability of detection*, which denotes the probability of a CR user declaring that a PU is present when the spectrum is indeed occupied by the PU. In terms of detection performance, Spectrum Sensing can further be separated into two techniques for implementation as shown in fig 1.2. below.

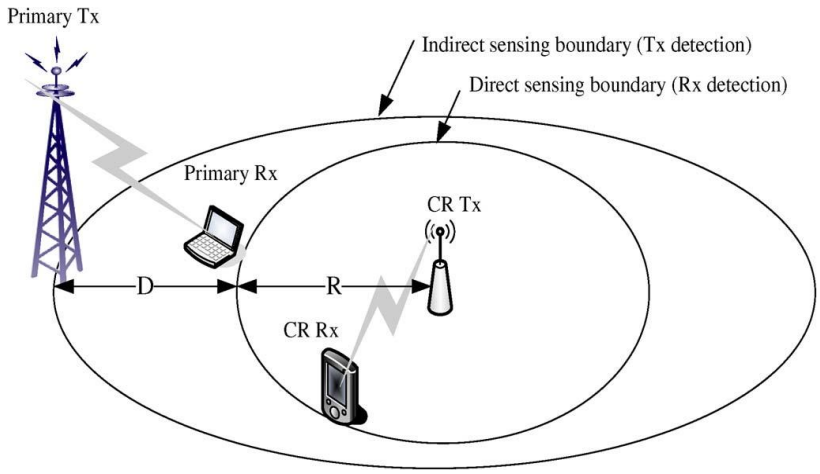

Fig.1.2: Principle of Spectrum Sensing [15]

Fig 1.2 shows the basic principle of how Spectrum Sensing works where the PU transmitter (Tx) sends data to its intended receiver in a certain licensed spectrum band. Sensing the nearby PU receiver (Rx) can directly identify the spectrum hole, which is called *direct Spectrum Sensing*. Similarly, sensing the surrounding PU-Tx environment can also identify the spectrum holes, but in an indirect way, which is called *indirect Spectrum Sensing*. Within the indirect Spectrum Sensing (SS) technique, there are a number of schemes that can be used for SS namely matched filter detection, energy detection, cyclostationary detection, covariance based detection and SS using multiple antennas.

In practice, spectrum sensing is usually hampered by two profound phenomena namely Multipath Fading and Interference, and their effects cannot be over emphasized. These drawbacks may significantly compromise detection performance, make Spectrum Sensing very unreliable and create the hidden node problems. A possible solution to these drawbacks lies in the concept of spatially distributed nodes in a network, as they are less likely to concurrently experience fading or receiver uncertainty. For example, if a number of CR users while performing their own local sensing, can exploit diversity by cooperatively sharing their sensing results with other users and the FC, the combined cooperative decision on spectrum utilization can combat multipath fading and improve overall detection performance.

Another crucial task in the design of CR is about how best the SUs can avoid interfering with the PU in their vicinity [14]-[16]. It becomes particularly challenging nowadays where the PU is seldom idle, such that the availability of spectrum holes becomes very limited [16]. In trying to find solutions to this problem, the focus of research has shifted towards IA [17], as it naturally fits in with the CR networks effort of managing interference between the PU and SUs [17] - [19].

1.3.Interference Alignment in Cognitive Radio Networks

IA is a radical cooperative interference management strategy that has emerged through rigorous analysis of interference channels (IC) and networks. This approach exploits the availability of multiple signaling dimensions either from multiple antennas, time slots or frequency blocks as the case may be. The transmitters linearly encode their signals over these multiple signaling dimensions, such that the resulting interference signal observed at each receiver lies in a lower dimensional subspace and is orthogonal to the one spanned by the signal of interest at each receiver while the other subspace is reserved for interference free

communication, hence achieving the IC's maximum multiplexing gain, or degrees of freedom (DoF) [17], [18].

The earliest work to explore the increase in DoF with message sharing in the manner of CR was done in [19], [20] for both the MIMO interference and "X"-channels. This is because the CR network can be seen as an IC when the SUs coexist with the PUs and the SU transmission is subjected to the PU-Rx threshold as well as the cross interference between the SUs themselves [11]. A number of other practical IA algorithms have also been developed in the manner of message sharing such as [21] to [23], where each Tx has an intended Rx, and the remaining Tx's are considered as interferers for that Rx. These studies have provided a significant research platform that has translated into basically two main paradigms in the design and implementation of IA in CR networks.

The first paradigm considers a CR network consisting of a number of SU pairs and the PU-Tx and Rx pair, where the PU-Tx is assumed far from its Rx and thus SU-Rx's are considered not to be influenced by the interference from the PU-Tx (which is similar to the *Direct Spectrum Sensing* scenario). The second paradigm considers the same CR network as the first paradigm, but the SUs are in closer proximity to the PU-Tx (in the manner of *Indirect Spectrum Sensing*). However, instead of sensing for spectrum holes left by the PU, this paradigm proposes that under a power-limitation, a PU which maximizes its own rate on its MIMO channel singular values might leave some of them unused *i.e.* no transmission takes place along the corresponding spatial directions. These unused directions may become TOs that can be opportunistically utilized by the SUs to avoid interfere with the signal sent by the PU-Tx [24].

1.4.Research Aims and Objectives

1.4.1. Aim

The main aim of this research is therefore to combat multipath fading between the SUs through optimizing cooperative spectrum sensing, mitigating interference using IA between the PU and SUs and optimizing the transmission sum rates in the CR network. The metrics that validate performance of these aims include *probability of detection* and sum rate graphs.

1.4.2. Objectives

In order to improve the performance of CR systems, many works have focused on the collaboration of multiple CR users in SS whereby the possibility of detection errors can be reduced by introducing spatial diversity [25]. Through this collaboration of Cooperative Spectrum Sensing (CSS), each user may independently perform local SS and then report a binary decision to a combining user or FC. The FC then makes a decision on the presence or absence of the PU signal in order to reduce the probability of detection errors by exploiting spatial diversity. In terms of local SS techniques, energy detection (ED) has been shown to be more optimal as a solution, than other techniques especially in low-noise scenarios [8], [9]. Thus, the design of an ED based CSS model will be the focus for this research work.

In CSS, the FC controls the three step process as follows: Firstly, the FC selects a frequency band for sensing and instructs all SUs to individually perform local sensing on the *sensing channel* i.e. the physical channel between the PU and each cooperating SU. Secondly, all the SUs report their local sensing results to the FC via a *reporting channel*. Lastly, the FC combines all the received local sensing information in order to determine the status of the PU, makes a decision on the presence/absence of the PU and then diffuses this information back to all cooperating SUs. The main objectives of this research will be centered on finding ways to optimize both the *sensing* and *reporting* channels.

Several works have shown that these reporting channels are also susceptible to fading effects and interference. It is shown in [26] that when the reporting channels become very noisy, CSS will get no advantages. Employing some additional forms of transmit diversity such as STBC can alleviate performance of decision reporting [27]. STBC can mitigate the effect of fading and improve the performance and reliability of digital transmission over wireless radio channels, hence its application in several SS research endeavors [28]. However, use of STBC becomes more impractical in higher mobility environments because of its dependence on global CSI. In order to optimize CSS, one of the main objectives of this research therefore is the optimization of *reporting channels* by incorporating differential strategies for decision reporting in CR networks that do not depend on availability of global CSI.

With regards to managing interference between the SUs and the PUs, this work will focus on critically evaluating the two main paradigms in the design of IA in CR networks. It is well known from the literature that the first paradigm of implementing IA in CR networks which is more biased towards *direct SS* is somewhat less optimal than the second paradigm (whose bias leans towards *Indirect SS*). This is because, like direct SS, detecting a PU-Rx is a more challenging task than detecting the PU-Tx. Thus, this work will focus more on the second paradigm used to implement IA in CR networks, with the key objective being to develop appropriate algorithms that will optimize detection performance of the SUs as well as maximizing the overall sum rates of the CR network.

For local sensing, since all CR users are tuned to the selected licensed channel to observe the PU on the *sensing channel*, it seems straightforward that some form of diversity can also be applied to the *sensing channels* in order to optimize its performance. However, the present demand on the licensed wireless spectrum makes it particularly challenging to find availability of spectrum holes. Interestingly, several studies have shown that when the PUs

transmission is maximized by a water-filling power allocation scheme over its spatial directions, some of these spatial directions (SD) could be left unused due to power limitations. As such, instead of the SUs sensing for spectrum holes, they can then opportunistically sense for these unused SDs as their TO, and IA can then be used to align the SUs transmission with these unused SD, thereby avoiding the SUs interfering with the PU transmission [24]. To optimize performance of the *sensing channels*, this work considers multiple cooperating SUs in the manner of CSS while implementing a WF scheme for PU link optimization. Since the success of SU communication depends on the accuracy of the sensing procedure for unused SDs [30], this work optimizes ED to give the SU a higher probability of correctly detecting TO's.

In terms of maximizing the achievable transmission rates for the SUs opportunistic link, several studies basically apply schemes such as uniform or optimal power allocation (UPA/OPA) and blind CSI estimation schemes, along with a few enhancements which makes them very optimal in terms of transmission rates. However, quite a number of these research studies are known to be more susceptible to noise impairments and are also mostly useful for high SNR regimes. Since implementing second order beamformers with optimal power allocation outperform UPA/OPA, this work considers that the multiple SUs use second order beamformers with OPA along with some form of transmit diversity in order to increase the data rates of the SU transmission without compromising the performance.

1.4.3. Contribution

CSS has been investigated in Rayleigh-fading environments over non-ideal reporting channels, where the simulation results have shown that its performance is limited by the probability of reporting errors. This work proposes a transmit diversity scheme using D-STBC where CSI is not required. By regarding multiple pairs of CRs as virtual antenna arrays

in multiple clusters, D-STBC is applied for the purpose of decision reporting over Rayleigh channels. Hard combination schemes are employed at the FC due to their minimal bandwidth requirements. Simulations results show that this method achieves full transmit diversity, albeit with slight performance degradation in terms of power. The results also show improvements in sensing performance when compared to conventional CSS over non-ideal reporting channels.

For a multiuser MIMO overlay CR network, a ST-OIA technique has been proposed that allows spectrum sharing between PU and SU while ensuring zero interference to the PU. The CR system consists of one PU and K SUs where local CSI is available at both the Tx's and Rx's of SUs. The PU uses ST-WF algorithm to optimize the PU's transmission and in the process, frees up unused eigenmodes that can be exploited by the SU. Because ST-WF achieves higher capacity per antenna than other methods at low to moderate SNR regimes, it makes it ideal for implementation in CR networks. The SUs align their transmitted signals in such a way their interference impairs only the PU's unused eigenmodes. For this solution with multiple SUs exploiting the benefits of CSS to work, there should be zero interference at the PU-Rx. Secondly, there should be zero interference to both the PU and SU Rx's. The third condition caters for the multiple SU scenarios which require limited cooperation between the PU-Rx and the multiple SUs to ensure interference from multiple SUs are aligned along unused eigenmodes. In order to optimize the SUs transmission rates, this work assumes a TDMA system for the SU network such that principle of Reciprocity can be utilized [12].

Naturally, the success of the SUs communication depends on the availability of unused DoFs as shown in the work in [15], which proposed a fast sensing method based on a generalized likelihood ratio test (GLRT) to more accurately decide the absence of individual PU streams

thereby determining the availability of unused DoFs. This work makes use of a double threshold (defined as λ_1, λ_2respectively) ED scheme similar to the work in [27], [28] for purpose of enhancing detection accuracy. The condition of this method states that "if the energy value exceeds λ_2, then the SU reports unavailability of used SD. Alternatively, if it is less than λ_1, then SU reports availability of unused SD. Furthermore, if energy value is between λ_1 and λ_2 , then the SU reports this observational energy value also, thus the FC receives two kinds of information; local binary decision and the observational value. This gives the SU a higher probability of correctly detecting TOs because the FC has a wider range of information from which available TOs can be found.

The SU communication in this work is also based on fixed-rate communication where the transmission rate is independent of SNR level, implying it would support medium to low range SNR values. As mentioned earlier, the Alamouti structure used for STBC is an effective way of providing diversity for MIMO systems, albeit with local CSI requirements at the SU-Rx's. Thus, this work has considered a DS-TBC scheme for independent, identically distributed (i.i.d) fading channels, where the channels spatial correlations were estimated without the need for local CSI or training symbols. With a focus on the SUs channels being spatially correlated, this would imply that even in fast-fading channel conditions, the channel's spatial correlations would typically change slowly to corroborate with the assumption of fixed rate transmission. Thus, a transmission scheme is developed here that combines beamforming with D-STBC, where each transmitter encodes symbols using Alamouti codes followed by beamformers that align interference at unintended receivers. Unlike the threshold beamforming (TBF) protocol, this work first provides a reference symbol followed by differentially phase-shifted symbols (known as codewords) and given the fact that the channels correlations are assumed relatively constant for at least two symbol

periods, the receiver processes the received data independent of CSI or training symbols. Any channels fluctuation outside this window implies outage and thus the SU remains silent. In order to improve sum rates of the SU transmission, a correlation matrix is computed which releases eigenvectors that are used to transmit the code words with proper power loading on each eigenvector, in a process called eigen-beamforming. The receiver removes the aligned interference and decouples symbols using interference cancellation followed by symbol-by-symbol decoding.

1.5.Organization

In Chapter 2, we design and analyze the performance of CSS in CR networks and IA in CR Networks. The rest of Chapter 2 is organized as follows: In Section 2.1, the properties of CSS in relation to local sensing are discussed and the cooperative system architecture is presented. In Section 2.2, we discuss the related mathematical statistics in terms of the *probabilities of detection, false alarm* as well as the receiver operating characteristics (ROC) of CR. Section 2.3 discusses the classification of CSS into three main categories while Section 2.4, discusses the various data fusion techniques used in CSS. The performance offered by the CSS strategy is analyzed via numerical and simulation results in Section 2.5. In addition, we show how the use differing combination schemes at the FC improves performance. Section 2.6 introduces IA as an interference management strategy, which leads to the discussion of IA in CR networks in Section 2.7. The first and second paradigms used to implement IA in CR networks are presented along with various mathematical algorithms used to achieve this. Comprehensive analyses for both paradigms are presented in Section 2.8 using simulations to ascertain the inherent advantages of IA in CR networks.

In Chapter 3, we present D-STBC schemes for CSS. Since the reporting channels are also susceptible to fading effects and interference, then some other form of transmit diversity can alleviate performance of decision reporting. STBC being one of such diversity techniques can be applied to CSS in CR networks. The rest of Chapter 3 is organized as follows: In Section 3.2, the network model is introduced (clusters based on metric distance). The performance limits of CSS are measured on the probability of reporting errors. In Section 3.3, a performance analysis of cooperative spectrum sensing over Rayleigh fading channels is given, which is followed by a transmit diversity model using DSTBC. In Section 3.4, the FC with hard and soft combinations is presented and detailed analyses for various fusion rules are presented. Simulation results and for multiple are clusters are presented in Section 3.4 and conclusions are drawn in Section 3.5.

In Chapter 4, we design space-time opportunistic interference alignment in CR networks. The rest of Chapter 4 is organized as follows. In Section 4.2, the system model is described, and the main assumptions required for analysis are introduced. In Section 4.3, a comparative analysis is done between the spatial water-filling (SWF) and ST-WF schemes for the PU link and Section 4.4 presents the space-time opportunistic IA scheme (ST-OIA) by presenting the original OIA approach and describing the steps taken towards achieving the novelty of this work. Section 4.5 provides the reciprocity technique used to optimize the transmission rates of the SU network. Simulation results as well as a performance comparison between this work and [21] – [24] were then presented in Section 4.6, while section 4.7 presents the concluding remarks of this chapter.

In Chapter 5, OIA is described where CSI acquisition is impractical. The rest of Chapter 5 is organized as follows: In Section 5.2, the system model and the main assumptions required for analysis are reviewed (given that the system model for this chapter is the same as Chapter 4).

In Section 5.3, a review on the comparative analysis between the MEB, SWF and ST-WF schemes is done, as well an analysis on outage probability of the ST-WF algorithm. Section 5.4 presents the OIA by presenting the sensing phase (along with the double threshold method) and the IA phase with the SU selection process. Section 5.5 presents OIA with STBC by briefly reviewing the literature before presenting the algorithms required for the STBC-beamforming-IA technique. Section 5.6 then presents the OIA with D-STBC approach that describes the steps taken towards achieving diversity and higher data rates. Section 5.7 provides an overview of simulation results as well as performance comparisons. Finally, Section 5.8 presents the concluding remarks.

Finally, Chapter 6 concludes the thesis and gives directions for further research.

2. Cooperative Spectrum Sensing

The process of CSS starts with local spectrum sensing at each cooperating CR user and similar to spectrum sensing without cooperation, the objective of local SS is PU signal detection. Being one of the crucial functionalities of CR in terms of learning the radio environment, the techniques used to carry out SS are crucial in helping networks achieve diversity and are one of the fundamental elements in CSS [30].

SS techniques can be classified into two broad categories namely coherent and non-coherent detection as shown in fig 2.1 below [30]. In coherent detection, the PU signal can be detected by comparing the received signal or the extracted signal characteristics with a priori knowledge of PU signals. Examples of coherent detection include matched filter detection and cyclostationary feature detection. In non-coherent detection, no priori knowledge is required for detection. Examples in this category include ED, compressed sensing and wavelet detection. Our discussion here focuses on the ED techniques, rather than an exhaustive search for all detection methods. This is due to its simplicity, low implementation costs, low computational complexity and its wider applicability as it works irrespective of the signal format to be detected [31]. The detailed discussion of other sensing techniques can be found in [32] – [35].

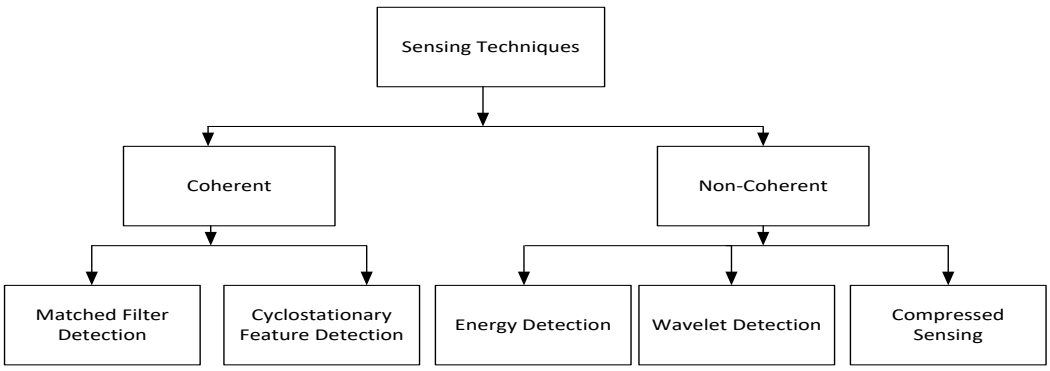

Fig. 2.1 Spectrum Sensing Techniques

2.1.Energy Detection Based Spectrum Sensing

When the considered deterministic PU signal is unknown, it is sometimes appropriate to consider the signal as a sample function of a random process even if its spectral region to which it is approximately confined is known. In the absence of much knowledge concerning the signal, it seems appropriate to use an ED [35], [36] to determine the presence of a signal assuming the noise is considered to be Gaussian and additive with zero mean. The ED technique is a simple and effective SS approach whereby the received signal energy is compared to a defined detection threshold to determine the presence or absence of the PU signal [34]. The received signal energy $y(t)$ at the CR user can be formulated as a binary hypothesis problem given as follows:

$$y(t) = \begin{cases} \sum_{i=1}^{m} n_i(t) & H_0 \\ \sum_{i=1}^{m} h_i(t)s_i(t) + n_i(t) & H_1 \end{cases} \tag{2.1}$$

where $y(t)$ denotes the received signal at the CR user, $s_i(t)$ is the transmitted PU signal, $h_i(t)$ is the channel of the sensing channel, $n_i(t)$ is the zero-mean additive white Gaussian noise (AWGN), H_0 and H_1 denote the hypothesis of the absence and the presence, respectively, of the PU signal in the frequency band of interest.

In energy detection, the energy of $y(t)$ is pre-filtered by an ideal bandpass filter in a fixed bandwidth W before being squared and integrated over an observation time window T. The energy collected in the frequency domain is denoted by E_i, which serves as a decision statistic given as follows [35] – [37]:

$$E_i \sim \begin{cases} \mathcal{X}_{2m}^2 & , \quad H_0 \\ \mathcal{X}_{2m}^2(2\gamma_i) & , \quad H_1 \end{cases} \tag{2.2}$$

Where $\mathcal{X}_{2m}^2$ denotes a central chi-square distribution with $2m$ DoF and $\mathcal{X}_{2m}^2(2\gamma_i)$ denotes a non-central chi-square distribution with m DoF and a non-centrality parameter $2\gamma_i$. The instantaneous SNR of the ith CR is given as γ_i, and $m = TW$ is the time-bandwidth product. The received signal energy is compared to a detection threshold λ, which is a value set depending on the requirements of detection performance. A decision saying that PU is idle H_0 is made if it is less than the threshold. Otherwise CR thinks that PU is active H_1.

$$d = \begin{cases} H_o \quad , & if \;\; y(t) < \;\; \lambda \\ H_1 \quad , & otherwise \end{cases} \tag{2.3}$$

ED is not without its drawbacks as it is well known that the detection performance is affected when the noise variance is unknown to the sensing node especially in the lower SNR regimes, which makes it difficult to distinguish between the radio signal and noise signal. Therefore the knowledge of the noise power can be used to improve the detection performance of the energy detector.

The CR's detection performance is commonly measured by the *probability of false alarm* P_f and *detection* P_d which are defined as follows:

$$P_d = P\{decision = \; H_1 | \; H_1\} = P\{y > \lambda | \; H_1\} \tag{2.4}$$

$$P_f = P\{decision = \; H_1 | \; H_0\} = P\{y > \lambda | \; H_0\} \tag{2.5}$$

Based on these definitions, the *probability of a missed detection* is defined as $P_m = 1 - P_d = P\{decision = \; H_0 | \; H_1\}$. The plot that demonstrates P_d versus P_f is called the ROC curve, which is the metric for performance evaluation of sensing techniques.

2.2.Related Mathematical Statistics

2.2.1. Probability of False Alarm

When PU is idle (H_0), the received signal $y(t)$ at the CR follows the central chi-squared distribution and non-central chi-squared distributed under (H_1) with $2m$ DoF [36].

Its PDF can be written as [38]

$$f(y|H_0) = \frac{\mathrm{y}^{m-1} e^{-\frac{y}{2}}}{\Gamma(m) \cdot 2^m} \tag{2.6}$$

Where $\Gamma(\cdot)$ is the gamma function

As there is only noise in the received signal, when PU is idle (H_0) as in(2.1), P_f is independent of the statistics of the wireless channel [36], thus:

$$P_f = \int_{\lambda}^{\infty} f(y|H_0)dy = \frac{\Gamma\left(m, \frac{\lambda}{2}\right)}{\Gamma(m)} \tag{2.7}$$

2.2.2. Probability of Detection

On the contrary, when PU is active (H_1) as in(2.1), the received signal energy is dependent on the channel type. The received signal energy for a particular instantaneous SNR also follows the non-central chi-squared distribution with $2m$ degree of freedom and non-centrality parameter of $2\gamma_i$, with the instantaneous SNR of γ_i. Its PDF can be written as [38]

$$f(y, \gamma_i|H_1) = \frac{\mathrm{y}^{m-1} e^{-\frac{(y+2m\gamma_i)}{2}}}{\Gamma(m) \cdot 2^m} \; 0F_1\left(m, \frac{m\gamma_i y}{2}\right) \tag{2.8}$$

Where $0F_1(.,.)$is the congluent function [39].

For an AWGN Channel, the instantaneous SNR at the CR user remains constant at $\overline{\gamma_i}$. The PDF for the received signal is given as

$$f(y|H_1) = \frac{\mathrm{y}^{m-1} e^{-\frac{(y+2m\overline{\gamma_i})}{2}}}{\Gamma(m) \cdot 2^m} \; 0F_1\left(m, \frac{m\overline{\gamma_i} y}{2}\right) \tag{2.9}$$

Similar to (2.7), P_d is given as

$$P_d = \int_{\lambda}^{\infty} f(y|H_1)dy = Q_m(\sqrt{2m}\,\overline{\gamma_i}\sqrt{\lambda}\,) \tag{2.10}$$

Where Q_m is the uth order Marcum-Q function, $\gamma_i = E_s|h|^2/N_0$, E_s is the power budget at the PU [39].

In conditions of multipath fading, the Rayleigh channel model is one of the most common and simple channel models that can be used. Assuming Rayleigh fading with random instantaneous SNR at the CR and a PDF of $f_h(\gamma_i)$, the PDF for the received signal energy can be obtained by

$$f(y|H_1) = \int_0^\infty f(y, \gamma_i|H_1) \cdot f_h(\gamma_i) dy$$

$$= \int_0^\infty \frac{y^{m-1} e^{-\frac{(y+2m\gamma_i)}{2}}}{\Gamma(m) \cdot 2^m} \, 0F_1(m, \frac{m\gamma_i y}{2}) \cdot \frac{1}{\overline{\gamma}_l} e^{-\frac{\gamma_i}{\overline{\gamma}_l}} d\gamma_i \tag{2.11}$$

In terms of the incomplete gamma function $\Gamma(\cdot)$, (2.10) can be rewritten as

$$f(y|H_1) = \frac{e^{-\frac{1}{2(1+m\overline{\gamma}_l)}y} \times [\Gamma(m-1) - \Gamma\left(m-1, \frac{m\overline{\gamma}_l y}{2+2m\overline{\gamma}_l}\right)]}{2 \cdot (1+\mathrm{m}\,\overline{\gamma}_l) \cdot (\frac{m\overline{\gamma}_l}{1+m\overline{\gamma}_l})^{m-1} \cdot \Gamma(m-1)} \tag{2.12}$$

Where $\overline{\gamma}_l$ is the average SNR received at the CR user.

Hence, in Rayleigh fading channel, P_d is given as

$$P_d(\lambda) = \int_\lambda^\infty f(y|H_1) dy$$

$$= \frac{\Gamma\left(m-1, \frac{\lambda}{2}\right)}{\Gamma(m-1)} + e^{-\frac{1}{2(1+m\overline{\gamma}_l)}} \times (1 + \frac{1}{m\,\overline{\gamma}_l})^{m-1} \times [1 - \frac{\Gamma\left(m-1, \frac{\lambda m\,\overline{\gamma}_l}{2(1+m\,\overline{\gamma}_l)}\right)}{\Gamma(\mathrm{m}-1)} \tag{2.13}$$

While in Nakagami fading channel, the derivation of P_d is presented in [36] as follows

$$P_{d,Nak}(g, m, \overline{\gamma}_l, \lambda) = \alpha \left[G_1 + \beta \sum_{n=1}^{m-1} \frac{\left(\frac{\lambda}{2}\right)^n}{2(n!)} 1F_1\left(g; n+1; {}^{\lambda}/_{2}\; {}^{\overline{\gamma}_l}/_{g + \overline{\gamma}_l}\right) \right] \tag{2.14}$$

Where

$$\alpha = \frac{1}{\Gamma(\mathrm{g}) 2^{g-1}} \left(\frac{g}{\overline{\gamma}_l}\right)^g$$

$$\beta = \Gamma(\mathrm{g})\left(\frac{2\,\overline{\gamma}_i}{g+\overline{\gamma}_i}\right)^{g} e^{-\frac{\lambda}{2}}$$

$$G_1 = \frac{2^{g-1}(g-1)!}{\left(\frac{g}{\overline{\gamma}_i}\right)^{g}} \frac{\overline{\gamma}_i}{g+\overline{\gamma}_i} e^{-\frac{\lambda}{2}\frac{g}{g+\overline{\gamma}_i}} \left[\left(1+\frac{g}{\overline{\gamma}_i}\right)\left(\frac{g}{g+\overline{\gamma}_i}\right)^{g-1} \times L_{g-1}\left(-\frac{\lambda}{2}\frac{\overline{\gamma}_i}{g+\overline{\gamma}_i}\right)\right.$$

$$\left. + \sum_{n=0}^{g-2}\left(\frac{g}{g+\overline{\gamma}_i}\right)^{n} L_n\left(-\frac{\lambda}{2}\frac{\overline{\gamma}_i}{g+\overline{\gamma}_i}\right)\right]$$

Where ${}_1F_1(.;.;.)$,$L_n(\cdot)$, g, m are the confluent hypergeometric function, Laguerre polynomial of degree n ,Nakagami parameter and time-bandwidth product respectively [40].

2.2.3. Receiver operating characteristics (ROC)

In order to compare the performances for different threshold values, ROC curves can be used to allow us to explore the relationship between the P_d and P_f of a sensing method for a variety of different thresholds, thus enabling the determination of an optimal threshold.

This section provides simulation results to verify the analytical framework, and to compare the ROC curves for different channel scenarios presented in section 2.2 above. We first show the performance of ED in non-cooperative cases (for AWGN and Rayleigh Fading channels), which is an important starting point of the investigation for cooperative cases.

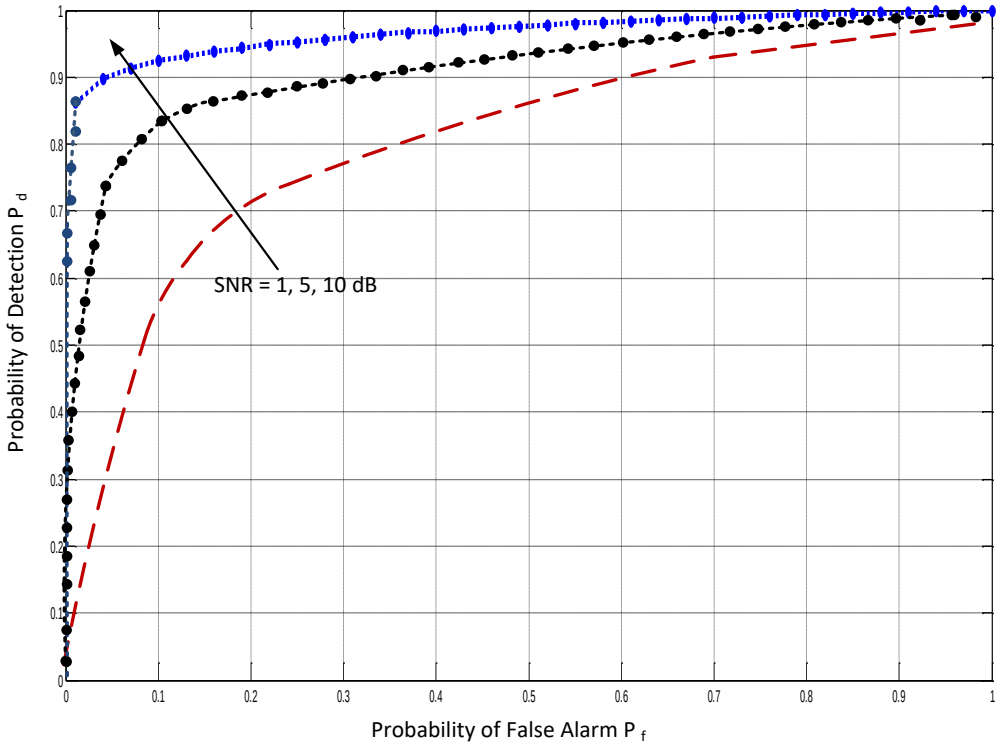

Fig 2.2 ROC curves for the ED for various SNR levels for the AWGN channel

It can be seen in fig 2.2 for that even for the AWGN channel with more ideal parameters; the ED capabilities degrade when the average γ_i of the channel decreases from 10 dB to 1 dB

Fig. 2.3 on the other hand illustrates ROC curves with the Rayleigh fading channel for different γ_i values, which shows a higher performance degradation of the energy detector when comparisons are made between Fig. 2.2 and Fig. 2.3. This deficit in performance can be attributed to the shadowing/fading effects of the channel.

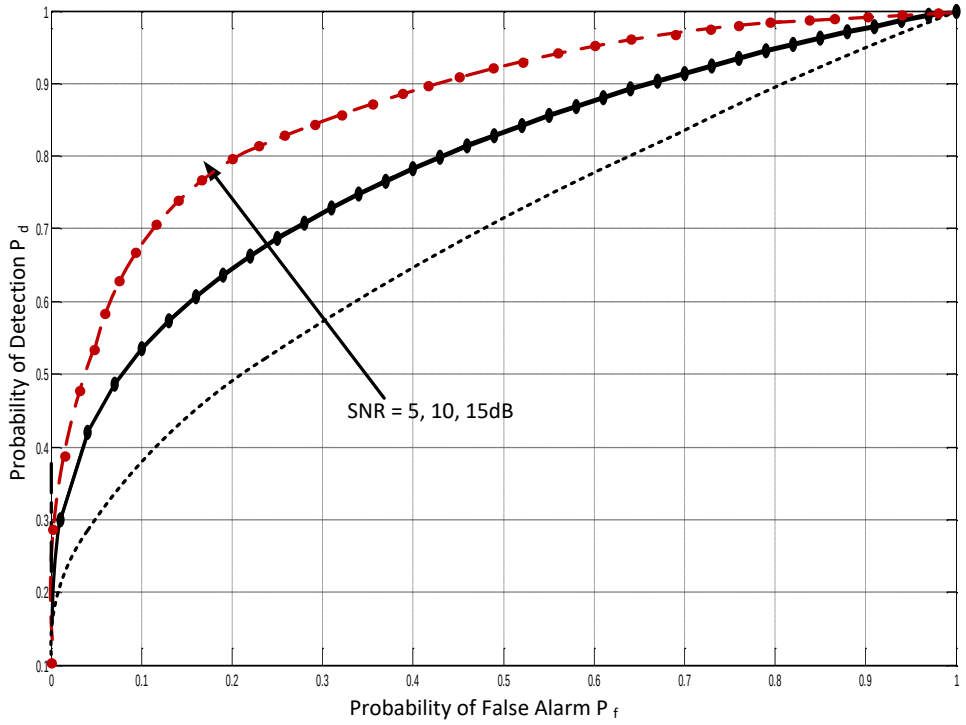

Fig 2.3 ROC curves for the ED for various SNR levels for the Rayleigh channel

2.3.Classification of Cooperative Spectrum Sensing

CSS mitigates the problems of noise uncertainty, fading and shadowing as shown in fig 2.5 below. The process starts with local SS where all CR users are tuned to the selected licensed channel or frequency band on a *sensing channel*. For data reporting, the channel linking each cooperating CR user and the FC for sending the sensing results is called a *reporting channel* [30]. To facilitate analysis, CSS can be classified into three categories based on how cooperating CR users share the sensing data in the network. These categories include centralized, distributed and relay-assisted [30], [31], [41] as illustrated in Fig. 2.4.

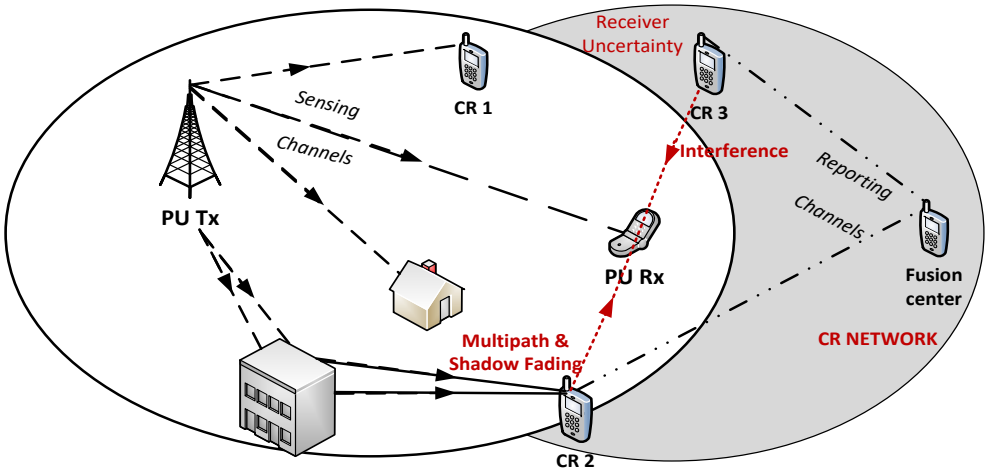

Fig 2.4 Receiver uncertainty and multipath/shadow fading [30]

2.3.1. Centralized CSS

In centralized CSS, the FC controls the three-step process by selecting a frequency band of interest for sensing and directs all the CRs to perform local sensing on the *sensing channel*. Secondly, all CR users report their sensing results via the *reporting channels*. Lastly, the FC collects the received local sensing information, identifies the available spectrum holes and diffuses the decision back to cooperating CR users [30].

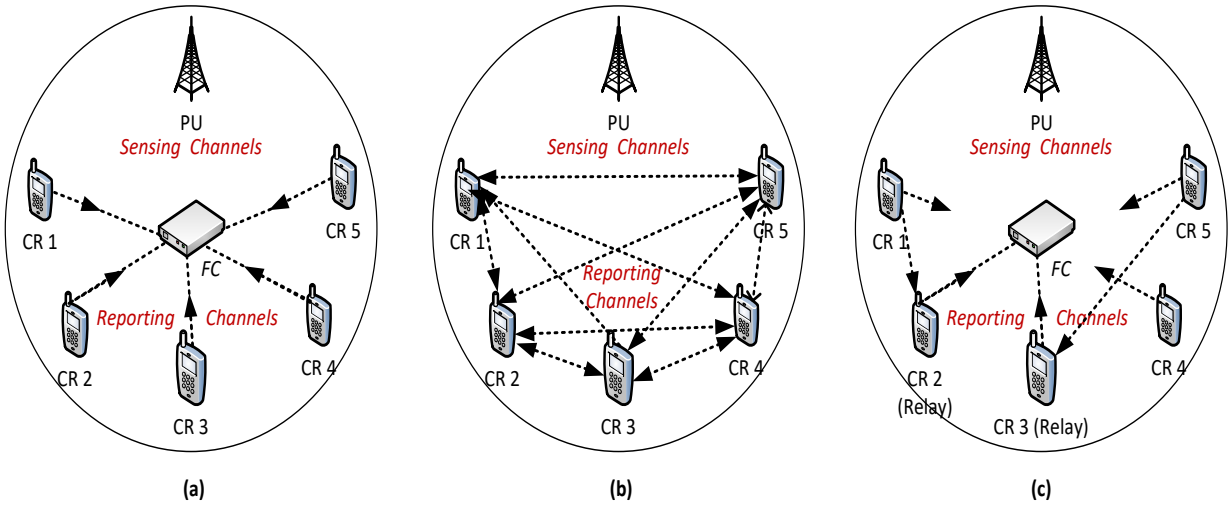

Fig 2.5 Classification of CSS: (a) Centralized (b) Distributed (c) Relay-assisted

2.3.2. Distributed CSS

Unlike centralized, distributed CSS does not rely on the FC for making the cooperative decision. Based on a distributed algorithm, CR users share sensing information between them and based on a local criterion, decide which portion of the spectrum is idle. If the criterion is not satisfied, CR users resend their sensing results to each other and repeat this process until there is convergence and a decision is reached. This category is more advantageous than centralized CSS in terms of cost because there is no need for a backbone infrastructure. Its major disadvantage lies in the fact that it may take several iterations to reach the unanimous cooperative decision, which can lead to large network overheads and prolonged sensing duration that will ultimately have a negative impact on the benefits of CSS.

Several algorithms have been proposed in the literature such as the work done in [42] – [45] to optimize this process. Of particular interest is gossiping updates for efficient spectrum sensing (GUESS) approach [43]. By performing efficient coordination between CRs, this work is shown to have low-complexity with reduced protocol overheads. Another noteworthy endeavour is the work done in [44], where only final decisions are shared to minimize overheads.

2.3.3. Relay Assisted

This category is based on CR users observing weak sensing and reporting channels in one part as well as strong sensing and reporting channel in another and trying to complement and cooperate with each other to improve the performance of CSS. As seen in fig 2.6(c), the relay-assisted CSS can exist in both distributed and centralized structures based on the demands on sensing and reporting at any given time. This category can also be operated as a multi-hop CSS category. It should be noted that the relay for CSS has a distinctly different purpose from the relays in cooperative communications [46].

Of the three categories outlined above, it becomes clear that the optimal strategy for deploying CSS is the centralized category because of its relative ease of implementation, reduced overheads and shorter sensing durations compared with the distributed and relay-assisted categories of CSS, thus will be the preferred choice for this research.

The centralized approach does have its drawbacks of incurring some overheads such as control channel bandwidth, energy efficiency, and reporting delay especially when a large number of CR users are involved in CSS.

Grouping the cooperating users into clusters for CSS has been shown to be effective in reducing the cooperation range and the incurred overhead [47], [48]. In [49], four clustering methods are considered for user selection depending on the availability of location information. Random clustering is a method adopted that randomly divides CR users into clusters of equal size when the actual positions of CR users and PUs are not known. This is followed by reference-based clustering which depends on CR user positions with respect to a given reference. The third method is called statistical clustering, where clusters are formed by using the statistical information and the proximities of CR users when only the positions of CR users are known. In the case of distance-based clustering, when the positions of both CR users and PUs are known, only the CR users closest to the PU in the cluster participate in CSS. In [21], clustering is utilized to exploit user selection diversity to improve the detection performance through reporting channels under Rayleigh fading. In each cluster, the CR user with the largest reporting channel gain is selected as the cluster head (CH) to reduce the reporting overheads.

As such, the next chapter of this research work (chapter 3) considers CSS in a more realistic environment showing how CSS performance is limited by the imperfect reporting channels, when both the sensing channels and reporting channels are characterized by fading. In order

to cope with this drawback, the work in Chapter 3 proposes a transmit-cluster scheme for the CR users to design a diversity based CSS method with STBC.

2.4.Data Fusion

There are a few fundamental elements of CSS that enables its successful operation and deployment. They include sensing techniques, hypothesis testing etc, which have already been introduced in earlier sections of this write up. The remaining elements which include the cooperation models and data fusion will be discussed in this section.

The cooperation model, which consists of the parallel fusion and game theoretical models, simply consider how CR users cooperate to perform SS. However, the game theoretical model was not considered further as it is beyond the scope of this research. The parallel fusion (PF) model is basically the model that has been used to describe CSS so far in this work, with the CR users observing the licensed spectrum for TOs and diffusing these observations to the FC, which then fuses the reported data and makes a decision based on hypothesis testing [41].

Data fusion, which is also an element of CSS, is the process of combining local sensing data for hypothesis testing by the FC in centralized CSS. Based on bandwidth demands, Data fusion can be carried out in two different ways namely (1) soft combining and (2) hard combining.

2.4.1. Soft combining (Quantized Soft combing)

CR users can either transmit the entire local sensing samples or the complete local test statistics for soft decision. Quantized Soft Combining is similar to the Soft combining, but the CR users have the ability to quantize the local sensing results and send only the quantized data in order to reduce control channel overheads [30]. For the case of our considered ED based CSS, existing and simpler receiver diversity techniques of equal gain combining (EGC)

and selection combining (SC) have been utilized for soft combing in [36], with the EGC method having a slightly higher gain than the SC method. Another method, which is based on log-likelihood ratio test is the Chair-Varshney (CV) combining rule, which was shown to be optimal for fading as well as noisy channels [50] ,[51].

2.4.2. Hard Combining

It is very easy and convenient to transmit the one-bit decision for hard combining after binary local decisions have been reported to the FC. The commonly used fusion rules are AND, OR and Majority fusion rules. In AND-rule, all sensing results should be H_1 for deciding H_1, where H_1 is the alternate hypothesis, *i.e.* the hypothesis that the observed band is occupied by a PU. In OR-rule, the CR decides H_1 if any of the received decisions plus its own is H_1 . M-out-of- N rule outputs H_1 when the number of H_1 decisions is equal to or larger than M [33]. Another less popular fusion rule that shows better performance than the AND/OR rules is the Dempster-Shafers theory of evidence rule [52].

Using Soft combining at the FC can achieve better detection performance than hard combining, but at the cost of channel overhead, although quantized Soft combining could reduce control channel overheads with the possibility of having a degraded performance due to the loss of information from quantization. Hard combining rules on the other hand are found to perform as good as soft decisions when the number of cooperating users is sufficiently high [53].

The false alarm Q_f and detection probabilities Q_d for CSS under this rule for data fusion are given by

$$Q_f = Prob\{ H_1 | H_0\} = \sum_{l=k}^{N} \binom{N}{l} P_f^1 (1 - P_f)^{N-l} \tag{2.15}$$

$$Q_d = Prob\{H_1 | H_1\} = \sum_{l=k}^{N} \binom{N}{l} P_d^1 (1 - P_d)^{N-l} \quad (2.16)$$

2.5.Numerical Comparison

This work focuses on cooperative cases were the impact of the number of CRs on detection performance is explored.

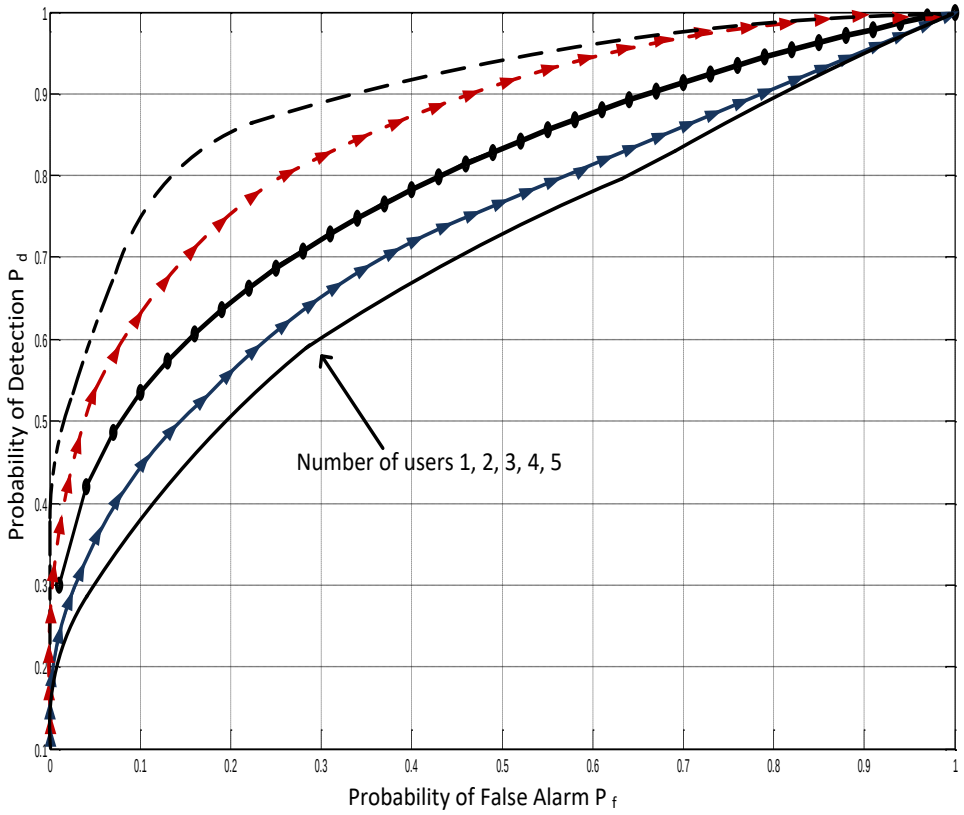

Fig 2.6 ROC curves for up to 5 users for the Rayleigh channel

The upper bound of P_d based on simulation results are shown in Fig. 2.6, where it is seen that increasing the number of CRs considerably improves the detection performance. The average SNR for other channels (from the PU to each CR and from each CR to the FC) is 5 dB. If these sensing channels are identical and independent, then every SU achieves identical P_f and P_d. As shown in fig 2.2 and 2.3, when the average SNR of the direct link is improved

from -5 dB to 5 dB, ROC curves move rapidly to the left-upper corner of the ROC plot, which means better detection capability.

Fig. 2.7 shows the ROC curves for k-out-of-n rule in decision fusion strategy for error-free channels, where three fusion rules: OR, AND, and Majority rules, are considered. The average SNR in each link (i.e. the sensing and reporting channels) is 5 dB. With error-free reporting channels, the OR rule always outperforms both AND and Majority rules because the FC can decide H_1 when at least one CR user detects the PU signal.

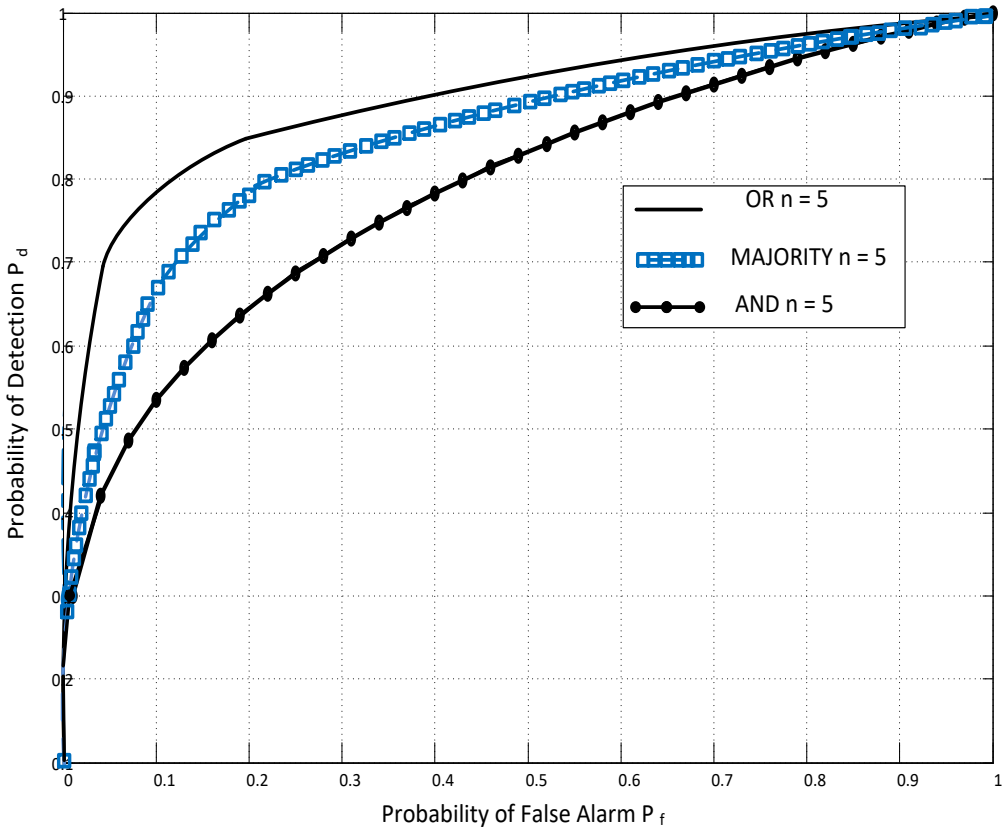

Fig 2.7 ROC curves for up to 5 users for the AND, OR and Majority Combination

However, deciding H_1 for the AND rule requires that all CR users must detect the PU signal. The Majority rule has better detection capability than AND rule. The simulation results shown fig 2.8, in which Maximum Ratio Combining (MRC) has been proved experimentally

to be a nearly optimal soft combination scheme are all under i.i.d. Rayleigh channels. MRC is a coherent technique, where all the signals are co-phased and weighted according to their signal voltage to noise power ratios. Out of all the soft combining techniques, MRC provides the best performance. One of its major drawbacks is its significant hardware requirements. The soft combining schemes exhibit much better performance than the conventional hard combination schemes, thus verifying advantages of soft combination especially with lower SNR values (Section *2.4.2*). It is observed from fig 2.8 that while the MRC scheme exhibits the best detection performance, it is completely dependent on full CSI. The SLC scheme, on the other hand does not require any CSI, but still gives less performance than the MRC scheme. In the absence of CSI, the SLC scheme provides the best performance.

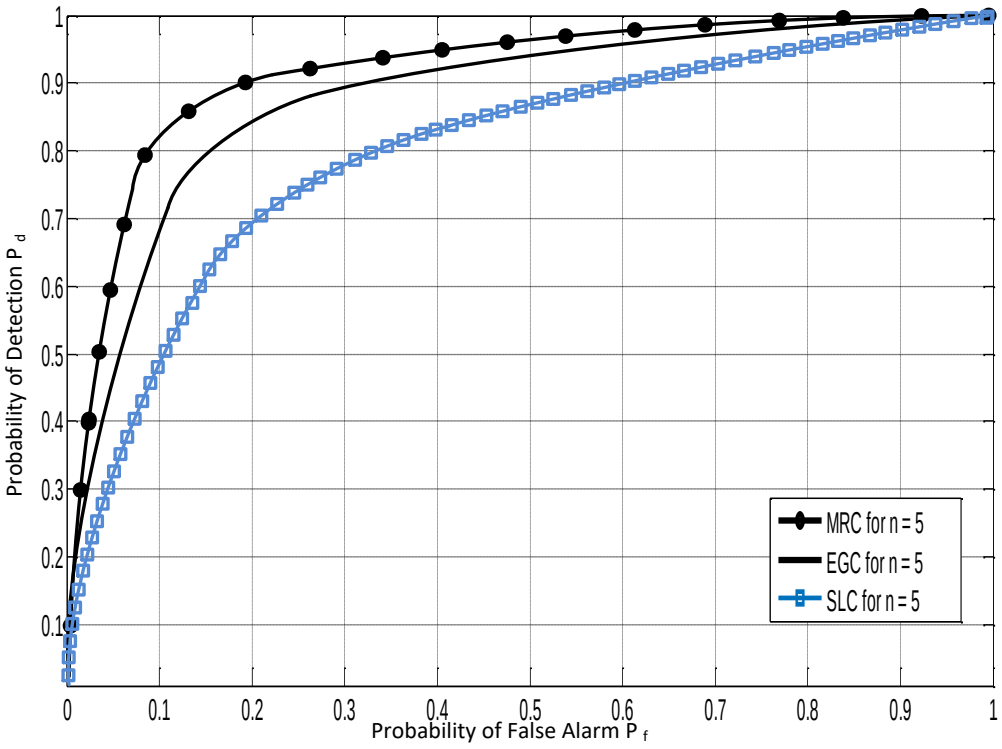

Fig 2.8 ROC curves for up to 5 users for Soft Combination

2.6.Interference Alignment

Traditionally, minimal interference is simply treated as background noise; considerable interference though, can first be decoded and then removed from the received signal (i.e., through interference cancellation); or avoided completely either by orthogonalizing the channels or adopting a medium access control (MAC) scheme [53, 54].

As stated in Chapter 1, recent research has found IA as a significant breakthrough in interference management; a linear pre-coding technique which exploits interference in interference limited wireless networks [17, 55]. It is by definition a cooperative interference management strategy that results in sum capacities scaling up linearly at high SNR by taking advantage of the multiple signaling dimensions provided by the Tx's time slots, frequency blocks or antennas to achieve the IC's maximum multiplexing gain or DoF [19], [53] – [57].

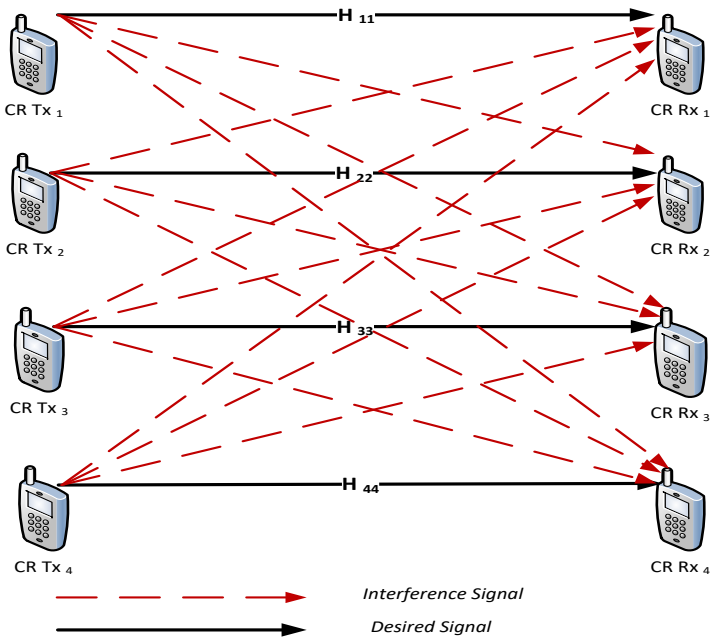

Fig 2.9 Interference Channel (IC)

The study of the DoF initiated in [55] presented the IA scheme in its linear form to be a *general* principle, in which users are able to transmit at a data rate equal to one-half of their capacity in an ideal interference-free channel to yield a normalized DoF i.e. the DoF could be

up to of $K/2$, where K is the number of interfering users. This is all achieved by users linearly pre-coding their transmissions such that each of the interference signals are fully contained in a lower dimensional space and lie in a subspace orthogonal to the one occupied by desired signal, while the other subspace is reserved for interference free communication. Thus substantial system throughput gain can be achieved with IA when $K \geq 1$ despite its strong requirement for the global CSI at every node.

Considering the symmetric K −user MIMO $M \times N$ Gaussian IC shown in Fig. 2.9, there are K Tx-Rx pairs with M antennas at each Tx and N antennas at each Rx. The Rx of $CR\ Tx_1$ user only needs to correctly decode the signal from the Tx of $CR\ Rx_1$ using zero forcing. There are therefore $K-1$ interfering signals at each Rx. The received signal $Y_k(n) \in \mathbb{C}^{(N\times 1)}$ at k^{th} receiver at time n can be expressed as

$$Y_i(n) = \sum_{j=1}^{i} H_{ij}(n)x_j(n) + z_i(n)\ ;\ \ \forall k \in \varkappa \triangleq \{1,2,\ldots\ldots,K\} \tag{2.17}$$

Where $Y_i(n) \in \mathbb{C}^{(N\times 1)}$ denotes the $N_i \times 1$ received signal (vector) at the i^{th} receiver

$z_i(n) \in \mathbb{C}^{(N\times 1)}$ denotes the $N_i \times 1$ zero mean unit variance circularly symmetric AWGN noise vector at the i^{th} receiver

$x_j(n) \in \mathbb{C}^{(M\times 1)}$ Denotes the $M_j \times 1$ signal (vector) transmitted from the j^{th} transmitter

$H_{ij}(n) \in \mathbb{C}^{(N\times M)}$ is the $N_i \times M_j$ matrix of the channel coefficients between the j^{th} transmitter and the i^{th} receiver

Also, $P_j = E\left[[||x_j(n)||^2\right]$

Where $P_j$is the transmit power of the j^{th} transmitter.

The DoF d for the k^{th} user's message is also defined as $k^{th} \leq \left(M_j, N_i\right)$

The next step in our review is to define the transmitted signal from the k^{th} user as

$$x_j = \sum_{d=1}^{d_k} V_j^{(d)} \tilde{x}_j^{(d)} = V_j \tilde{x}_j \tag{2.18}$$

Where $\tilde{x}_i$ is a $d_i \times 1$ vector that denotes the independently encoded signal from the $k^{[th]}$ user

V_j Is the $M_j \times d_j$ transmit pre-coding (beam-forming) matrix

The pre-coding filters are designed to ensure overlap of interference subspaces at the Rx's while also ensuring desired signals remain linearly independent of the interference. This makes it possible for the Rx's to zero-force all interference signals independent of the desired signals.

Defining the zero-forcing filters as $U^{[i]}$, the DoF allocation d for each SU is feasible if there exists a set of transmit pre-coding matrices $V^{[j]}$ and receive suppression matrices $U^{[i]}$ defined as follows:

$$V_j : M_j \times d_j, \qquad V_j^{\dagger} V_j = I_{d[j]} \tag{2.19}$$

$$U_i : N_i \times d_i, \qquad U_i^{\dagger} U_i = I_{d[i]} \tag{2.20}$$

If interference is suppressed into the null space of U_i, then the following IA conditions must be satisfied

$$U_i^{\dagger} H_{ij} V_j = 0, \forall j \neq i \tag{2.21}$$

$$rank(U_i^{\dagger} H_{ij} V_j) = d_i, \forall i \in \{1,2,\ldots..,K\} \tag{2.22}$$

For the constant MIMO IC considered here, the channel matrix is assumed to remain constant for the duration of one extended symbol, i.e., each block in the extended channel matrix is the same and the channel coefficients are assumed to be drawn from a continuous distribution and all Tx's and Rx's are assumed to have global CSI of all links.

The receiver i premultiplies $Y_i(n)$ with a linear filter $W_i^H \in \mathbb{C}^{Sd_i \times NS}$ to obtain

$$\hat{Y}_i = W_i^H H_{ii} x_i + \sum_{j=1, j\neq i}^{K} W_i^H H_{ij} x_j + W_i^H z_k \quad (2.23)$$

The first term in the above represents the desired signal, while the second term represents the interference from the other Tx's, and the last term is due to the noise at the Rx.

IA can be therefore be summarized as a technique that calculates a set of precoders such that any user can cancel the interference it observes from all other users without destroying its desired signal [58], [59].

2.7.Interference Alignment in Cognitive Radio

It was interesting to see that the potential interference free dimensions or DoF that can be created largely depended on the alignment techniques involved, implying that the signal space could potentially have as many spatial dimensions as the total number of Tx and Rx antennas across all the nodes in the network [60]. However, achieving optimal signal alignment is still a very challenging task [17] of which techniques such as message sharing, beamforming, zero forcing and successive decoding may be combined in many different ways across users, data streams, and antennas to establish inner bounds on the DoF [16].

The earliest work to explore the increase in DoF with message sharing in the manner of CR was done in [19], [20], [55] for both the MIMO interference and X-channels. This is because the CR network can be seen as an IC when the SUs coexist with the PUs and the SU transmission is subjected to the PU-Rx threshold as well as the cross interference between the SUs themselves. Thus the IA technique tends to naturally fit in with CR systems effort of managing interference between the PU and SU [57]. The work in [19], [20] and [55] explored the impact of sharing one user's message with other user's Tx or Rx in that manner of singularity. In terms of performance, the DoF for the MIMO IC remained the same as without any form of cognition at either transmitters or receivers. Indeed, even this was a good enough

result for further research bearing in mind that all nodes were assumed to have equal number of antennas, and increasing the number of antennas always led to higher data rates anyway. However, the IC was shown to achieve higher DoF if both users have some form of cognition at the same time i.e. they both have cognitive Txs, or they both have cognitive Rx's or one has a cognitive Tx while the other has a cognitive Rx.

A number of other practical IA algorithms have been developed in the manner of message sharing such as [21] to [22], but these have been primarily developed for the single-tier K-user IC. These studies focusing on single-tier systems have provided a significant research platform that has translated into mainstream two-tier CR networks i.e. CR networks consisting of both PUs and SUs, of which there are basically two main paradigms in the design for implementing IA in CR networks.

2.7.1. First Paradigm of IA in CR

The first paradigm considers a CR network consisting of a number of SU pairs and the PU-Tx and PU-Rx, where the PU-Tx is assumed far from its Rx and the SU-Rx's are considered not to be influenced by the interference from the PU-Tx, which is somewhat similar to the Direct SS scenario [15]. The main goal of this IA approach is to choose appropriate Tx precoding matrices and Rx interference suppression subspaces for the SUs to make sure that each SU-Rx can decode its own signal while also keeping an allowable interference level to the PU-Rx within the specified threshold. The transmit precoders and interference receiving matrices are chosen to minimize the interference leaked into the received signal subspace while simultaneously imposing an upper limit on the interference temperature, without the constraint on the number of SUs. This design is solved iteratively until the algorithm converges monotonically, where Tx's and Rx's shape the precoder and Rx subspaces by turns.

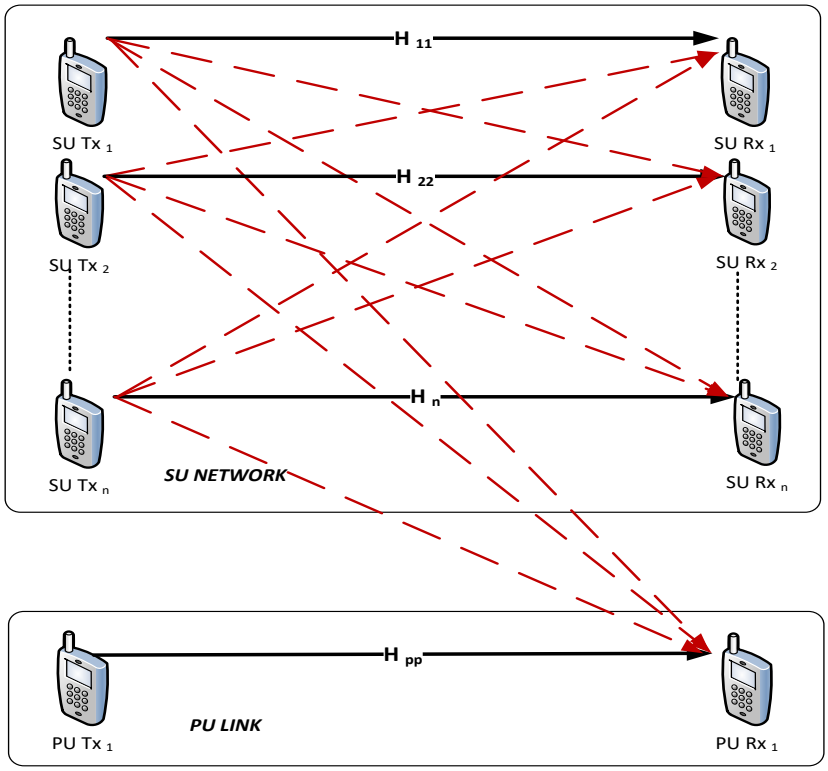

Fig 2.10 First paradigm of IA in CR [61]

Consider a *K*-user MIMO IC with a single PU link and *K* SUs, depicted in Fig 2.10. Each Tx/Rx pair are equipped with M_k and N_k antennas, respectively. It is assumed that the interference from the PU-Tx does not affect the SUs Rx's. From the point of view of IA with a d_i dimensional transmit signal vector $d_i \in \mathbb{C}^{d_i \times 1}$, the signal obtained at receiver i is given as

$$y_i = H_{ii}V_i x_i + \sum_{l=1, l\neq k}^{i} H_{ij}x_j + n_i, \;\; i = 1, \ldots . K \tag{2.24}$$

Where $H_{ij} \in \mathbb{C}^{M \times N}$ denotes the channel between *j*th transmitter to *i*th receiver, $V_i \in \mathbb{C}^{N \times d_k}$ is the precoding matrix with columns comprising of d_i, $n_i \in \mathbb{C}^{M \times 1}$ denotes the receiver thermal noise, modelled as complex additive white Gaussian noise vector.

The PU transmission is a point-to-point communication without considering the SU links. It is also assumed that the PU channel matrix H_{ii} is perfectly known at PU-Tx and PU-Rx. In

designing IA in single-tier networks (without PU links) over MIMO block fading channel, the precoding matrices $\{V_i\}_{i=1}^{K}$ k =1 and interference receiving matrices $\{U_i\}_{i=1}^{K}$ satisfy the conditions of (2.19) and (2.20).

Condition (2.19) and (2.20) ensures no interference from other SU links at the output of the kth SU-Rx, and guarantees that the desired signal space at the kth receiver achieves d_i DoF when H_{kk} is full rank. The desired message for the kth SU can be decoded by projecting onto the orthogonal complement of U_i and zero forcing the interference. Note that, it is still an open problem for general IC to determine closed-form precoding matrices and received interference subspaces. Only for three-user IC has a closed-form solution of V_i for any d_i been found [55], [58].

For the two-tier CR network, the goal of IA is to choose precoder matrices $\{V_k\}_{k=1}^{K}$ and interference receiving matrices $\{U_k\}_{k=1}^{K}$ such that each SU-Rx can decode its own signal by forcing interfering SUs to share a reduced-dimensional subspace while keeping an allowable interference level to the PU within the specified limit. Firstly, Tx j adjusts V_j to make sure the most of its induced interference at other Rx falls into the subspaces $\{U_i\}_{i=1}^{K}$, and keep the interference to the PU below a pre specified level. Secondly, each SU-Rx chooses a subspace U_i to guarantee most of interference falls into the interference subspace when Tx precoding V_j is fixed. This distributed system model is the foundation on which various enhancements have been applied towards optimizing the operation of the first paradigm.

One of such techniques is the idea of symbol extensions, where linear IA (i.e., those based on spatial beamforming) operate within the spatial dimensions provided by multiple antennas at the transmitting and receiving nodes, and seeks to divide those spatial dimensions into separable subspaces to be occupied by interference and desired signals at each Rx. This idea was first introduced in [19], [55] for the two user MIMO X channel where all nodes equipped

with M >1 antennas achieved enlarged DoF by using linear beamforming across multiple channel uses [53]. For the two-tier CR network, one way of exploiting symbol extensions was shown in the work in [61], where the SUs are trying to gain access to the licensed spectrum, without degrading performance of the PU network. The unique condition that avoids degrading the sum rate of the PU's is a *zero-impact* threshold for the number of SU-Tx antennas, which is set in such a way that those SU-Tx's with more (or equal) antennas than this threshold can utilize the licensed spectrum. A specific *Successive IA* (SIA) precoding is also proposed and shown to be optimum for various network setups determined by the number of PUs, SUs and antennas at each node [62].

While the work presented in [19], [54] were significant, their closed form expressions still had significant drawbacks such as reliance on global CSI. Secondly, closed form solutions have only been found in certain cases. In general, analytical solutions to IA problem are difficult to obtain and even the feasibility of IA over a limited number of signaling dimensions remains an open problem. Thirdly, while IA performs well at high SNR, it can be far from optimal at moderate to low SNR [60].

These challenges have inspired the work done in [63], an IA scheme known to minimize leakage interference with only local CSI requirement in order by progressively reducing leakage interference at each Rx. For a two-tier CR network, the distributed IA algorithms can be applied with some enhancements such as the work in [64], which introduces the concept of matrix distance so that at Rx *i*, the distance between the subspace spanned by the interference signals $H_{ij}V_j, k \neq 1$ and its interference receive subspace spanned by $\boldsymbol{U_i}$ is kept as close as possible. Unlike the work done in [63], this work has no constraints on the number of users. Thus by assuming perfect local CSI, the distributed algorithm iteratively solves the optimization problem. Each secondary Tx updates its precoding matrix to minimize the total

interference leakage from interference subspace to signal subspace and guarantees its interference to the PU to be below a certain level. The matrix distance, used as a measurement metric, can be defined as the distance between two orthonormal matrices *A* and *B*, such that the following expression holds $||A - BB^H A||_F$ [63]. The work in [64] is shown to improve sum rates of the CR network and employs a similar technique to [62] to protect the PUs, even though this particular solution consists of multiple PUs [65], [66].

To make improvements to the leakage interference performance at low-and-moderate SNR, [67] proposes a robust joint signal IA (JSIA) design that transforms the transmit optimization and Rx subspace selection constraints into a finite number of linear matrix inequalities that are both optimal and solvable by interior point methods [68]. The proposed design then simultaneously minimizes the leakage of interference signals from the SU-Tx while maintaining interference to the PU-Rx below an acceptable level. The drawback of this solution however, lies in its intricacy making it impossible to prove that the iterations converge to the global optimum [15].

2.7.2. Second Paradigm of IA in CR with Water filling

It is well known that detecting the PU-Rx can be quite a significant challenge due to the fact that the PU-Rx does not transmit when the PU is active. This justifies the reason why most existing spectrum sensing schemes identify spectrum holes by detecting the PU-Tx [11], [15], [58]. A similar challenge is faced by the first paradigm of IA in CR due to the fact that the SUs are more concerned about the PU-Rx and how best to limit the interference level within the specified limit. As described above, the approach of the first paradigm is neither inferior nor less optimal than the approach of the second paradigm, because there are a number of solutions in the literature such as [61] that provide very interesting results. It is rather another aspect of this subject that this particular research will not focus on.

The second paradigm therefore considers the same CR network as the first paradigm, but the SUs are in closer proximity to the PU-Tx in the same manner of Indirect Spectrum Sensing where the SUs are required to detect the PU-Tx. This paradigm proposes that under a power-limitation, a PU which maximizes its own rate by water-filling on its MIMO channel singular values might leave some of them unused *i.e.* no transmission takes place along the corresponding SDs [69], [70]. These unused directions may be opportunistically utilized by the SU-Tx with OIA since its signal would not interfere with the signal sent by the PU-Tx. A linear pre-coder is designed, which perfectly aligns the interference generated by the SU-Tx with such unused SDs, thereby enabling the SUs to share the PU's spectrum with zero interference to the PU transmission. An optimization scheme can also be designed to maximize the transmission rates of the SUs [24]. The system model consists of a single PU link (PU-Tx and PU-Rx) and a single SU link (SU-Tx and SU-Rx) as shown in Fig. 2.11. Every user is assumed to have M transmit and N receive antennas, where the PU and SUs operate in the same frequency band and all channels are Rayleigh flat-fading.

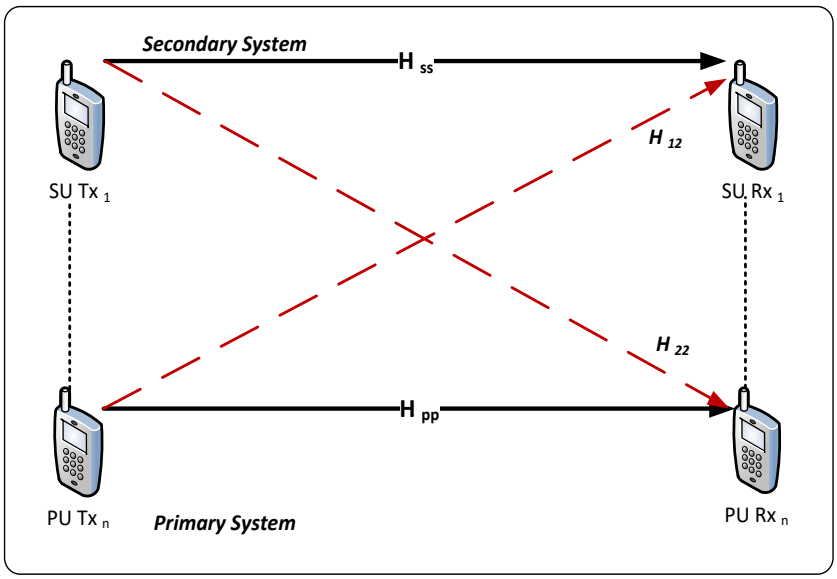

Fig. 2.11 Two-user MIMO interference channel for Second Paradigm of IA in CR [24]

The PU link is a single-user MIMO channel which is represented as a $N_{pp} \times M_{pp}$ matrix, H_{pp} whose capacity can be defined as

$$C = \max_{Q:Tr(Q)=P} log\left|I_N + H_{pp} Q H_{pp}^H\right| \quad (2.25)$$

Where Q is the $M \times M$ input covariance matrix.

The channel matrices for both the PU and SU links are assumed fixed for the whole transmission duration or constant over each data block, which extends to the case of slow-fading channels. The SU is assumed to have global CSI of all the channel transfer matrices which provides an upper bound on the achievable rate of the SU.

Similar to(2.24), the IA condition states that the PU and SU received signals are given by

$$y_i = \mathrm{H}_{ii} V_i x_i + \sum_{j=1}^{K} \mathrm{H}_{ij} V_j x_j + z_i \quad (2.26)$$

where y_i denotes the $N_i \times 1$ received signal vector at the i^{th} receiver; z_i denotes the $N_i \times 1$ zero mean unit variance circularly symmetric AWGN noise vector at the i^{th} receiver; x_i denotes the $M_i \times 1$ signal vector transmitted from the j^{th}transmitter; $\mathbf{H}_{ij}$ is the $N_i \times M_i$ matrix of the channel coefficients between the j^{th} transmitter and the i^{th} receiver; Also, $P_i = E[x_i\, x_i^H]$, where P_i is the transmit power of the j^{th} transmitter. It should be noted that i and j are used as a generalization denoting each Rx and Tx pair.

2.7.3. Water-filing

One of the attractive features of MIMO systems is spatial multiplexing gain and consequently a higher capacity performance over single-input single-output (SISO) system, achieved by the classical water-filling (WF) algorithms [70]. WF algorithms are known to provide capacity achieving scenarios arising from MIMO systems taking advantage of the DoF offered by antennas to increase spectral efficiency as well as maximizing the mutual information

between the input and the output of a channel composed of several sub-channels with the availability of global CSI at the Tx's [68].

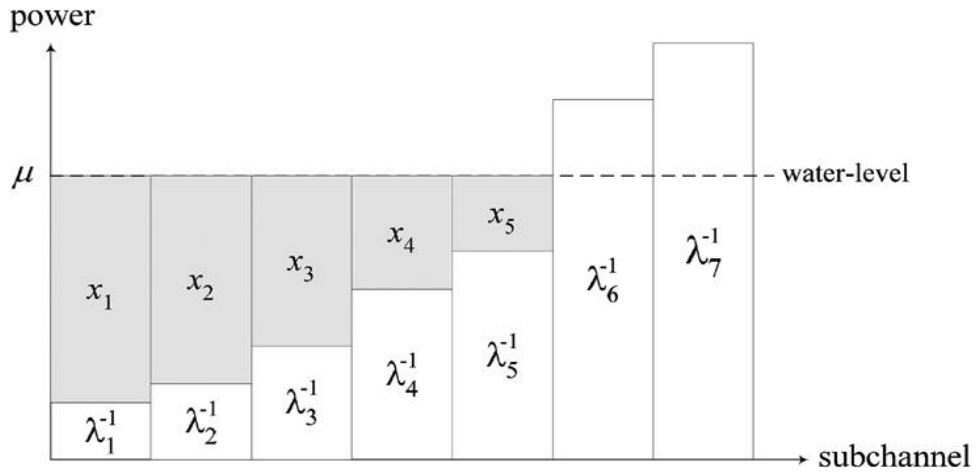

Fig. 2.12 Classical water-filling power allocation [71]

The diagram in Fig. 2.12 describes how the classical WF works, where units of water per sub-carrier are filled into the vessel and μ is the height of the water surface. For some sub-carriers, the bottom of the vessel is above the water and no power is allocated to them, making them the unused spatial directions that could be utilized by the SU transmission. In these sub-carriers, the channel is too poor for it to be worthwhile to transmit on, thus allocates more power to the stronger sub-carriers.

This WF technique can be broken down into the following steps:

Step I: Solve the capacity maximization problem using WF algorithms.

Under the assumption that the channel matrix H_{pp} is known at the Rx and Tx, the PU chooses its pre-coding V_p and post-processing U_p matrices in a way that their channel transfer matrix is diagonalized, which satisfies the singular value decomposition (SVD) $H_{pp} = U_p \Lambda_p V_p^H$ where $U_p \in \mathbb{C}^{(M_{ss} \times M_{ss})}$ and $V_p = \mathbb{C}^{(N_{pp} \times N_{pp})}$ are unitary matrices and Λ_p is a diagonal matrix which contains $\min(N_{pp}, N_{ss})$ non-zero singular values, $\lambda_1, \ldots \ldots \lambda_{\min(N_{pp}, N_{ss})}$.

Then, the achievable rate of the PU is maximized by the power allocation P_p matrix as

$$max \log \left| I_{N_r} + \frac{1}{\sigma^2} H_{pp} V_p P_p V_p^H {H_{pp}}^H \right| \tag{2.27}$$

$$subject\ to \qquad trace(\mathrm{Q}) \leq \mathrm{P}$$

Where H_{pp} is the MIMO channel between the PU-Tx and PU-Rx

Q Is the autocorrelation matrix of the output vector x, defined as $Q = E[xx^{\dagger}]$

P_p is the power allocation matrix

The solution to (2.27) is the classical WF algorithm. The general power optimization process can be carried out as $\tilde{Q} = UQU^{\dagger}$ with $\tilde{Q}$ being the capacity maximizing matrix [23], [24] such that

$$\forall_n \in \{1, \ldots . N_t\}, \qquad P_1(n,n) = \left(\Gamma_0 - \frac{\sigma^2}{\lambda_i} \right)^+ \tag{2.28}$$

Where σ^2 is the noise variance ;

a^+ Is the matrix $\max\{0, a\}$;

The constant Γ_0 is a Lagrangian multiplier that is determined to satisfy

$$\sum_{j=1}^{N} P_p(j,j) = p_{max}$$

Step II: Compute the Transmit Opportunities

The power allocation matrix P_p might contain zeros in its main diagonal implying that no transmission takes place along the corresponding spatial direction. This means that the SU can align its transmitted signal with the unused singular modes such that it does not interfere with the signal transmitted by the PU.

The PU allocates it's transmit power over an equivalent channel defined as a $N_p \times M_p$ matrix which consists of parallel sub-channels with non-zero singular values, (also referred to as the

transmit dimensions used by the PU). The used dimensions can be denoted as $m_1 \in \{1, \ldots\ldots, M\}$, while $N_1 - m_1$ denotes the unused dimensions without any PU signal.

This channel can be transformed from a set of m_1 used transmit dimensions into a set of receive dimensions and a set of $N_1 - m_1$ unused receive dimensions without any PU signal.

Step III: Design the Opportunistic SU transmitter

In order to design IA pre-coding matrices that will take advantage of unused dimensions, a set of IA conditions must be defined that the SUs must meet in order to make use of the TO's. The first condition states that the opportunistic transmitter has to avoid interfering with the m_1 dimensions used by the PU-Tx i.e. interference from the SU is made orthogonal to the m_1 receive dimensions used by the PU link, which is achieved by aligning the transmission from the SU using linear precoding, with the $N_1 - m_1$ unused receive dimensions of the PU link.

As a consequence, in the spatial domain, the corresponding orthogonality condition (such that the SU generates no interference on the primary link is given by

$$U_p^H H_{ps} V_s = \alpha \bar{P}_p \tag{2.29}$$

where the matrix $\bar{P}_p$ is a diagonal matrix with entries

$$\forall_n \in \{1, \ldots\ldots N_t\}, \;\; \bar{P}_p(n,n) = \left[\frac{\sigma^2}{\lambda_n^2} - \beta\right]^+ \tag{2.30}$$

It can easily be verified since both matrices are diagonal.

Additionally, the constant α is chosen to satisfy the power constraints with $i = 2$. Assuming that H_{pp} and H_{ps} are available at the SU-Tx, then the SU precoder can be computed as:

$$V_{ss} = \alpha H_{ps}^{-1} U_p \bar{P}_p \tag{2.31}$$

For the case where $N_s > N_p$, *i.e.* the Rx has more antennas than the Tx, it is still possible to obtain the pre-coding matrix by using the Moore-Penrose pseudo-inverse relation [23].

Once (2.31) has been satisfied at the SU-Tx, then no additional interference impairs the PU. The next step is to consider the interference that the SU-Rx undergoes from the PU-Tx, which has the effect of a being a colored noise [24] with covariance $Q \in \mathbb{C}^{N_s \times N_p}$ due to the channel H_{sp} and the pre-coder V_p. Thus

$$Q = H_{sp} V_p P_p V_p^H H_{sp}^H + \alpha^2 I_{N_r} \tag{2.32}$$

The received signal at the SU can be solved by $D_i = Q^{-(\frac{1}{2})}$ so that

$$r_2 = Q^{-(\frac{1}{2})} H_{ss} V_s s_s + n_s' \tag{2.33}$$

Where $n_s' = Q^{-(\frac{1}{2})}(H_{ss} V_s s_s + n_2)$ is an i.i.d process with zero mean. The second condition also states that the opportunistic link is said to satisfy the IA condition if the PUs transmission achieves the same rate as a single-tier system (with no SUs), with the objective being to calculate the pre-processing matrix to satisfy the IA condition. This is followed by the post-processing matrix, which optimizes the SUs transmission rate.

Step IV: Optimize the Opportunistic SU's transmission rates

The proposed pre-coding scheme is described in Step III guarantees that no interference is generated on the PU. Step IV defines the processes required in order to optimize the transmission rate for the SUs. For this purpose, the choice of the power allocation of the SU-Tx termed $\tilde{P}_{pp}$ needs to be optimized. The first process is the simplest scheme implemented with UPA, before the second process which implements the optimization scheme using an OPA in order to maximize the SU transmission rates [24].

Given that V_{ss} and D_{ss} are satisfied, the $\tilde{P}_{ss}$ input covariance matrix, which maximizes the achievable transmission rate for the opportunistic link is computed as follows:

$$\max_{P_2} \ \log_2 \left| I_{N_{ss}} + D_{ss} H_{ss} V_{ss}{}^H H_{ss}^H D_{ss}^H V_{ss} Q^{-1/2} \right| \tag{2.33}$$

$$s.t. \qquad Trace\left(V_{ss} V_{ss} V_{ss}{}^H\right) \leq M_2 p_{2,\max}$$

Uniform Power Allocation: The SU-Tx does not perform any optimization on its own transmit power, but rather uniformly spreads its total power among the TOs. The input covariance matrix is set to $P_s = I_{N_t}$ so that the rate achieved by the SU while generating zero-interference to the PU-Rx is

$$R_s = \log_2 \left| I_{N_r} + Q^{-\frac{1}{2}} H_{ss} V_{ss} V_{ss}^H H_{ss}^H Q^{-\frac{1}{2}} \right| \tag{2.34}$$

Optimal Power Allocation: The transmission rate for the secondary link is maximized by adopting a power allocation matrix P_s which is a solution of the following optimization problem,

$$\underset{P_s}{\text{argmax}} \quad R_s(P_s) \tag{2.35}$$

$$s.t. \quad Trace\left(P_{ss} V_s V_s^H\right) \leq p_{max}$$

where

$$R_s(P_s) = \log_2 \left| I_{N_r} + Q^{-\frac{1}{2}} H_{ss} V_{ss} P_s V_{ss}^H H_{ss}^H Q^{-\frac{1}{2}} \right| \tag{2.36}$$

Note that solving this optimization problem requires the knowledge of the covariance matrix Q, which is calculated at the SU-Rx based on the knowledge of the channel H_{sp}. This can be done if the SU-Rx estimates Q and feeds it back to the SU-Tx. Here, we assume a perfect knowledge of Q is available at the SU-Tx. Another process was then proposed for (2.35) which led to a WF solution. The idea here is to solve a priori non-trivial optimization problem defined by (2.35) by introducing an equivalent channel matrix G to simplify the problem by applying a singular value decomposition to the new channel.

The outcome of the work in [21] shows that the zero interference constraint to the PU-Rx that has to be satisfied theoretically diminishes opportunities for some of the IA algorithms under

the first paradigm, such as Interference Cancellation (IntCan) and Distributed IA to be used as enhancements to improve overall performance of IA in CR.

Given this fact, subsequent research such as the work done in [72] on interference cancellation introduce novel techniques other than the more conventional IA algorithms, that will provide enhancements to the base model of the second paradigm in [24] to improve overall performance of IA in CR. These techniques are mostly focused on the PU link optimization, spectrum sensing employed by the SU as well as the SUs transmission rates.

For example, the work in [73] investigates both orthogonal and non-orthogonal transmission of the SU, with the aim of determining spectral efficiency gain of an uplink MIMO CR system, where SU is allowed to share the spectrum with the PU by using a unique space alignment technique along with an interference temperature threshold technique to ensure a non-zero SU rate. The proposed scheme adopts a successive IntCan (SIntCan) technique so that the SU is not limited to exploiting the unused TOs of the PUs transmission, but it's also allowed to exploit the used eigenmodes of the PU by respecting both total power and interference temperature constraints. Furthermore, this work analyses the SIntCan's operational inaccuracy as well as the CSI estimation imperfection on the SUs power allocation. Taking this further, the research work done in [74] ensures zero LIF is only feasible when the SU-Tx has at least the same number of antennas as the DoF of the PU system. As the success of the SU communication depends on the availability of unused TOs, the work in [74] focuses on two very specific contributions. The first is a fast coarse sensing method that detects unused TOs, based on the eigenvalues of the received signal covariance matrix. Secondly, a more accurate sensing method based on the generalized likelihood ratio test (GLRT) is applied after coarse sensing to fine tune detection of the unused TOs.

On the subject of spectrum sensing, the work done in [75] described the SUs as sensing for the unused eigenmodes in the manner of cooperative spectrum sensing (CSS). After the decision made by the fusion center (FC) on which eigenmodes to use, the SUs were made to align their transmitted signals to the SDs associated with the PUs unused eigenmodes to ensure orthogonality between the PU and the SUs. This work proposed using maximum eigen-beamforming (MEB) algorithms to optimize the PUs transmission. While its operation is very close to the WF schemes used in [76], [77], the main advantage of using the MEB protocol is that the Tx of the PU puts all its power on the antenna corresponding to the largest eigenmode of its transmission channel, thus by default, the rest of the eigenmodes are left unused for the SUs' transmission. The benefit of using the MEB scheme over existing WF approaches is its slightly lower computational complexity. However, this slight advantage is still very much debatable as the MEB scheme suffers from rigid allocation of power to the largest eigenmode given the fact that the largest eigenmode mode might not always be the optimum for the opportunistic transmission (as shall be discussed further in Chapter 5). Furthermore, this work proposed using a distributed power-allocation strategy called the threshold beamforming (TBF) algorithm to maximize the SUs transmission rates. It enables the SU links with a maximum eigenvalue above a certain threshold to transmit data at full power, while the rest remain silent, thus enabling the CR network to maximize the sum rate of both the PU and SUs. The overall solution causes no interference to the PU-Rx, provides significant throughput gain and senses the TOs of the PU network with higher detection probability.

2.8.Simulation Results and Analysis

For the first paradigm, this work considers a single-tier $3 - user$ 2×2 MIMO (as shown in Fig. 2.10) system configuration against a two-tier CR network consisting of a PU link and *3*

SUs where the algorithm converges when the total interference power is less than 10^{-4}, depicted in Fig 2.11. Each Tx/Rx pair are equipped with $N_k = M_k = 2$ antennas, respectively. It is assumed that the interference from the PU-Tx does not affect the SUs receivers. The numerical results presented in Fig. 2.14 illustrate the various performances of the SUs for the single-tier network, the first paradigms distributed CR network model as well as the enhanced matrix-distance model described in [64], which are measured by the sum rate achieved over the IC, i.e., the sum of the rates achieved by the 3 users, measured in bits per channel use versus SNR in dB.

As expected, the single-tier IA algorithms are upper-bounded, linearly scaling upwards as SNR approaches infinity. As shown in Fig 2.13, the single-tier algorithms outperform the algorithms of the first paradigm owing to the presence of the PU as well as the SUs sacrificing performance to keep interference to the PU below the specified threshold. The difference in performance becomes clearer as the SNR increases.

The distributed algorithm which minimizes the interference leaked into the received signal subspace while simultaneously imposing an upper limit on the interference temperature is seen to have the least performance in terms of sum rates. Enhancements such as the one described in the work in [63] has a better performance compared to the base model, which implies that a higher multiplexing gain is achievable with improved optimization.

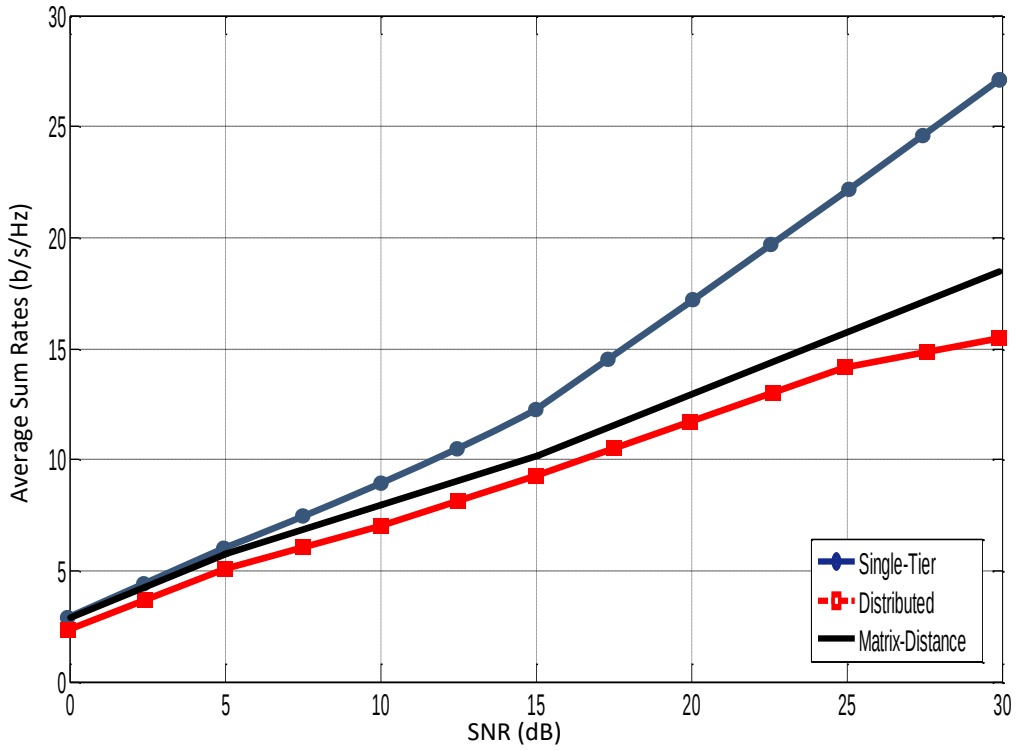

Fig. 2.13 Performance comparison of the Single-Tier IA against First Paradigm of IA in CR algorithm for the three-user IC with two antennas at each node

A similar trend in performance can be seen in the numerical results obtained for the second paradigm (as seen in Fig 2.14), which compares the single-tier network with the OPA/UPA and the threshold based beamforming (TBF) schemes, where the performance of the single-tier network remains upper bounded. The TBF scheme serves as a distributed power-allocation strategy that is effective tool for sparing transmit power in poor channel conditions where the Rx of SU*k*, for $k = 1, \ldots, K$, estimates only its local CSI and feeds back the Tx antenna index to the corresponding Tx if the largest eigenvalue of its own channel matrix, denoted as $\lambda_{k,max}$, is greater than a pre-specified threshold level λ_{th}. If $\lambda_{k,max} > \lambda_{th}$, SU*k*'s Tx puts all its power on the antenna corresponding to the fed back index; otherwise, it remains silent and thus improves the spectrum efficiency for SUs.

While the two-tier algorithms experience a drop in performance as SNR increases, the SU-Tx always sees a nonzero number of TOs, even though the number of TOs is a non-increasing function of the SNR, thus opportunistic communications are always feasible [24]. This drop in performance can be attributed to the limited singular values left unused by the PU link. It is observed that for small number of antennas, the UPA and OPA have identical performances. This implies that the upper bound of performance depends on antenna ratios at the Tx and Rx as well as the number of SUs because a single SU is unlikely to perform reliable detection due to factors such as noise, multipath fading impairment and sensing time constraints [16].

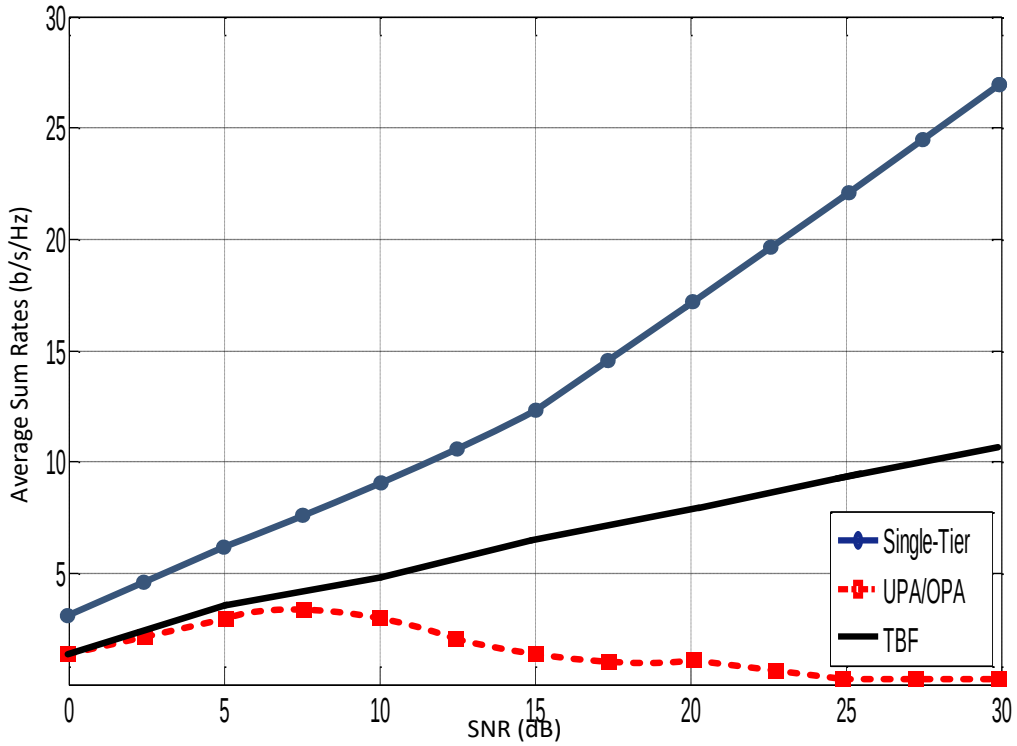

Fig. 2.14 Performance comparison of the Single-Tier IA against the Second Paradigm of IA in CR algorithm for the three-user IC with two antennas at each node.

Fig. 2.14 above also demonstrates the impact of one of the enhancements applied to the second paradigm, namely the TBF algorithm on the performance of the SUs.

Firstly, the TBF scheme employs a number of SUs, which increases the average sum rate due as a result of diversity gain introduced by multiple SUs. The diversity gain states that there is a higher probability of at least one of the SUs meeting the interference power requirement and ensuring reliable detection of the TOs.

Secondly, the performance of the TBF algorithm increases exponentially when the SNR increases because with the TBF algorithm, the PU-Tx assigns all its power to the antenna that corresponds to maximum eigenmode of the channel matrix, thus leaving the other eigenmodes as TOs for opportunistic transmission. Therefore, there is always a nonzero numbers of TOs for the SU to exploit. Another reason for the improved performance of the TBF algorithm is because it separates the SUs with the better and poorer channel conditions, according to a pre-specified threshold, so that those above the threshold are able to transmit. The SUs with the poorer channel condition stay on the silent mode to cooperate with the other links in order to enhance the performance of the network through controlling the interference among the SUs. Thus, the SUs transmission rates improve substantially in comparison with the UPA/OPA schemes when all the SUs employ the TBF protocol. Another observation is that, for intermediate SNRs, the SU's data rate increases without significantly affecting the PU's data rate [75].

2.9.Summary

A review of the concise literature required in order to optimize spectrum sensing in CR using IA was given a critical evaluation in this chapter in the following steps. Since CSS is usually a three step process starting with local spectrum sensing, the first part of this chapter reviewed the various techniques used to carry out local spectrum sensing. Given the wide scope of literature available in this aspect, this work focused specifically on ED given its ease of implementation with due consideration to its inherent drawbacks. The related

mathematical statistics used to evaluate the performance of ED in ideal and non-ideal channel environments were reviewed and simulations carried out were presented using ROC curves.

The next step involved classification of CSS into its various categories and the data fusion rules employed by the FC in deciding the presence or absence of spectral opportunities. Centralized CSS was shown to be the optimal solution in terms of implementation costs and performance. The results of the simulations carried out with similar parameters and channel conditions showed that SS using ED and cooperation performed better than the initial ROC presented for spectrum sensing using ED but without cooperation. Thus, the first strategy considered for optimizing CSS in CR using IA is ED based CSS.

The general IA technique was then reviewed as a cooperative interference management strategy that results in sum capacities linearly scaling up at high SNR by taking advantage of the multiple signaling dimensions to achieve the IC's maximum DoF. We then reviewed earliest work to explore the increase in DoF with message sharing in the manner of CR that gave the necessary impetus to integrate IA in CR. The research work done to implement in IA in CR seemed to have been done along two main areas, the first paradigm being in a direct way where the PU-Tx is assumed far from its Rx and the SU-Rx's are considered not to be influenced by the PU-Tx. The second paradigm is more conventional, where SUs are in closer proximity to the PU-Tx in the same manner of indirect SS where the SUs are required to detect the PU-Tx. However, this second paradigm proposes that under a power-limitation, a PU which maximizes its own rate (mostly through WF) on its MIMO channel singular values leaves some of them unused. These unused directions may be opportunistically utilized by the SU-Tx since its signal would not interfere with the signal sent by the PU-Tx. As such, this chapter then provided a critical review on WF and the steps involved in making

the unused spatial dimensions into TOs that can be used to enhance the transmission of the SUs.

The results of the simulations carried out for the two paradigms were compared to the conventional IA in a single-tier network, and the results showed that IA in single-tier networks performed significantly better than the work of the first and second paradigms. Interestingly, the first paradigm seemed to have better performance than the second, implying that there is a higher challenge as well as a wider opportunity with the second paradigm to improve its performance hence the objective of this work to introduce novel techniques that will provide performance gains for the second-paradigm. These techniques will touch on the PU link maximization under a power limitation; the sensing mechanisms adopted by the SU as well as optimization of the SUs transmission rates.

3. Cooperative Spectrum Sensing with Space-time Block Coding

3.1.Introduction

As discussed in the introductory chapter, the main aim of this research work is optimizing CSS in CR, with the objectives being to optimize the performances of the *reporting* and *sensing* channels. Thus, optimizing the performance of *reporting* channels in realistic channels conditions will be the main objective of this chapter.

It has been well established that the FSA policy is fixed in terms of frequency band utilization [5]. As a result, spectrum usage is limited to certain parts of the frequency spectrum. With several research studies indicating that the rest of the spectrum remains under-utilized [5], dynamically accessing the spectrum with CRs can help improve spectrum utilization. CR is designed to sense and learn from the environment in order to provide the best services to users. Since it was first introduced by Mitola [9], CR has become the enabling technology for supporting DSA in wireless communications.

The CRs detect *spectrum hole*s and dynamically change their radio parameters to exploit the unused parts of the spectrum, making SS by far the most important component in the establishment of CRs [10]. Most existing SS schemes employ indirect sensing techniques which focus on PU-Tx) detection [15], where ED is the preferred local sensing solution for this research work [32], [36]. Despite the optimality of ED, it is well known that the detection channels are still impaired due to shadowing and fading conditions resulting in degraded sensing performance of CR. In order to alleviate detection performance especially against the *hidden terminal* [8], [10] problem, CSS has been proposed as a possible solution. In CSS, SUs individually perform *local sensing* and then report this information to a FC via a *reporting channel*. The FC then makes a decision on the presence or absence of the PU signal based on its received information. In other words, CSS can alleviate the *hidden terminal*

problems by exploiting spatial diversity, with the aim of reducing the probability of detection errors [34].

In practice however, the *reporting channels* are also susceptible to fading effects and interference. It is shown in [34] that when the reporting channels become very noisy, CSS will get no advantages and that the probability of false alarm is lower bounded and the bound tends to linearly increase with the probability of reporting errors.

3.1.1. Diversity Techniques

As discussed in Chapter 2, CSS with particular emphasis on centralized CSS may incur high overhead such as control channel bandwidth, energy efficiency, and reporting delay when a large number of CR users need to cooperate and report to the FC. To alleviate this problem, grouping the cooperating users into clusters is an effective approach aimed at reducing overheads [78], [79]. Employing some other form of transmit diversity can alleviate performance of decision reporting. By introducing *probability of reporting error* P_e in the CR network, the work in [34], [80] proposed a transmit diversity based CSS method which applies some existing STBC and space-frequency (SF) coding for multiple antennas systems to CRs that are coordinated to form a transmit cluster to mitigate the effect of reporting errors and improve the performance and reliability of CSS.

The work done in [34], [80] also applied STBC to improve performance of spectrum sensing in realistic environments with the condition that SUs were aware of each other's decision. At high SNR, this work achieved higher diversity gain and reduced probability of reporting errors P_e, albeit with huge time losses. These time losses have been addressed in the research work done in [81], where clusters with higher sensitivity are set to adapt different sensing durations in order to overcome unnecessary energy consumption and ultimately improve performance.

The literature in [82] makes good use of the *inter-user* CSI and provides a dynamic STBC based-clustering scheme, which overcomes the limitation of fixed clustering. More recently, literature in [83] proposed a similar approach to [82], but the clustering scheme instead focuses on the quality of *inter-user* channels to achieve better results. There are clearly gains achieved from the existing literature in terms of performance. However, use of STBC becomes more tedious and impractical in realistic environment where both the sensing channels and reporting channels are characterized by fading channels.

This then justifies the need to incorporate differential strategies to improve decision reporting in CR networks. The idea of differential strategies span from the use of differential schemes in multiple antenna systems [84], [85] and the work done in [85], [86] have shown that existing differential STBC are suitable for both single and multiple antenna networks, thus the need for a DSTBC based CSS scheme that does not require knowledge of CSI.

3.1.2. Decision Fusion

In practical wireless network scenarios, the reporting channels will most likely introduce errors in decision reporting, which may have a significant impact on performance of CSS [87] – [90]. Thus in the presence of non-ideal reporting channels between the CR and the FC, the question arises as to how to design the FCs decision rules [74]. Before applying the fusion rules, statistical hypothesis testing is typically performed to test the sensing results by each cooperating SU on the presence of PUs. There are two basic hypothesis testing methods in spectrum sensing namely the Neyman–Pearson (NP) test and the Bayes test [31].

For the NP test, the objective is to maximize P_d under the constraint that $P_f \leq \alpha$, where α is the maximum P_f. It can be shown that the NP test is equivalent to the following likelihood ratio test (LRT) given by

$$\Lambda(y) = \frac{f(y|\mathrm{H}_1)}{f(y|\mathrm{H}_0)} = \prod_{k=1}^{N} \frac{f(y_k|\mathrm{H}_1)}{f(y_k|\mathrm{H}_0)} \gtrless_{\mathrm{H}_0}^{\mathrm{H}_1} \lambda \tag{3.1}$$

Where $\Lambda(y)$ is the likelihood ratio, λ is the detection threshold and N is the number of samples, of which the equality holds as long as the observations are independent and identically distributed (i.i.d.). As a result, the optimal test at FC in CSS is the NP-based LRT if the conditional independence is assumed [16]. Thus, the detector (local sensing) or the FC (cooperative sensing) declares H_1 if $\Lambda(y) > \lambda$ and declares H_0 otherwise. The design in the presence of possible channel errors has been previously addressed under the NP criterion [91] where it is shown that the optimal decision rule that maximizes the P_d for fixed P_f at the FC is the NP. Furthermore, it is shown that, in the case of noisy channels, the decision made by each SU will depend on the reliability of the corresponding transmission channel. Moreover, the P_f at the FC is restricted by the channel errors. For a given decision rule, the probability of any channel being in error must be kept at a certain level in order to achieve a desired probability of false alarm at the FC.

In a Bayes test, the objective is to minimize the expected cost called the Bayes Risk by declaring H_i when H_j is true. In other words, the Bayes risk to be minimized is the sum of all possible costs weighted by the probabilities of two incorrect detection cases (P_f and P_m) and two correct detection cases. The LRT of a Bayes test can be represented as

$$\Delta(y) = \frac{f(y|\mathrm{H}_1)}{f(y|\mathrm{H}_0)} \gtrless_{\mathrm{H}_0}^{\mathrm{H}_1} \lambda \frac{P(\mathrm{H}_0)(\mathrm{C}_{10} - \mathrm{C}_{00})}{P(\mathrm{H}_1)(\mathrm{C}_{01} - \mathrm{C}_{11})} = \lambda \tag{3.2}$$

Thus, the detector or the FC can minimize the Bayes Risk by declaring H_1 if $\Delta(y) > \lambda$ and declaring H_0 otherwise.

3.2.System Model

For the purpose of this chapter, we consider a CR network that consists of a source PU, N single antenna SUs, an FC and wireless channels (reporting, sensing and inter-user channels) where transmission occurs over two phases. We will consider optimizing the second phase of transmission where the SUs make use of the reporting channels to send their sensing decisions to the FC. Assume that N SU nodes are separated into a group of clusters based on their geographical proximity, where each cluster is composed of two nodes to ease computational complexity (as shown in fig 3.1) and form a virtual MIMO array. Differential space-time coding (DSTBC) for a two-to-one scenario can then be applied to exploit spatial diversity and improve performance.

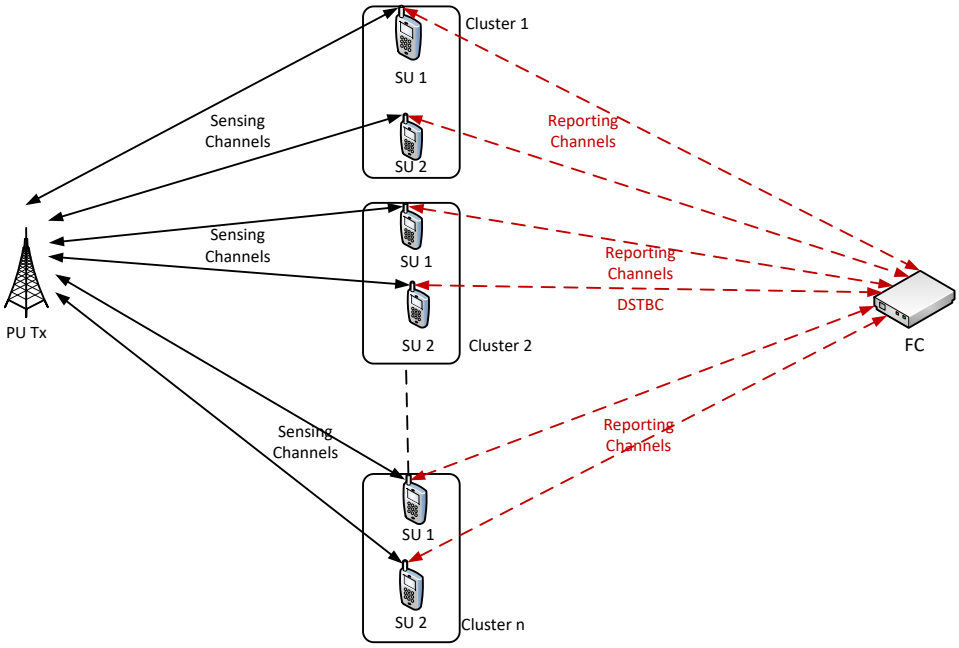

Fig. 3.1 CR Network model showing CR clusters

Assume that the wireless links between the SUs and the FC are independent flat fading Rayleigh channels and as such, received signals for each CR are conditionally independent and identically distributed (i.i.d.) under each hypothesis. Thus, the detector or the FC can minimize the Bayes Risk by declaring H_1 if $\Lambda(y) > \lambda$ and declaring H_0 otherwise.

3.2.1. Local Spectrum Sensing

In order to counter the problem of coherent detection, non-coherent CSS detection can be achieved optimally with the use of energy-detectors [4], [6], which begins with a three-step process controlled by the FC. Recalling from chapter 2, the FC selects a licensed frequency and sends an instruction to all SUs to begin "*local sensing*", a binary hypothesis testing problem denoted as

$$y(t) = \begin{cases} \sum_{i=1}^{m} n_i(t) & H_0 \\ \sum_{i=1}^{m} h_i(t)s_i(t) + n_i(t) & H_1 \end{cases} \tag{3.3}$$

Where $y(t)$ = Received signal at the CR user

$n_i(t)$ = Additive white Gaussian noise (AWGN)

$s_i(t)$ = The transmitted PU signal

$h_i(t)$ = The channel gain of the sensing channel

D_0/D_1 = Absence/Presence of the PU signal in the frequency band of interest

Using energy-detectors, each SU collects the relevant information on the spectrum and calculates the individual sensing statistic over a sensing duration independently. Recall that E_i represent the output of the energy detector for the ith SU and that there are $2m$ samples over each sensing duration T_s, according to [15], E_i follows a central chi-square distribution with $2m$ DoF if H_0 is true; otherwise E_i would follow a non-central chi-square distribution with $2m$ degrees of freedom. That is

$$E_i \sim \begin{cases} \mathcal{X}^2_{2m} & , \quad H_0 \\ \mathcal{X}^2_{2m}(2\gamma_i) & , \quad H_1 \end{cases} \tag{3.4}$$

Where $\gamma_i = |h_i(t)|^2 E_s/\sigma_i^2$ Instantaneous SNR of the ith SU;

$E_s = \sum_{k=1}^{2m}|x(k)|^2$ Transmit energy during each sensing;

$m = T_s B$ Is the time-bandwidth product

When the detecting channels follow Rayleigh distribution, the P_d, P_f and P_m for the local SS at a single SU under Rayleigh fading are given respectively as [15],

$$P_d = Prob\{Y > \boldsymbol{\lambda} | H_1\} = \frac{\Gamma(\frac{m}{2}, \frac{\lambda}{2 + 2\gamma})}{\Gamma(\frac{m}{2})} \tag{3.5}$$

$$P_f = Prob\{Y > \boldsymbol{\lambda} | H_0\} = \frac{\Gamma(\frac{m}{2}, \frac{\lambda}{2})}{\Gamma(\frac{m}{2})} \tag{3.6}$$

$$P_m = 1 - P_d$$

where λ = threshold value of the energy detector,

Γ = complete gamma function

Then the complementary ROC curves can be given to describe the performance of energy detector for the different values of average SNR and *m*.

3.2.2. Performance Limits of Cooperative Spectrum Sensing

It is impossible to transmit the decisions in practice without errors over the wireless channels. For example, when one SU reports a sensing result denoting the presence of the PU to the FC through a realistic fading channel, the common receiver will likely detect it to be the opposite result (i.e. denoting the absence of the PU) because of the disturbance from the random complex channel coefficient and CSI estimation errors. Eventually, the performance of CSS will be degraded by error reporting channels [80]. The performance of CSS is evaluated by taking the $P_{e,i}$, defined as the error probability of signal transmission over the reporting channels between the ith CR and the FC, into full consideration.

Recalling (2.15) and (2.16), Q_f and Q_m can then be given as,

$$Q_f = 1 - \prod_{i=1}^{K}\left[\left(1 - P_{f,i}\right)\left(1 - P_{e,i}\right) + P_{f,i}P_{e,i}\right], \tag{3.7}$$

$$Q_m = \prod_{i=1}^{K}\left[P_{m,i}\left(1 - P_{e,i}\right) + \left(1 - P_{m,i}\right)P_{e,i}\right], \tag{3.8}$$

Where $P_{f,i}$ and $P_{m,i}$ are the false alarm probability and missed detection probability of the local SS of the ith CR, respectively.

Suppose that every CR has an identical local SS performance and experiences identical but independent reporting errors such that $P_{e,i} = P_e, \forall_i = 1,2\ldots\ldots, K$

The false alarm probability is lower bounded by $\bar{Q}_f$ such that

$$Q_f \geq \bar{Q}_f = 1 - (1 - P_e)^K \tag{3.9}$$

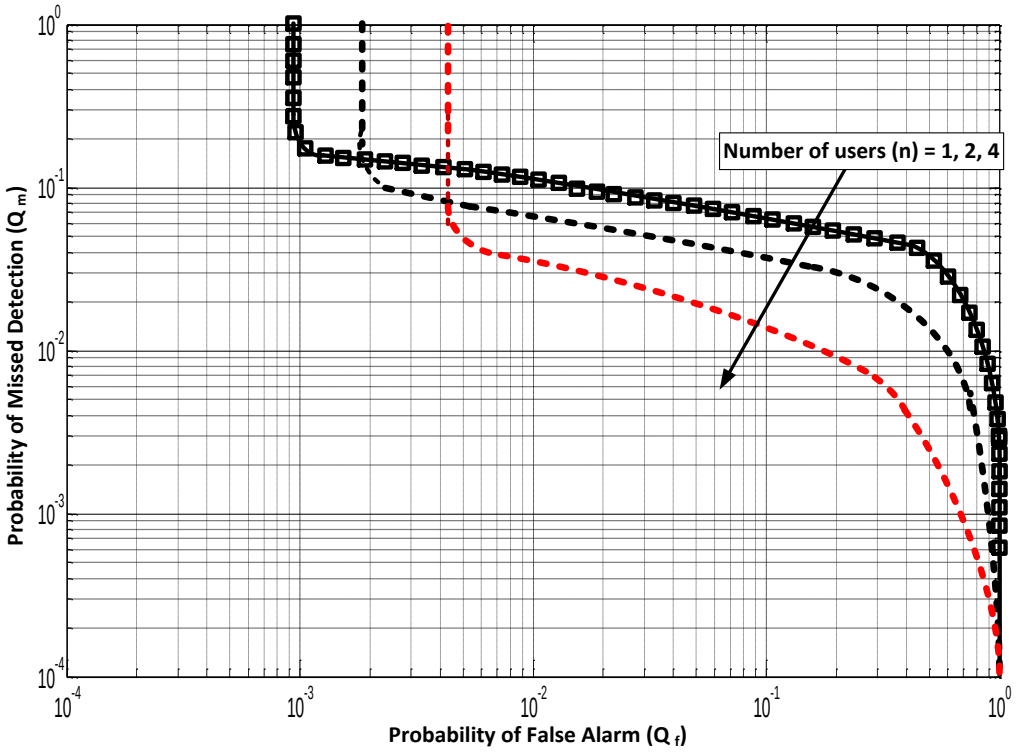

Fig. 3.2: Performance of Cooperative Spectrum Sensing for different number of SUs $n = 1,2,4$ with SNR $\gamma_i = -1dB$ and reporting error rate $P_e = 0.001$

For a very small step P_e, the bound reduces to $Q_f \geq KP_e$

It is also assumed that the local SS conducted by CR i results in the very ideal scenario of $P_{f,i} = P_f$ and $P_{m,i} = P_m = Pm$, for all $i = 1, \ldots\ldots, K$, and that the P_e is identical for all CRs. The ideal scenario is considered for the purpose of this research work. Furthermore, Q_f is bounded by $Q_f \geq \bar{Q}_f \triangleq lim_{P_f \to 0} Q_f$

The performance of CSS with respect to the number of CRs for an SNR $\bar{\gamma} = 1dB$ and $P_e = 0.001$ has been simulated to show that the higher number of cooperating SUs diminishes performance.

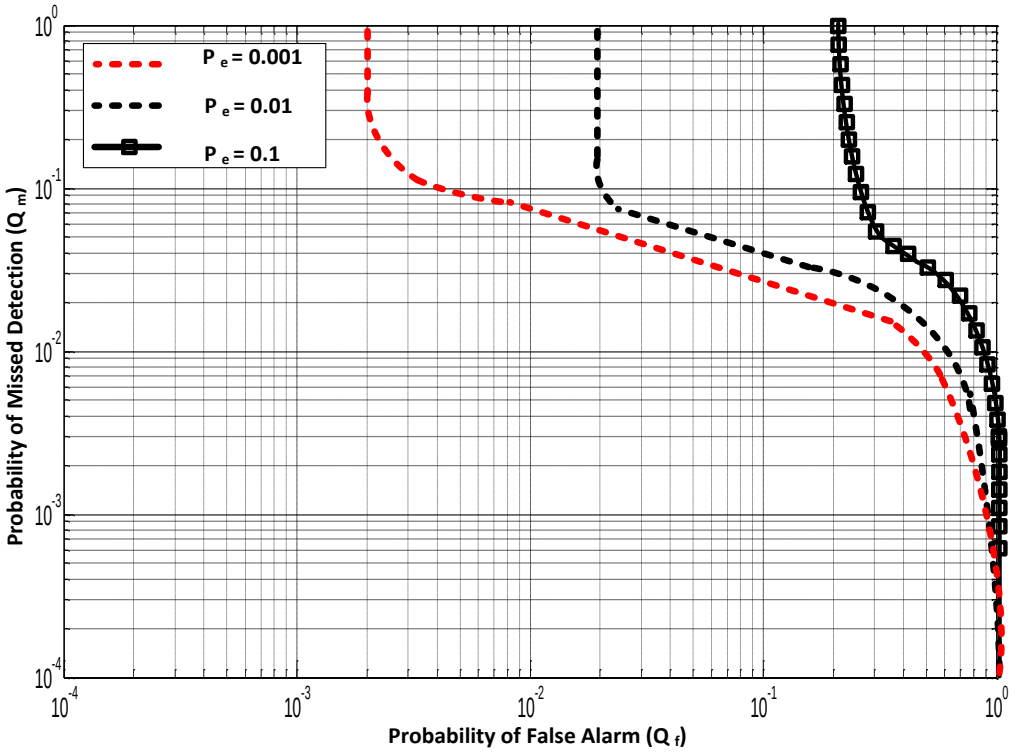

Fig. 3.3: Performance of Cooperative Spectrum Sensing for $n = 2$ with SNR $\gamma_i = -1dB$ and different values of reporting error rates P_e

For two SUs, the performance of $Q_f$is slightly higher than four SUs (as seen in fig 3.2). However, Q_m will increase when Q_f decreases to the lower bound $\overline{Q}_f$. Equivalently, the

probability of detection Q_d will quickly fall down to zero. Thus, CSS will be impractical when $Q_f \rightarrow \bar{Q}_f$. Moreover, $\bar{Q}_f$ increases with the increased number of CRs. Fig. 3.3 compares the performance results under different probabilities of reporting errors for two CRs and $\bar{\gamma} = 1dB$. Fig 3.3 shows that the larger P_e is, the larger the bound of Q_f. Given that Q_f is the probability that the FC erroneously reports the presence of the PU while it is in fact absent, the graphs clearly show that a larger value of P_e signifies a higher probability that the licensed frequency band will be vacant but not utilized. This can lead to significant loss of bandwidth efficiency loss. From Fig. 3.3, it can be concluded that the bandwidth efficiency loss increases with the increase of P_e.

3.3.Differential Space-time Block Codes on the Reporting Channels

The second-step involves each SU reporting a binary *local sensing* decision to the FC via the *reporting channel*. Assuming that D_0 and D_1 denote the local sensing decision from SU1 and SU2 respectively. In order to implement differential STBC, SU1 and SU2 are coordinated to form an array cluster where they can exchange their decisions and send these decisions to the FC (as seen in Fig 3.1).

3.3.1. Differential Encoding

For a single transmit antenna, differential schemes such as differential phase-shift keying (DPSK) exist that do not require knowledge of channel/ pilot symbol transmission. Such schemes have found applications in scenarios such as the one employed in the IEEE's IS-54 standard. Extensions of these differential schemes have been considered to provide simple differential encoding and decoding algorithms to either MIMO or virtual MIMO systems [84], [86]. The key to generating these codes depends on computing a set of coefficient vectors (R_1, R_2) and mapping a block of information bits into the coefficient vector sets.

Although not very realistic in practice, we assume inter-user interference between SUs in each cluster is negligible; then the SUs can exchange their decisions and send these decisions to the FC [6]. This assumption is made in order to lessen the computational complexity that would otherwise be incurred if inter-user interference is taken into consideration. Also ssuming message exchange among the nodes is perfect due to geographical proximity, D-STBC has been applied so that signal transmission begins by sending an arbitrary pair of signals D_{s0} and D_{s1} at time t_1 simultaneously from the two SUs, followed by the related pair of signals $-D_{s1}^*$ and D_{s0}^* at time t_2. These two transmissions do not carry any data but rather, provide the Rx with a known *frame of reference* for facilitating the D-STBC process.

The SU's encode the data sequence in a differential manner so that the signals to be transmitted are subsequently represented as linear overlays of those times at t_1 and t_2, thus generating (D_{s0-1}, D_{s1}) and $(-D_{s1}^*, D_{s0-1}^*)$ from the two SUs at times $2t-1$ and $2t$. With information bits D_0, D_1 at the encoder used to select (R_1, R_2), the modulated symbols for the next two transmissions are given as

$$\{D_0, D_1\} = R_1(D_{s0-1}, D_{s1}) + R_2(-D_{s1}^*, D_{s0-1}^*) \tag{3.10}$$

This process is mapped into the coefficient vector sets and inductively repeated until the end of the frame, the mapping process computing the transmitted symbols for different combinations of decision statistics until the end of the transmission.

3.3.2. Differential Decoding

For the sake of simplicity, we assume that only one Rx antenna is employed which is the FC in this case. The received data are processed by computing the differential phases between any two consecutive symbols. The differential phases are given by

$$\hat{\theta}_t = arg\, r_{t-1}^* r_t \tag{3.11}$$

Since $e^{j\theta_t} = e^{\frac{2\pi c_t}{M}}$ and $c^t = \frac{M\hat{\theta}_t}{2\pi}$; the decision rule can be formulated as follows

For $i - 1/2 \leq \frac{M\hat{\theta}_t}{2\pi} \leq i + 1/2, \quad \hat{c}_t = i$ (3.12)

Where $\hat{c}_t$ is the estimate of the transmitted data symbol c_t and $i \in \{0,1,2\ldots\ldots\ldots, M-1\}$.

The following parameters are defined as follows

$r_t =$ Received signal at time t

$n_t =$ Noise sample at time t,

$h_1, h_2 =$ Fading coefficients from transmit antennas one and two to the receive antenna. Let

$$H = \begin{pmatrix} h_1 & h_2^* \\ h_2 & -h_1^* \end{pmatrix} \quad (3.13)$$

and

$$N_{2t-1} = (n_{2t-1}, n_{2t}^*)$$

$$N_{2t} = (n_{2t}, -n_{2t-1}^*)$$

The vector representation of the received signals are given as

$$(r_{2t-1}, r_{2t}^*) = (D_{0i-1}, D_{1i}) \cdot H + N_{2t-1} \quad (3.14)$$

$$(r_{2t}, r_{2t-1}^*) = (-D_{1i}^*, D_{0i-1}^*) \cdot H + N_{2t} \quad (3.15)$$

A decision statistics $\widehat{R}_1$, at the FC is defined as the inner product of the two received signal vectors in (3.12) and (3.13).

$$\widehat{R}_1 = r_{2t+1} r_{2t-1}^* + r_{2t+2}^* r_{2t} \quad (3.16)$$

From [17] and [18], (3.14) can be rewritten as

$$\widehat{R}_1 = (|h_1|^2 + |h_2|^2) R_1 + N_1 \quad (3.17)$$

Similarly, another decision statistic can be defined as the Inner product of the received signals in (3.12) and (3.13) as

$$\widehat{R}_2 = (|h_1|^2 + |h_2|^2) R_2 + N_2 \quad (3.18)$$

These two decision statistics can summarized as follows

$$(\widehat{R}_1, \widehat{R}_2) = (|h_1|^2 + |h_2|^2)(R_1, R_2) + (N_1, N_2) \quad (3.19)$$

The ML decoder then chooses the closest coefficient vector to the decision statistics $(\widehat{R}_1, \widehat{R}_2)$ and inverse mapping is applied to decode the transmitted block of bits (D_0, D_1) [92], [93].

3.4.Fusion Centre

After NP hypothesis testing is complete, the FC combines all the local sensing information, determines the presence or absence of a PU and diffuses the decision back to the SUs. When local decisions are reported to the FC, it is convenient to apply linear fusion rules to obtain the cooperative decision. In general, the sensing results reported to the FC will be combined using *Soft Combining* and *Hard Combining* in descending order of demanding channel bandwidth [94], [95].

- Hard Combining

The three decision rules used include *AND, OR,* and *MAJORITY* rules [31]. Consider all the individual test statistics Δ_N given as either a 1 or 0 as the hard decision from FC, with the *AND* rule stating that a signal is present if ***all*** users have detected a signal i.e.

$$H_1: \sum_{i=1}^{N} \Delta_N = K$$

$$H_0: otherwise \tag{3.20}$$

The *OR* rule states a signal is present if ***any*** of the users detect a signal i.e.

$$H_1: \sum_{i=1}^{N} \Delta_N \geq 1$$

$$H_0: otherwise \tag{3.21}$$

The *MAJORITY* rules is a voting rule which decides the presence of a signal if a minimum of M out of the N users have detected a signal where $1 \leq M \leq N$, i.e.

$$H_1: \sum_{i=1}^{N} \Delta_N \geq M$$

$$H_0: otherwise \tag{3.22}$$

It can thus be said that the cooperative sensing probabilities of detection Q_d, false alarm Q_f and missed detection Q_m can be represented by (3.7) and (3.8) and as follows:

$$Q_d = 1 - \prod_{i=1}^{N} \left[P_{d,i} P_{e.i} + \left(1 - P_{d,i}\right)\left(1 - P_{e.i}\right) \right] \tag{3.23}$$

- Soft Combining

In soft data fusion, CR users forward the entire local observations or test statistics E_k to the FC without performing any local decision and the decision is made by combining these results at the FC by using appropriate combining rules such as square law combining (SLC), MRC and selection combining (SC). Soft combination provides better performance than hard combination, but it requires a larger bandwidth for the control channel [49]. It also generates more overhead than the hard combination scheme [53].

Square Law Combining (SLC) is one of the simplest soft combining schemes, where the outputs of the square-law devices (i.e. the estimated energies) are sent to the FC to be added to yield a new decision statistic. The decision is carried out in the FC when the summation is compared to a threshold to decide on the existence or absence of the PU [51]:

$$E_{slc} = \sum_{k=1}^{K} E_k \tag{3.24}$$

Where E_k denotes the statistic from the kth CR user. The detection probability and false alarm probability are formulated as follows [52]:

$$Q_{d,\ slc} = Q_{mK}\left(\sqrt{2\gamma_{slc}}\sqrt{\lambda}\right) \tag{3.25}$$

$$Q_{f,\ slc} = \frac{\Gamma(mK,\ \ \lambda/2)}{\Gamma(mK)} \tag{3.26}$$

Where $\gamma_{slc} = \sum_{k=1}^{k} \gamma_k$ and γ_k is the received SNR at the kth CR user.

The difference between the MRC method and the SLC is that the energy received at the FC from each user is pondered with a normalized weight which depends on the received SNR of the different CR users, before being added. The statistical test for this scheme is given by:

$$E_{mrc} = \sum_{k=1}^{K} w_k E_k \tag{3.27}$$

The probabilities of false alarm and detection over Rayleigh channels can be given as

$$Q_{d,\ mrc} = Q_m\left(\sqrt{2\gamma_{mrc}}\sqrt{\lambda}\right) \tag{3.28}$$

$$Q_{f,\ mrc} = \frac{\Gamma(m,\ \ \lambda/2)}{\Gamma(m)} \tag{3.29}$$

Where $\gamma_{mrc} = \sum_{k=1}^{k} \gamma_k$

In Selection Combining (SC), the FC selects the branch with highest SNR on a continuous basis aided by a time constant. $\gamma_{sc} = \max(\gamma_1, \gamma_2, \ldots\ldots \gamma_k)$

Thus, the probabilities of false alarm and detection over Rayleigh channels can be given as

$$Q_{d,\ sc} = Q_m\left(\sqrt{2\gamma_{sc}}\sqrt{\lambda}\right) \tag{3.30}$$

$$Q_{f,\ sc} = \frac{\Gamma(m,\ \ \lambda/2)}{\Gamma(m)} \tag{3.23}$$

Equal Gain Combining (EGC) is the simplest technique in terms of complexity of implementation. Similar to MRC, all weights are equal but co-phasing is still required to produce acceptable outputs from the FC. Of all the combination schemes, EGC has generated the least amount of research interest owing to the difficulty of finding the probability density function (PDF) of its output SNR.

3.5.Simulation Results and Numerical Analysis

The PU is assumed to be transmitting a signal in the frequency range between 470MHz and 710MHz whose bandwidth is 6MHz; modulation type is BPSK, code rate of ½, bit rate of the system being $f_s = 27$ Mbit/s with a transmission power of 20dB. The average occupancy rate for the PU is set to 50% i.e. the probability of presence and absence of the PU signal is fixed to an equal probability (0.5), respectively. A Rayleigh channel is considered and a cluster of pairs of SUs are distributed randomly within a 500m-by-500m region. The SU's employ ED to perform spectrum sensing with the received SNR γ_i of each SU's detector set around -1dB, with the channel having a noise floor of -10dB and a local sensing time of $25\mu s$. The simulation is based on Monte Carlo method with 1,000,000 iterations.

The simulation results presented in this section demonstrates that this work achieves full transmit diversity as well as improvements in detection performance through the ROC curves in relation to SNR.

3.5.1. Probability of Reporting Errors

Decision reporting to the FC is only able to employ transmit diversity based on the quality of the inter-user channel i.e. the channel between the SUs. Ideal conditions are thus assumed for the inter-user channel so that the SUs can always correctly decode their exchanged signals for DSTBC reporting to be implemented. Fig.3.4 below shows performance comparison of CSS with DSTBC reporting for two CRs against STBC reporting at SNR $\gamma_i = 5dB$, where the reporting channels are subjected to reporting errors.

CSI has to be estimated before detection of the transmitted symbols can take place. In practice however, channel estimators cannot provide perfect CSI and the resulting channel estimation errors will cause a degradation of reporting performance [79], [80]. From fig. 3.4 above, it is seen that the bandwidth efficiency is increased because of the obvious diversity

gain achieved as well as the negation of CSI estimation errors (channel estimation error reduces the effective SNR and causes saturation).

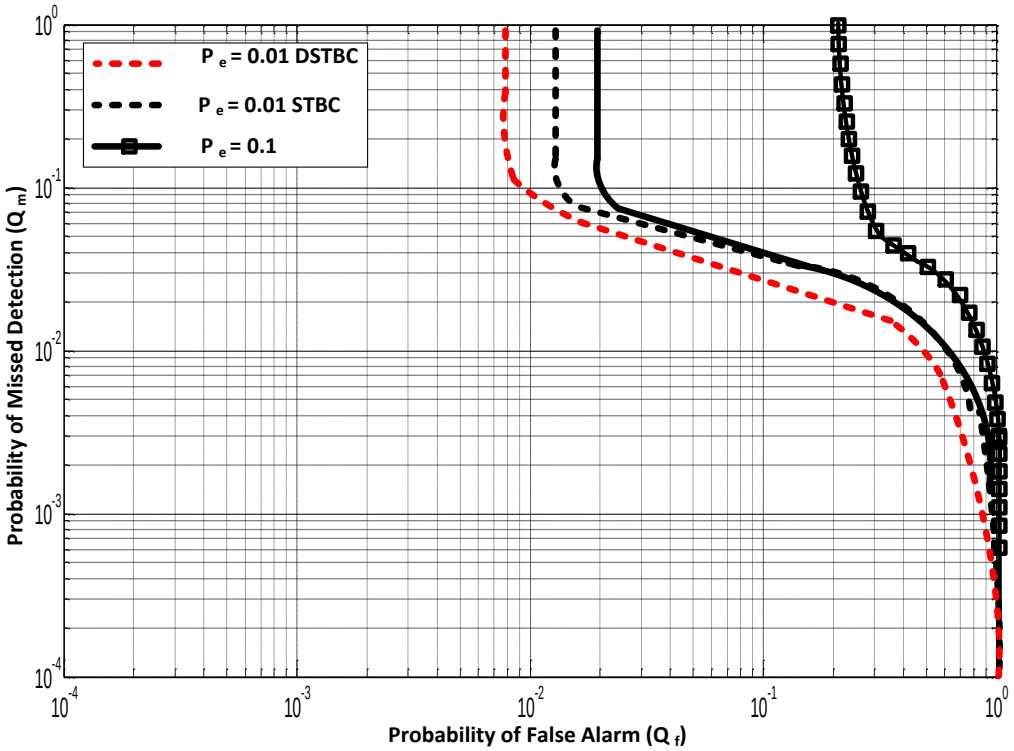

Fig. 3.4: Performance of Cooperative Spectrum Sensing for $n = 2$ with SNR $\gamma_i = -1dB$ and different values of reporting error rates P_e

Also, Q_f of DSTBC reporting is bounded, implying that even with the expected loss of 3dB, DSTBC reporting provides a slightly upper bound of performance compared with STBC reporting. It can thus be concluded that with the increase of *N*, the bound of Q_f will only increase.

3.5.2. Diversity Gain

Fig. 3.5 illustrates the bit-error-rate (BER) simulated performance of the differential scheme over Rayleigh fading channels with the two SUs sending their sensing decisions to the FC. The results for BPSK constellations are illustrated for non-coherent spectrum sensing without diversity, with STBC diversity and with DSTBC diversity. The performance curve of the

DSTBC scheme follows the same pattern to the one with STBC schemes implying that the orthogonality of the differential schemes also provides full transmit diversity. However at the threshold BER of 10^{-3}, the DSTBC scheme has an approximate 3dB loss when compared to the STBC scheme. This can be attributed to the fact that neither the SUs nor the FC requires CSI, hence the degraded performance [94].

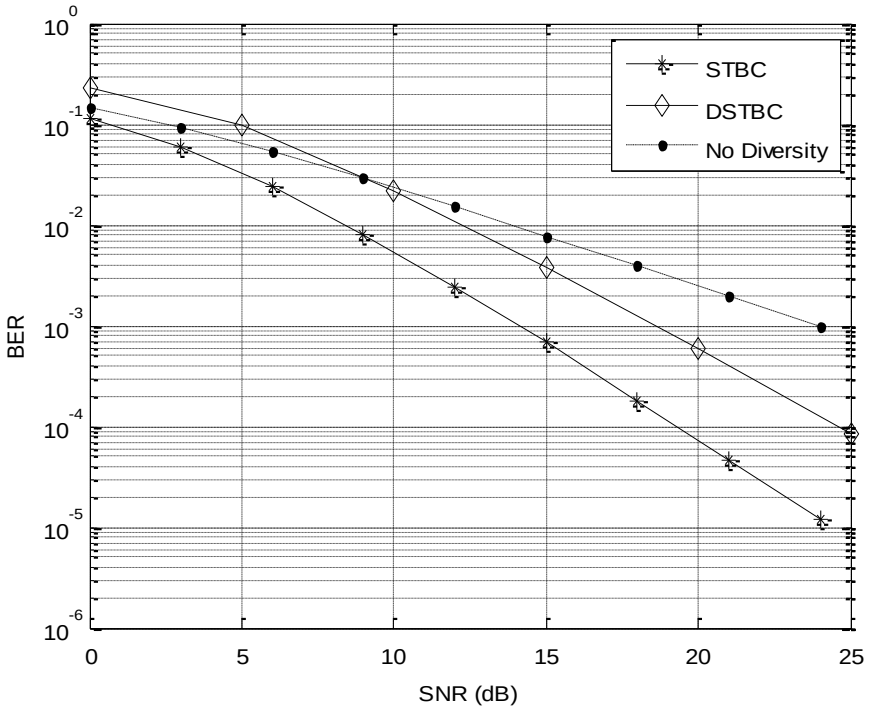

Fig. 3.5: Performance comparison of CSS with STBC and with differential-STBC

3.5.3. Hard Combination

For the hard combination decisions, we present the ROC curves for the *AND* rule in Fig.3.6 and the *OR* rule in Fig. 3.7 respectively. In Fig. 3.6, the cooperative sensing probability of detection Q_d is plotted against the cooperative sensing probability of false alarm Q_f for three clusters i.e. 6 nodes respectively firstly under ideal conditions (i.e. error-free reporting), then without D-STBC reporting and with D-STBC reporting. Additional simulations are carried out for four and five clusters with D-STBC reporting, of which their ROC curves are also

plotted. All simulations are carried out and with a locally received SNR γ_i of $-10dB$ at each SU node.

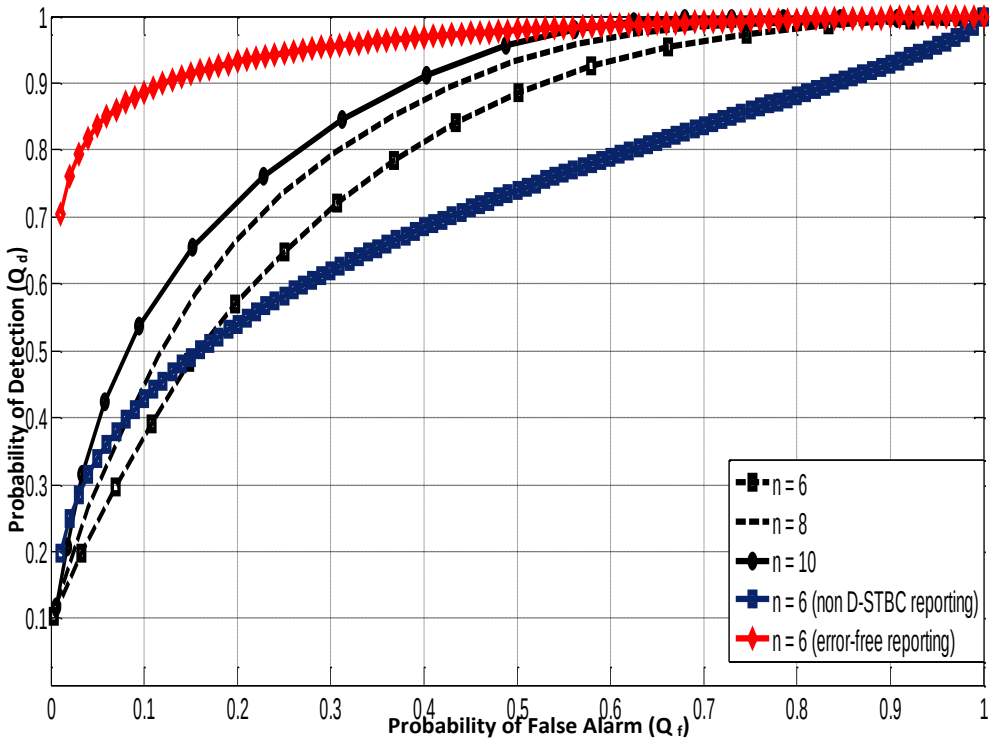

Fig. 3.6: Performance of Cooperative Spectrum Sensing with differential-STBC (n=6, 8 and 10) with SNR γ_i= 5dB for *AND* fusion rule.

The work done in [94] shows that for error-free reporting channels, the ROC curves for *OR* combination rule at an average received SNR of 5dB outperforms *AND* rule. However, with channels under deep fading, the relative performance of these rules can be quite varied.

For 3 clusters each having a local SNR γ_i of 5dBm, the *AND* rule's performance is below that of *OR* fusion. However, the comparative performance of CSS with diversity in [94] showed better performance than [80] for both the *OR* as well *AND* rules at $\gamma_i = 5dB$.

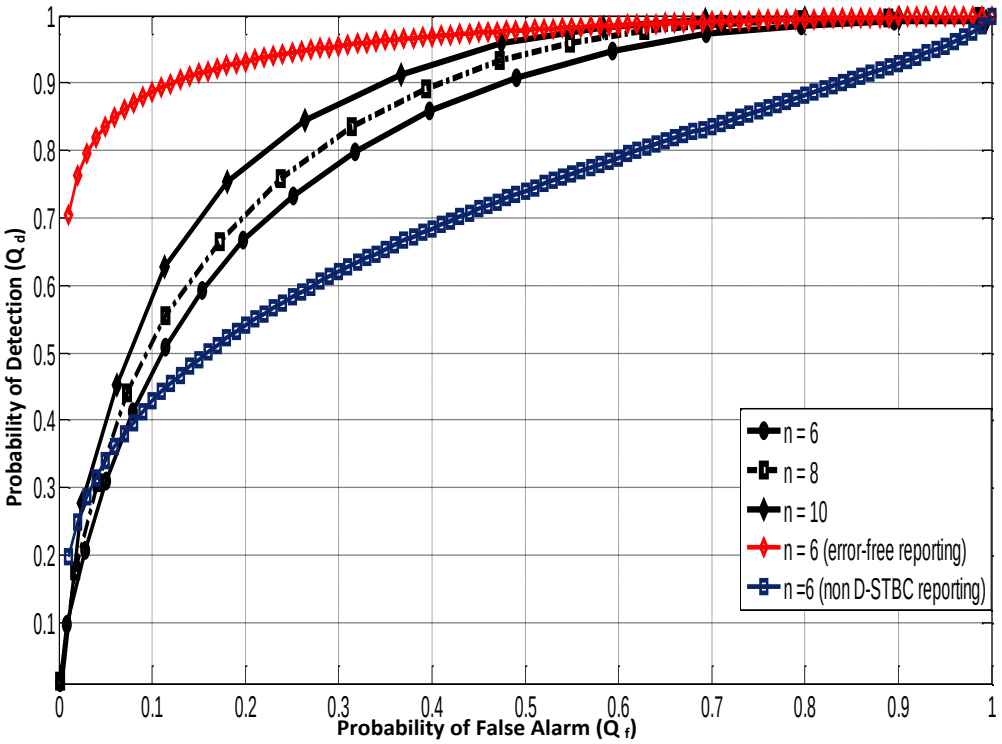

Fig. 3.7: Performance of Cooperative Spectrum Sensing with DSTBC (n=6, 8 and 10) with SNR γ_i= 5dB for *OR* fusion rule.

For this work, it can be seen that the performance curves of DSTBC reporting are worse than the ideal curves but generally better than the performance of non-DSTBC reporting. It can be observed for example that at Q_f =0.1, the probability of detection for 3 clusters is approximately 0.35 for CSS with DSTBC. Even with the low SNR values γ_i and expected performance degradation of DSTBC, its performance is just slightly worse than that of non-DSTBC reporting with *AND* fusion rule under the same conditions. It can also be seen that the sensing performance increases as the number of cooperative nodes/clusters increases, which is consistent [84], [94]. Similarly, in Fig. 3.7, the performance curves for the *OR* fusion rule are plotted at an average SNR $\gamma_i$value of $5dB$ for 3 clusters with DSTBC and without DSTBC reporting respectively.

When Rayleigh fading is considered, the work in [80] uses orthogonal channels based on TDMA for diversity to forward decisions to the FC. Comparing the results in [80] with the results in this work, it can be seen in Fig. 3.7 that the DSTBC CSS scheme performs better despite the lower values of γ_i . With regards to this work, it was observed that the performance curves for non-DSTBC reporting initially outperform the DSTBC reporting scheme, albeit for a very short period of time.

The DSTBC scheme evidently has significant performance gains. For example, for 3 clusters, at $Q_f = 0.1$, P_e is about 0.45 for D-STBC reporting, while it is less than 0.4 for non-DSTBC reporting. These results are consistent with the fact that *OR* fusion rule generally performs better than *AND* fusion, especially in cases of practical interest. It can also be seen that the sensing reliability increases as nodes increases.

Due to the orthogonality between the sequences coming from the two transmit antennas, this scheme can achieve the full transmit diversity, despite the fact that the CSI is not available at the nodes [93]. Therefore, by exploiting DSTBC among nodes in a cluster, the sensing performance can significantly be improved for the reporting channel.

3.5.4. Soft Combining

For the soft combination decisions, we present the ROC curves for the *EGC* rule in Fig.3.8 and the *MRC* rule in Fig. 3.9 respectively. In Fig. 3.8, the cooperative sensing probability of detection Q_d is plotted against the cooperative sensing probability of false alarm Q_f for three clusters i.e. 6 nodes respectively firstly under ideal conditions (i.e. error-free reporting), then without D-STBC reporting and with D-STBC reporting. Additional simulations are carried out for four and five clusters with D-STBC reporting, of which their ROC curves are also plotted. All simulations are carried out and with an SNR γ_i of $-10dB$ at each SU node.

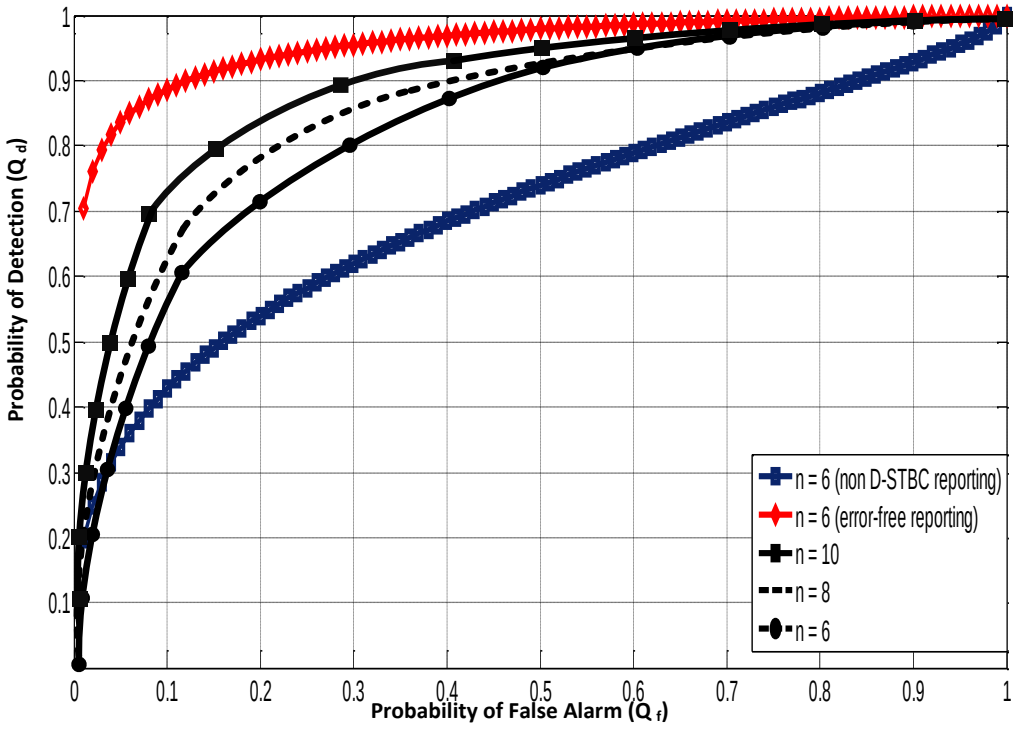

Fig. 3.8: Performance of Cooperative Spectrum Sensing with differential-STBC (n=6, 8 and 10) with SNR $\gamma_i = 5dB$ for *EGC* fusion rule.

The work done in [34] shows that for error-free reporting channels, the ROC curves for *EGC* combination rule at an average received SNR of 5dB outperforms *the hard combination rules*. For this work, it can be seen in Fig. 3.8 that the performance curves of DSTBC reporting CSS are not as good as the ideal curves but generally better than the performance of non-DSTBC reporting for *AND* fusion.

It can be observed for example that at Q_f =0.1, the probability of detection for 3 clusters is approximately 0.55 for CSS with DSTBC. It can also be seen that the sensing performance increases as the number of cooperative nodes/clusters increases, which is consistent [84], [94].

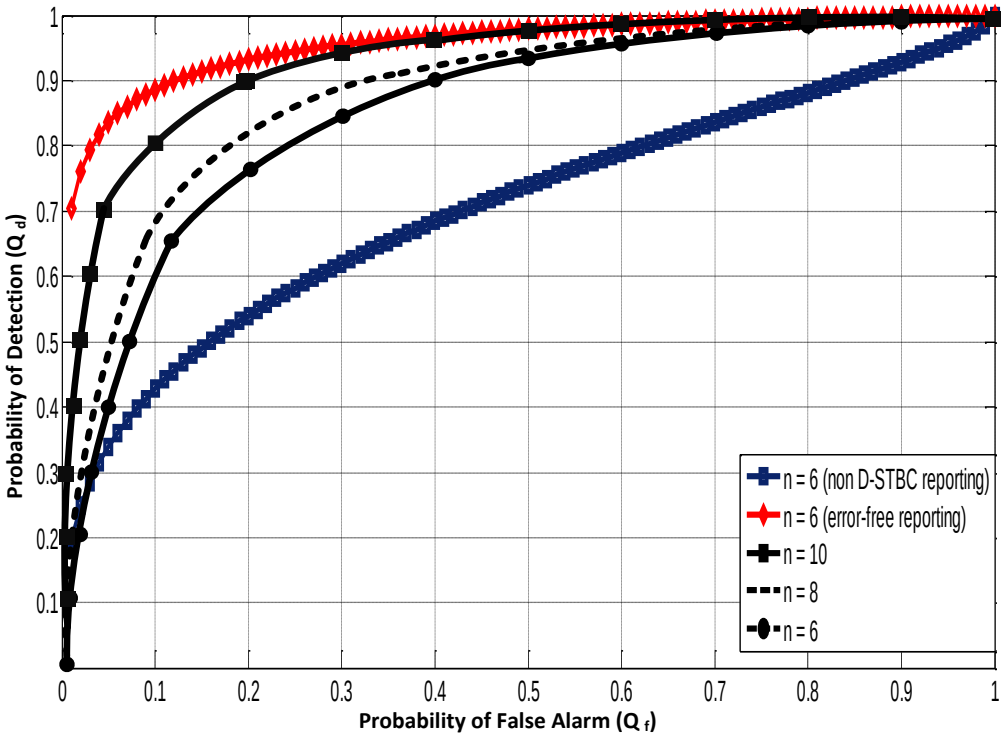

Fig. 3.9: Performance of Cooperative Spectrum Sensing with differential-STBC (n=6, 8 and 10) with SNR γ_i= 5dB for *MRC* fusion rule.

Similarly, in Fig. 3.9, the performance curves for the *MRC* fusion rule are plotted at an average SNR $\gamma_i$value of -10dB for 3 clusters with DSTBC and without DSTBC reporting respectively.

The overall performance is just slightly worse than that of error-free reporting, even though channel conditions are ideal in the case of error-free reporting. Comparing the results in [80] with the results in this work, it can be seen in Fig. 3.9 that the DSTBC CSS scheme performs better despite the lower values of γ_i as the MRC is able to maximize SNR at the output of the combiner. The DSTBC scheme evidently has significant performance gains. For example, for 3 clusters, at $Q_f = 0.1$, the probability of detection is about 0.60 for DSTBC reporting, while it is approximately 0.4 for non-DSTBC reporting. These results are consistent with the fact

that *MRC* fusion rule generally out performs EGC fusion, although in cases of practical interest, it is difficult to implement MRC due to its inherent implementation complexities. It can also be seen that the sensing reliability increases as nodes increases. Due to the orthogonality between the sequences coming from the two transmit antennas, this scheme can achieve the full transmit diversity, despite the fact that the CSI is not available at the nodes [93]. Therefore, by exploiting DSTBC among nodes in a cluster, the sensing performance can significantly be improved for the reporting channel.

3.6.Summary and Conclusion

This work has presented a DSTBC cooperative sensing scheme in order to improve overall sensing performance of CR networks by improving performance of non-ideal reporting channels under deep fading conditions. Firstly, it was shown through simulation results that DSTBC follows the same pattern in terms of BER performance, proving that it can also achieve full transmit diversity, albeit at the cost of approximately 3dB loss for DSTBC. Secondly, it was again shown through simulation results that despite not having prior knowledge of the reporting channel, DSTBC reporting with hard fusion rules *(OR/AND)* outperformed typical non-DSTBC reporting under the same conditions for various number of CR clusters. Therefore, not only can cooperative sensing be implemented with DSTBC, but its performance was shown to increase as the number of CR nodes increasers and at higher SNR. Thirdly, employing the *OR* fusion rule showed in simulations results significantly better performance than the *AND* fusion rule, making it the preferred option for future endeavors.

Further simulations results were presented which compared the soft fusion rules, and as was expected, the MRC fusion showed higher performance gain compared to the EGC rules.

These results were obtained without taking the overheads introduced by soft fusion rules into consideration, therefore both hard fusion remain the optimal solutions.

Given the fact in the presence of non-ideal reporting, the performance differential between the hard combinations rules do not always follow convention [35], i.e. the OR rule does not always outperform the AND rule in the presence of errors. With the introduction of DSTBC, the pattern of performance was seen to be restored, implying that the diversity gain achieves its main objective.

Possible future work to this scheme includes taking path losses between CR nodes in a cluster into consideration. Also employing techniques that can achieve full diversity when linear receivers, such as zero-forcing (ZF) and minimum mean square error (MMSE) receivers are used could also be considered in future research work.

It very clear that the number SUs in a cluster have been limited due to huge overheads and complexities a higher number of SUs will introduce into to the overall system model. In practice however, a higher number of SU nodes will introduce higher order block coding will which actually help to improve performance [84], [85]. There is thus a compelling reason for a higher number of SU to be considered as a vital part of the future work on this novelty.

A significant part of this Chapter has been published in the proceedings of the 26th IEEE Annual Symposium on Personal, Indoor and Mobile Radio Communications (PIMRC) held in September, 2015 in Hong Kong, China (http://ieeexplore.ieee.org/document/7343515/).

4. Space-Time Opportunistic Interference Alignment in Cognitive Radio

4.1.Introduction

The previous chapter has provided both the description and analysis of a technique used to optimize the performance of *reporting channels*. It is therefore appropriate that subsequent objectives of this research work focus on optimizing the performance of *sensing channels* used in CSS. As previously discussed, the increased deployment of wireless services is not the main reason for the greater scarcity of the licensed frequency spectrum, but rather the under-utilization of the licensed spectrum due to the FSA policy. In recent times, CR technology whose main idea is based on the DSA policy has emerged as the technology for meeting this under-utilization of the licensed spectrum [15], [91]. The CRs sense for spectrum holes in the licensed spectrum and make use of these spectrum holes either in an opportunistic or concurrent manner, as long as the PU transmission can be protected [15], [91]. Since the SU transmission is considered of a lower priority than that of the PU, a crucial task in the design of CR is about how best the SU can avoid interfering with the PU in their vicinity [15], [16] and [96]. In the present circumstances of wireless communications, the PU is seldom idle such that the availability of spectrum holes becomes very limited [97]. In trying to find solutions to this problem, IA has recently been considered as it tends to fit in with the CRs effort of managing interference between the PU and SU [17], [18] and [98].

The earliest work done to achieve IA in CR for the single-tier K-user IC developed a number of practical algorithms in the manner of message sharing between the PU and SU [19], [20], which have provided a significant research platform for continuous development of IA in CR. As a consequence, two main paradigms in the design of IA in CR networks have emerged, the first paradigm as mentioned earlier in Chapter 2 not being the main focus of this research, owing to the challenge involved in trying to detect the PU [11], [15] and [58]. The second

paradigm considers the same CR network, but the SUs are in closer proximity to the PU-Tx in the same manner of Indirect Spectrum Sensing where the SUs are required to detect the PU-Tx [11].

One of the earlier research studies done towards implementing this second paradigm was OIA [23], [24], where the PUs link makes use of a WF PA scheme to maximize its transmission over its SDs. In doing so, the PU leaves some of the SDs unused due to power limitations. Instead of sensing for spectrum holes, the SU-Tx senses for these unused SDs and opportunistically takes advantage of them with a linear pre-coder that aligns the transmission from the SUs with the unused SD thus avoiding any interference to the PUs transmission. As discussed in Chapter 2, the OIA solution was broken down into a 3-step process as follows: The first step involved the PU performing SVD on its MIMO channel and then applying a WF algorithm to maximize capacity of the MIMO channel leaving some unused SDs. These translate into TOs for the SUs. The second step involved the PUs computing these TOs while the SUs make use of a linear precoder that would enable them to align their transmission with the TOs, thus satisfying a zero-interference constraint to the PU-Rx. The third and final step involved optimizing the SUs transmission rates. Satisfying the zero interference constraint to the PU-Rx implies that opportunities for the IA algorithms [63], [65] used to improve overall performance of IA in CR are quite diminished. Alternatively, subsequent research such as the work done in [73], [75] as well as this research endeavor are focused on introducing novel techniques that will optimize each of the above mentioned steps used to implement the OIA. The work in this chapter also follows on the 3-step process of implementing IA in CR by performing SVD on the PUs channel matrices, but unlike the OIA solution [24], this chapter will maximize the channel capacity by using an alternative ST-WF owing to the research done in [77], which shows that ST-WF achieves higher capacity per antenna than SWF at low

to moderate SNR regimes [20]. One factor common with [24], [100] is that their models make use of a single-user MIMO SU link thus ignoring the effect of multiple SUs on the performance of a CR network. In fact, a single SU is unlikely to reliably detect the presence of a PU due to factors such as multipath fading impairments, low SNRs and sensing time constraints [30], [101]. Thus the work done in [75], [102] – [105] have considered implementation of multi-user MIMO SUs that employ CSS, a CR technique that caters for multi-path fading and the hidden node problem. The SUs individually perform *local sensing* in order to detect the absence or presence of the unused SDs by a binary hypothesis test and then report this information to the FC. The FC then makes a final decision based on its received information. In this work, this issue is addressed for a MIMO overlay cognitive system consisting of one PU link and multiple SUs. A technique similar to the OIA of [24] was then proposed, where the PU computes the TOs and the multiple SUs compute a linear precoder that would enable them align their transmission with the TOs.

The third and final step is optimization of the SUs transmission rates. While the OIA technique of [24] made use of an OPA/UPA to optimize transmission rate of the SU, this research introduced a novel technique that will enhance the UPA scheme to maximize the achievable transmission rate for the SUs opportunistic link. While the UPA/OPA schemes of [23] and [24] are very optimal in terms of transmission rates for a single user MIMO link, they will be more susceptible to noise impairments for multi-user SUs. They are also mostly useful for a higher number of antennas, which introduces higher computational complexity where IA is concerned. Hence this research will consider that the multiple SUs uses a TDMA mechanism and so channel reciprocity is assumed between the forward (Tx to Rx) and reverse (Rx to Tx) channels. Based on this, the SU receivers will periodically transmit

feedback through reverse channels in timeslots with channel parameters indicating a loss of fidelity or a change in the PUs transmission parameters.

It is worth noting that, although close in notion to the research done in [24], [75] and [100], this paper distinguishes itself in the following key aspects. Firstly, this work adopts an SVD scheme for the PU link that is based on the ST-WF technique to achieve better channel capacity from the PU. Secondly, the work done in [24], [98] and [100] would be inefficient in CSS as their respective system models include a single SU link for the CR system. This work employs multiple SUs, similar to [94] to enhance performance by taking advantage of CSS. Finally, while the above mentioned research employs different schemes in order to optimize the transmission rates of SUs; this work utilizes channel feedback in the form of reciprocity to optimize the transmission rates of the SUs.

The remainder of this chapter is organized as follows. In Section 4.2, the system model is described, and the main assumptions required for analysis are introduced. In Section 4.3, a comparative analysis is done between the SWF and ST-WF schemes for the PU link and Section 4.4 presents the space-time opportunistic IA scheme (ST-OIA) by presenting the original OIA approach and describing the steps taken towards achieving the novelty of this work. Section 4.5 provides the reciprocity technique used to optimize the transmission rates of the SU network. Simulation results as well as a performance comparison between this work and that of [the work done so far in the literature] were then presented in Section 4.6, while section 4.7 presents the concluding remarks of this chapter.

4.2.System Model and Assumptions

The system model for this paper is an overlay MIMO CR network that consists of a single PU link (PU-Tx and PU-Rx) and k SUs ($SU_1, \ldots, SU_k$) as shown in Fig. 4.1 below. Every user

has M Tx and N Rx antennas. The PU link is a point-to-point MIMO link, while the SU network is a multi-user MIMO network.

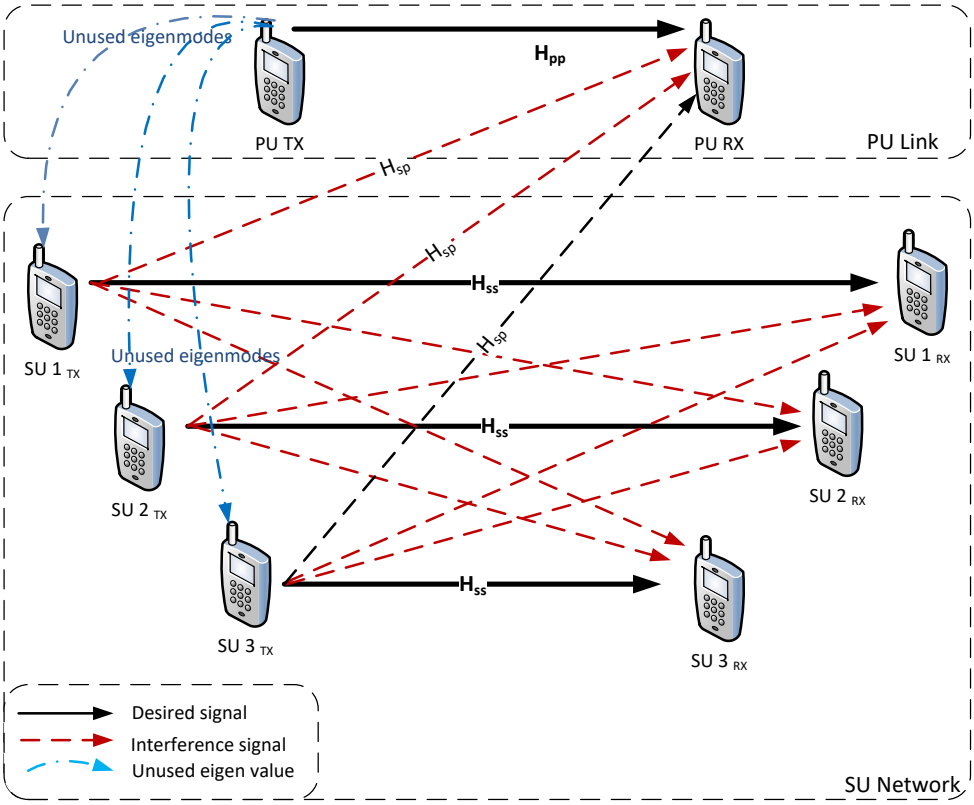

Fig. 4.1: Multiuser CR network model consisting of one PU link and multiple SUs

The following assumptions are made for the purpose of the system model as follows:

(I). The PU and SUs operate in the same frequency band and all channels are Rayleigh fading.

(II). The PU link is a single user MIMO channel which is represented as a $N_i \times M_j$ matrix, $\boldsymbol{H_{ij}}$ with channel coefficients between Tx j and Rx i, where elements of H_{ij} are drawn i.i.d. from a continuous distribution. The channels are assumed to be block fading, i.e., the channel state is fixed within a time slot and changes independently from one slot to the

other, and the CSI is known to all the nodes. The signal received at the PU-Rx can be defined as

$$Y_i = \sum_{\boldsymbol{j=0}}^{\boldsymbol{K}} \boldsymbol{H_{ij}} V_j x_j + n_i \tag{4.1}$$

Where V_j is the $M_j \times d_j$ precoding matrix of the ith user and d_i represents the number of transmitted streams, x_j is the $M_j \times 1$ transmitted vector, n_i is the $N_i \times 1$ additive Gaussian noise vector at the ith receiver. The transmitted power is subject to an average power constraint $E\left[x_j^H x_j\right] \leq P$.

(III). It is assumed the PU-Tx is oblivious to the presence of the SUs. We also assume that the PU channel matrix is known at the PU-Tx and PU-Rx [4]. The PU-Tx chooses its precoding matrix V_j and the PU-Rx chooses its post-processing matrix U_j such that the PU link channel transfer matrix is diagonalized.

Then once SVD has taken place on $\boldsymbol{H_{ij}}$ of the PU, each SU will receive independent $min(M, N)$ parallel non-interfering channels. Since the sum capacity of MIMO broadcast channels increases linearly with $min(M, N, K)$ (where K is the number of SUs), then having a number of SUs makes up for deploying considerable number of antennas for a single SU link [11], [23]. The received signal of at each SU-Rx is thus defined as

$$Y_{ss}^k = \boldsymbol{H}_{ss}^k x_{ss} + n_{ss} \tag{4.2}$$

And the transmit covariance of the input signal is $\sum_x \triangleq \mathbb{E}[x_{ss} x_{ss}^H]$ which is subject to an average power constraint, implying $Tr(\sum_x) \leq P$.

(IV). The SU setup is assumed to be a multi-user MIMO channel. The PU has reserved rights to the spectrum, the SU-Tx's sense vital information about the PU in order to avoid causing interference at the PU-Rx.

In the standard IA conditions, each Tx therefore transmits a sequence of Gaussian encoded symbols to its corresponding Rx by processing its symbols using a $M_i \times d_i$ precoding matrix V_i to form the transmitted signal vector $V_i x_i$. The received signal at the ith Rx is linearly processed by the post-processing matrix $U_i = N_i \times d_i$ to extract the symbols sent by the ith Tx. The IA condition states that the primary and secondary received signals are represented by

$$Y_i = \mathbf{H}_{ii} V_i x_i + \sum_{j=1}^{K} \mathbf{H}_{ij} V_j x_j + z_i \tag{4.3}$$

where y_i denotes the $N_i \times 1$ received signal vector at the j^{th} receiver; z_i denotes the $N_i \times 1$ zero mean unit variance circularly symmetric AWGN noise vector at the i^{th} receiver; x_i denotes the $M_i \times 1$ signal vector transmitted from the j^{th}transmitter; $\mathbf{H}_{ij}$ is the $N_i \times M_i$ matrix of the channel coefficients between the j^{th} transmitter and the i^{th} receiver; Also, $P_j = E\left[x_j\, x_j^H\right]$, where P_j is the transmit power of the j^{th} transmitter [20]. It should be noted that i and j are used as a generalization denoting each Rx and Tx pair.

4.3.PU Link Optimization

4.3.1. The Numerical Comparison

Most of the work on OIA in CR networks such as in [24], [97], [98] utilize SWF scheme for the PU link. The work in [75] makes use of the MEB scheme where the PUs Tx places all its power on the antenna that corresponds to the largest eigenmode of its channel matrix H_{pp}. Its

advantage being that all other dimensions are clearly left unused for the opportunistic SUs to exploit. However, with the comparative study carried out in [76], [77], it is clear that the ST-WF offers improved SU performance for the same PU parameters. Most significantly though is the ST-WF's higher capacity at low to moderate SNR regimes, which fits well with CR networks [76].

In order to implement the ST-WF algorithm, we take a look at the original approach for WF [70], [106] i.e. the SWF approach. For a single MIMO PU channel, recall that

$$\max_{Q} log \left| I + \frac{1}{\sigma^2} H_{pp} Q H_{pp}{}^{\dagger} \right| \quad subject\ to\ tr(Q) \leq P \tag{4.4}$$

where Q is the $M \times M$ input covariance matrix

where H_{pp} is the MIMO channel, Q is the autocorrelation matrix of the input vector x, defined as $Q = E[xx^{\dagger}]$, P is the instantaneous power limit, $|A|$ denotes the determinant of A, and $tr(A)$ denotes the trace of matrix A and σ_i is the noise variance. Let the SVD on matrix H_{pp} be given as $H_{pp} = U_{pp} \Sigma V_{pp}^{H}$ where U_{pp} is $M_{pp} \times M_{pp}$ and unitary while V_{pp} is $N_{pp} \times N_{pp}$ and unitary, Σ is $M_{pp} \times N_{pp}$ and diagonal with non-negative entries i.e. $\Sigma = \text{diag}\{\lambda_1, \ldots\ldots \lambda_M\}$. The diagonal elements of the matrix Σ are the singular values of H_{pp}, H_{pp} has exactly R_H positive singular values, where R_H is the rank of H_{pp} which satisfies $R_H \leq \min(M_{pp}, N_{pp})$. The transmitter/receiver chooses precoding matrices as the columns of $V_{pp}(U_{pp})$ that corresponds to a non-zero PA that is used to maximize the rate of the PU link under power constraints as shown (4.4).

SWF can be used to optimally allocate power to the parallel channels as defined by the following equation [70]:

$$P_{\mathrm{i}} = \left(\beta - \frac{{\sigma_i}^2}{\lambda_i}\right)^+ ; 1 \le i \le R_H \tag{4.5}$$

Where P_{i} is the power of x_{pp}. The WF level β is chosen such that $\sum_{i=1}^{R_H} P_{\mathrm{i}} = \mathrm{P}$ as defined in equation (4.5).

Once the PA matrix using SWF is set up according to [12], the diagonal matrix Σ contains m_1 non-zero/used entries and $N_1 - m_1$ zero/unused entries which crucially translate into a set of m_1 used receive dimensions and a set of $N_1 - m_1$ unused receive dimensions with no PU signal.

4.3.2. Space-Time Water-filling

In terms of implementing the ST-WF algorithm, the PU-Tx also chooses precoding matrices as the columns of $V_{pp}(U_{pp})$ that corresponds to a non-zero PA that is used to maximize the rate of the PU link under power constraints as shown in (4.6) below. It should be noted that for ST-WF, the function $E[tr(Q)]$ is present in all MIMO channel realizations, implying that the symbol rate changes faster than the channel variation where Q can be computed from all symbols but within one channel realization.

$$\max_{Q} E\left[log\left|I + \frac{1}{\sigma^2} H_{pp} Q {H_{pp}}^{\dagger}\right|\right] \quad subject\ to\ tr(Q) \le P \tag{4.6}$$

For computation of the diagonal PA matrix by applying the so-called ST-WF algorithm, β can be found as follows

$$P_{\mathrm{i}} = \left(\bar{\beta} - \frac{{\sigma_i}^2}{\lambda_i}\right)^+ ; 1 \le i \le R_H \tag{4.7}$$

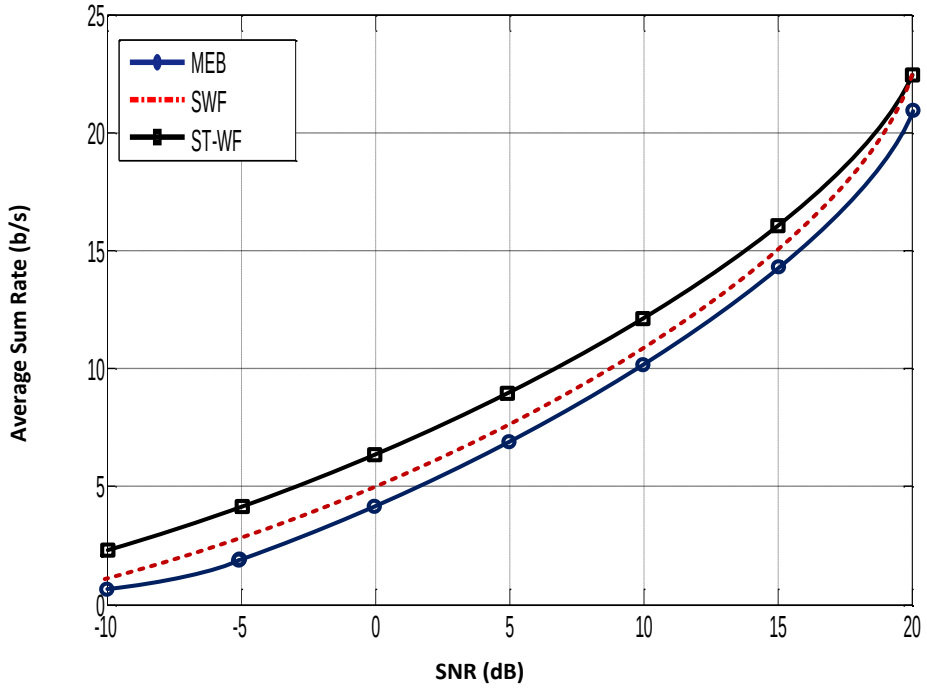

Fig. 4.2: Average sum rate versus the SNR at the PU's link for both water-filling (SWF and ST-WF) and MEB algorithms

where $\bar{\beta}$ is the mean water-level that can be solved by the equation given below

$$\sum_{l=1}^{L_p} \int_{\frac{\sigma_i^2}{\beta}}^{\infty} \left(\bar{\beta} - \frac{\sigma_n^2}{\lambda_i} \right) f(\lambda_i)\, d\lambda_i = \mathbf{P} \tag{4.8}$$

where $f(\lambda_i)$ is the marginal probability density function (pdf) of the random variable(λ_i). To gain more insight into this issue, Fig. 4.2 shows the average sum rate versus the SNR for a single user PU MIMO link with the SWF, ST-WF and MEB PA schemes.

For the Rayleigh channels in this work, Rayleigh fading is assumed to be pure due to the PU-Tx and PU-Rx assumed to be in close proximity and hence the shadowing effect is negligible. The ST-WF algorithm with no shadowing variance achieves higher spectral efficiency over SWF at low SNRs, and has the highest gain of 5dB SNR over equal power distribution at a

spectral efficiency of 2.5bps/Hz/antenna. Furthermore, fig. 2 shows that the numerical results obtained from the Monte Carlo simulations support theoretical results [70], [77].

Implementing the MEB algorithm achieves a performance that is only close to that of the SWF scheme. The simulation results clearly shows that the ST-WF scheme outperforms the other schemes and shows the possibility of increased sum rates in two-tier CR networks when the PU participates in IA.

4.4.Space-Time Opportunistic Interference Alignment

The proposed ST-OIA will be divided into two phases, (a) the sensing phase and (b) the interference alignment phase.

4.4.1. The Sensing phase

This section describes how the SUs perform SS without causing interference at the PU's Rx [24]. The unique feature of this work is that the SUs are only involved in sensing the TO's. Because both PU and SU have been assumed to be operating in the same frequency band, the SUs will always opportunistically make use of the licensed spectrum as long as the TOs are available.

We consider the channel with the PU-Tx acting as a base station transmitting in a broadcast mode to multiple SU's. In this case, it would be recalled that the maximum achievable rate of the PU with the ST-WF algorithm is given as [77]

$$p(\lambda) = \left(\beta - \frac{\sigma^2}{\lambda_i}\right)^+ \tag{4.9}$$

At high SNR, the ST-WF PA strategy gets no benefit because it allocates equal power to each of the R_H channels, thus the PU utilizes all its channels eigen-modes.

At low SNR however, the ST-WF algorithm allocates power to the strongest R_H parallel channels according to the water-level β. These channels translate into the m_1 used SDs, while the others can be classified as the $N_1 - m_1$ unused dimensions or TOs. The SUs make independent decisions about the unused $N_1 - m_1$ dimensions by setting the appropriate SS parameters, so that each SU can sense the absence or presence of the TO by the following binary hypothesis test [43], [75]:

$$\begin{cases} H_0;\ i^{th}\ eigenmode\ unused\ by\ PU \\ H_1;\ i^{th}\ eigenmode\ used\ by\ PU \end{cases} \tag{4.10}$$

This is a somewhat static approach to SS due to the very deterministic nature of the system model. In practical environments however, there would always be multiple PU's in which case the SUs would have to deploy dynamic SS which is beyond the scope of this work. As described in Chapter 2 (2.1), each SU employs the decision rule to make a decision about the unused SDs according to a threshold set either above or below the water-level as follows

$$d(t) = \begin{cases} y(t) \leq \beta & H_0 \\ y(t) > \beta & H_1 \end{cases} \tag{4.11}$$

Each SU sends a summary of its own observations to the FC in the form of either P_d, P_f for the SUs. The FC uses the hard combination fusion rule [46] – [48] for making the final decision based on the received information from SUs and relaying these decisions to the SUs.

This work utilizes probability of missed detection as one of the parameters for measuring performance. It can be observed that the simulation results in fig. 4.3 are quite optimal yielding near perfect results when sensing ONLY for TOs.

This work utilizes probability of missed detection as one of the parameters for measuring performance. It can be observed that the simulation results in fig. 4.3 are quite optimal

yielding near perfect results when sensing ONLY for TOs. From the analysis of chapter 2, the OR rule is the best among the fusion rules in many cases of practical interest due to its relative ease of implementation, therefore, it shall be considered for this phase of ST-OIA. The OR rule used compared very well to theoretical analysis, and the disparity in performance could be attributed to be the case when the SUs experience shadowing or fading.

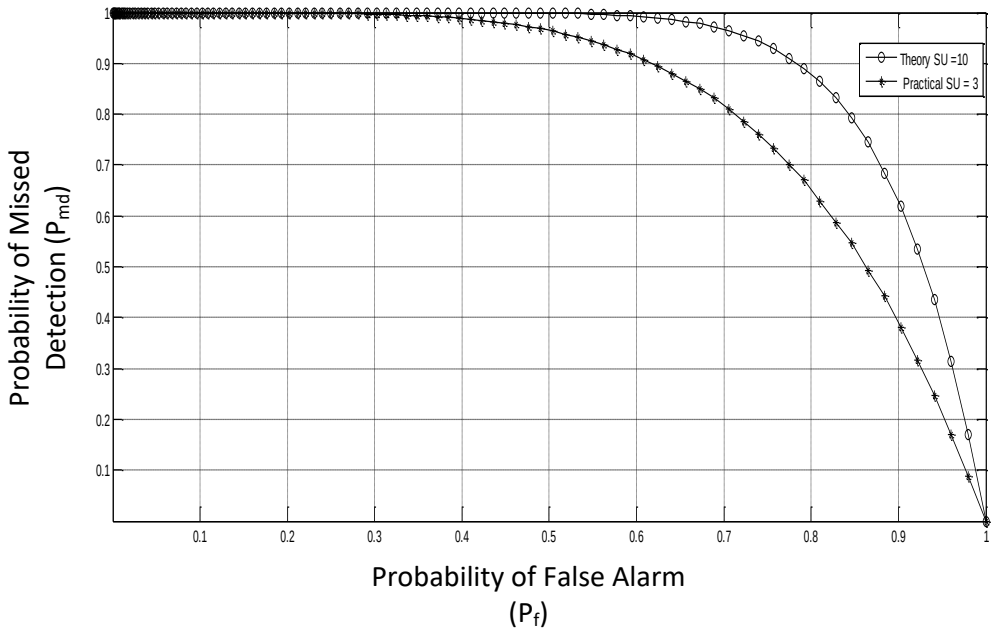

Fig. 4.3: ROC curve showing the theoretical and simulated results for 2 SUs

4.4.2. The Interference Alignment phase

The main goal of this phase is to derive appropriate pre-coding and post-coding matrices which align the SUs transmissions to the $N_1 - m_1$ unused SD left by the PU. In order to achieve that, an ST-OIA strategy is proposed in which three separate conditions must be satisfied. The first condition defines a pre-processing matrix for the SU-Tx that aligns its transmission with orthogonal spaces at the PU-Rx. The opportunistic SU link is said to satisfy the IA condition if its opportunistic transmission is such that the PU link achieves the same transmission rate of an equivalent single-tier system. Similar to the first condition, the second

condition defines a post-processing matrix to be met by the SU-Tx, but this time by aligning its transmission with orthogonal spaces at the SU-Rx. These two conditions were sufficient in the earlier work done in [97], [100]. However, our research work consists of multiple SUs used in the manner of CSS and thus requires a third condition to be defined to ensure that each SU successfully aligns its transmission with the orthogonal spaces at both the PU and SU.

Firstly, given the SVD channel matrix of the PU link as $\boldsymbol{H_{pp}} = U_{pp}\Sigma_p V_{pp}^H$ where V_{pp} and U_{pp} are the $M_{pp} \times M_{pp}$ and $N_{pp} \times N_{pp}$ singular vector matrices and $\boldsymbol{\Sigma_p}$ is a $N_{pp} \times M_{pp}$ diagonal matrix containing singular values, the cognitive IA problem is formulated by defining the required conditions for IA. Given that the received signal at the ith receiver due to the jth transmitter lies in the subspace spanned by the columns of $H_{ij}V_j$, the SU-Tx's are guaranteed not to generate any interference on the PU-Rx as long as the following precoding and post-processing condition are met

$$U_{pp}^H \boldsymbol{H_{pj}} V_j = 0_{d_p}; \quad \forall_i = 1, \ldots \ldots K \tag{4.12}$$

$$U_i^H \boldsymbol{H_{ip}} V_{pp} = 0_{d_i}; \quad \forall_i = 1, \ldots \ldots K \tag{4.13}$$

Equation (4.12) is the post-processing matrix that satisfies the orthogonality between the SU-Rx's and the PU-Tx, thus guaranteeing the PU link achieves similar data rates as an equivalent single-tier system despite the opportunistic transmission of the SUs. d_i is defined as the DoF [8], thus satisfying **the first condition**.

The second condition requires that the SU and PU signals be aligned to orthogonal subspaces at not only the PU receiver, but the SU receiver as well i.e. at output of the post-

processing matrices of its unintended receivers. Therefore, a different strategy is used to design the SUs post-coding matrix in order to satisfy the second interference constraint.

The first part of this constraint defined in (4.14) ensures that interference from each SU-Tx is aligned at the output of its corresponding unintended receivers.

$$U_i^H \boldsymbol{H_{ij}} V_j = 0_{d_i}; \quad \forall_i = 1, \ldots \ldots K \tag{4.14}$$

$$rank\{U_i^H \boldsymbol{H_{ii}} V_i\} = d_i; \quad \forall_i = 1, \ldots \ldots K \tag{4.15}$$

The constraint in (4.15) guarantees that the ith SU can achieve d_i DoF.

However, because this work consists of multiple SUs, **the third condition** that must be satisfied requires that ALL the SUs do not impose any interference on the PU receiver

For this third condition, it will be assumed that the channel coefficients are time varying such that constrained IA can be employed over multiple channel realizations to achieve the available $K(M - d_0)^+/2$ DoF. The first step towards achieving this transforms the cognitive IA problem into an unconstrained standard IA problem for a general cognitive system with K secondary pairs operating in the presence of a primary link with d_0 DoF. Defining the matrices $\{\tilde{V}_i\}_{i=1}^K$as $(M_i - d_0) \times d_i$ and the matrices $\{\tilde{U}_i\}_{i=1}^K$ as $(N_i - d_0) \times d_i$ such that

$$V_j = A_j \tilde{V}_j \quad \forall_j = 1, \ldots \ldots K \tag{4.16}$$

$$U_i = B_i \tilde{U}_i \quad \forall_i = 1, \ldots \ldots K \tag{4.17}$$

where the A_i matrix $(M_i - d_0) \times M_i$ spans the nullspace of the matrix $U_0^H H_{0i}$ i.e. $U_0^H H_{oi} A_i = 0_{d_0 \times (M_i - d_0)}$. Similarly, the B_i matrix $(N_i - d_0) \times N_i$ spans the nullspace of the matrix $V_0^H U_{0i}^H$ i.e. $V_0 H_{oi} B_i^H = 0_{d_0 \times (N_i - d_0)}$ [87].

Using the expressions defined (4.16) and (4.17) above for the precoding and post-processing matrices of the SUs eliminates the initially defined constraints in [102] due to the presence of the PU link, by substituting equations (4.16) and (4.17) in (4.14) and (4.15) to get the following equations

$$\widetilde{U}_i^H B_i^H H_{ij} A_j \tilde{V}_j = 0_{d_i \times d_j} \quad \forall_{i,j} = 1, \ldots\ldots K, i \neq j \tag{4.18}$$

$$rank\{\widetilde{U}_i^H B_i^H H_{ii} A_i \tilde{V}_i\} = d_i \quad \forall_i = 1, \ldots\ldots K \tag{4.19}$$

It can clearly be seen that the modified problem in (4.18) and (4.19) is a standard IA problem in the variables $\{\tilde{V}_i\}_{i=1}^{K}$ and $\{\widetilde{U}_i\}_{i=1}^{K}$. Recall that $\tilde{V}_i = \in \mathbb{C}^{(M_i - d_0) \times d_i}$ and $\widetilde{U}_i = \in \mathbb{C}^{(N_i - d_0) \times d_i}$, which is in accordance the remark 2 where the effect of the presence of a PU link with active d_0 DoF is equivalent to removing d_0 antennas from each SU-Tx and SU-Rx.

The conditions for estimating B_i by the i-th SU-Rx is done by listening to the PU-Tx and estimating the subspace spanned by $H_{i0}V_0$. Similarly, the j-th SU-Tx can estimate A_i by listening to the transmission and estimating the subspace spanned by listening to the transmission from the PU-Rx and estimating the subspace spanned by $\overleftarrow{H}_{j0}U_0$.

Since the work in [11] proposed a precoding scheme for the K-user symmetric MIMO IC that can asymptotically achieve a DoF of $KM/2$ with M antennas at each node, then using the above equations in (4.18) and (4.19), the K–user cognitive MIMO channel with M antennas at each node equates to a standard IC with $(M - d_0)^+$antennas at each node where the channel between the ith equivalent Tx and the jth equivalent Rx is given by $B_i^H H_{ii} A_i$. Hence, this same technique [5] can then be used to prove that $K(M - d_0)^+/2$ DoF are asymptotically achievable for the CR network.

4.4.3. Feasibility Conditions

This third condition is essentially equitable to having two non-interfering systems in the cognitive system, the first being a PU that equates to a MIMO-PTP channel with transmit and receive antennas. The second is a *k*–user IC having transmit and receive antennas where the presence of the PU is equivalent to removing antennas from the Tx/Rx of the SU, thus converting its own channel to a MIMO-PTP channel as well.

Following [11], the outer bound in can be obtained by picking two secondary users and ignoring the interference from the other secondary users, because in the presence of the PU, the DoF d_0 of the ith user cannot exceed those that can be obtained in the absence of the other $K-1$ SUs. The DoF of the resulting 2-user IC can be found using the results of [4] and is given by in (18) for the pair. Since there are user pairs resulting in times the sum of the individual rates, we get (4.18).

In this section, the feasibility of the proposed method and the conditions in which the cognitive system can limit the number of SUs that will be picked to ensure perfect IA will be discussed. The conditions for which the system is proper were first determined, i.e., the number of variables to be determined is greater than or equal to the number of equations in the system. In order to find the number of equations, the IA conditions were reformulated in (5) as the following:

$$N_v \geq N_e \Rightarrow M + N - (K+1)d \geq 0 \tag{4.20}$$

For the sake of simplicity, we limit our initial design to a 3-SU cluster i.e. each SU having $M = N = 3$ antennas. It is well know from the Bezout's theorem that generic polynomial systems are solvable if and only if the number of equations does not exceed the number of variables. As such, signal space IA problems can either be proper or improper [76]. Thus,

from the Theorem of Proper Characterization [49] which states that "A symmetric system $(M \times N, d)^K$ is proper if and only if $N_v \geq N_e \Rightarrow M + N - (K+1)d \geq 0$".

Simply comparing the total number of variables of equations and the total number of variables suffices to determine if a system is proper or improper. As an example, consider a $(1 \times 1,1)^4$ system i.e. a four user system where each Tx has $M = N = 1$ antennas with each user demanding a 1 DoF. From(4.20), this system can be categorized as being proper and can subsequently have four Tx's with one antenna each and two Rx's with two antennas each [49]. Therefore this example will automatically achieve 4 DoF, which automatically surpasses the DoF achievable by the X channel.

Thus, this system can be designed according to the algorithms defined in equations (4.14) and (4.15) to satisfy the IA condition of (4.18). Similarly, we can also design the CR as an Asymmetric system whose conditions state that "if a system is improper, then simply comparing the total number of equations and total number of variables may suffice

i.e. "An Asymmetric system defined as $\pi_{k=1}^{K}\left(M^{[k]} \times N^{[k]}, d^{[k]}\right)$ is improper if

$$N_v < N_e \Leftrightarrow \sum_{i=1}^{K} d^{[i]}\left(M^{[i]} \times N^{[i]}, d^{[i]}\right) < \sum_{\substack{i,j \in K \\ i \neq j}}^{K} d^{[i]} d^{[j]} \qquad (4.21)$$

This advantage of this optimization technique is that it will show how the DoF limitations of the X channel can be improved and it also allows more nodes to be incorporated into the CR network. From the analysis of results done in cfapter 2; detection performance of CSS is considerably enhanced with increased number of nodes. However, this does create a greater number of IA conditions to be met thus increasing computational complexity.

4.5.Optimizing SU transmission rates

The work in [24] proposed an OPA as described in Chapter 2, where the transmission rate for the SU link is maximized by adopting a power allocation matrix P_s which is a solution of the following optimization problem,

$$\underset{P_s}{\text{argmax}} \qquad R_s(P_s) \tag{4.22}$$

$$s.t. \quad Trace\left(P_{ss}V_sV_s^H\right) \leq p_{max}$$

where

$$R_s(P_s) = \log_2 \left| I_{N_r} + Q^{-\frac{1}{2}} H_{ss} V_{ss} P_s V_{ss}^H H_{ss}^H Q^{-\frac{1}{2}} \right|$$

This optimization problem requires the knowledge of the covariance matrix Q, which can be done if the SU-Rx estimates Q and feeds it back to the SU-Tx. In simpler terms, it is assumed there is a perfect knowledge of Q at the SU-Tx. Furthermore, the transmission rates for the SUs can also be optimized as shown in [12], which adopts a UPA scheme by spreading its total power among the identified TOs. In other endeavors, the work in [100] enables the SU link to estimate required CSI by blindly estimating its covariance matrices Q, albeit with a huge computational complexity.

Since the conditions for estimating B_i and A_i have been defined earlier where the i-th SU-Rx/ SU-Tx listens to the PU-Tx/PU-Rx in order to estimate the subspace spanned by $H_{i0}V_0/\overleftarrow{H}_{j0}U_0$, this provides an opportunity for this work to consider the multi-user SUs and not the PU link as using a time division duplex (TDD) mechanism [90] so that channel reciprocity is assumed between the forward (Tx to Rx) and reverse (Rx to Tx) channels.

The Reciprocity property of wireless networks is considered due to the drawbacks of existing closed form solutions of IA which typically include global CSI requirements optimal

performance only in high SNR conditions. The work done in [63] is was a technique designed to address the drawbacks of such existing closed form solutions of IA for the IC with arbitrary number of antennas at each transmitter and receiver to achieve the following objectives: require only local CSI, improve performance of IA solutions in lower SNR conditions and introduce diversity techniques in IA solutions [55]. These objectives all come about due to the reciprocity property of wireless networks is considered which states that "the signaling dimensions along which a receiving node sees the least interference is the same dimension along which this node will cause least interference when the roles of Tx's and Rx's are switched.

Considering the same $K-user$ IC as per the "**third condition**" for our design, let K^{th}Tx and Rx have M Tx antennas and N Rx antennas respectively, such that the channel is defined as stated in (2.17)

$$Y_i(n) = \sum_{j=1}^{i} H_{ij}(n)x_j(n) + z_i(n)\ ; \qquad (4.23)$$

Where symbols have the same meanings as previously discussed in(2.17).

For the $K-user$ IC defined above, a reciprocal channel can be defined as the role of Tx's and Rx's being switched so that all elements on the original channel corresponds equally but opposite to the elements on the reciprocal channel.

If interference is nulled into the null space of U_i as defined in equation (4.14), then the IA condition of equation (4.15) must be satisfied, where the desired signals are then received through a $d_i \times d_i$ full channel matrix defined as $\overline{H}_{ii} \triangleq U_i H_{ii} V_i$

The Reciprocity then goes on to state that for the $K-user$ reciprocal channel defined above, "if IA is feasible on the original IC, then it is also feasible on the reciprocal IC".

In mathematical terms, if $\overleftarrow{V_i}$ and $\overleftarrow{U_i}$ denote the transmit pre-coding and interference suppression filters on the reciprocal channel, then the IA conditions on the reciprocal channel can be defined as defined in equations (4.24) and (4.25)below [55]:

$$\overleftarrow{V_i}: N_i \times \overleftarrow{d_i},\ \ \overleftarrow{U_i}^{\dagger}\ \overleftarrow{U_i} = I_{d[i]} \tag{4.24}$$

$$\overleftarrow{U_i}: M_i \times \overleftarrow{d_i},\ \ \overleftarrow{U_i}^{\dagger}\ \overleftarrow{U_i} = I_{d[i]} \tag{4.25}$$

such that feasibility conditions on the reciprocal channel can be similarly satisfied as follows

$$\overleftarrow{U_i}^{H\dagger}\overleftarrow{H_{ij}}\overleftarrow{V_j} = 0_{d[i]\times d[j]}, \forall_{i,j}\ i \neq j \tag{4.26}$$

$$rank\{\overleftarrow{U_i}^{H\dagger}\overleftarrow{H_{ii}}\overleftarrow{V_i}\} = d_i, \forall i = 1, \dots \dots \mathcal{K} \tag{4.27}$$

This shows the duality of reciprocity with the original feasibility of IA. We will design transmit and receive filters that iteratively update their filters to approach interference alignment. The quality of IA is measured by the power in the *leakage interference* at each receiver, i.e., the interference power remaining in the received signal after the receive interference suppression filter is applied. The aim of this iterative approach is to progressively and iteratively reducing the leakage interference until it converges to zero [63]. The total leakage interference due to undesired transmission at each SU is given as $I^{[i*]} = Tr\left[U_i^{\dagger}Q_iU_i\right]$ Where $Q_i = \sum_{j=1,j\neq i}^{d_i}\frac{P_i}{d_i}H_{ij}V_jV_j^{\dagger}H_{ij}^{\dagger}$ is the interference covariance matrix at receiver i. For the reciprocal channel, if $\overleftarrow{P}^{[k]} > 0$ is the power constraint at every SU, then the total leakage interference can also be defined as

$$\overleftarrow{I}^{[j*]} = Tr\left[\overleftarrow{U_i}^{\dagger}\overleftarrow{Q_i}\overleftarrow{U_i}\right] \tag{4.28}$$

Where

$\overleftarrow{Q_i} = \sum_{j=1,j\neq i}^{d_i}\frac{\overleftarrow{P_i}}{d_i}\overleftarrow{H_{ij}}\overleftarrow{V_j}\overleftarrow{V_j}^{\dagger}\overleftarrow{H_{ij}}^{\dagger}$ is the interference covariance matrix at Rx i.

Recall that the SU-Rx can estimate by listening to the PU-Tx and estimating the subspace spanned by U_i. Similarly, the SU-Tx can estimate by listening to the transmission from the PU-Rx and estimating the subspace spanned by U_j

- The algorithm is modeled to alternate between both the original and reciprocal network.
- The iterations for the pre-coding matrices are set as$\tilde{V}_j$: $M_j \times V_j, V_j V_j^{\dagger} = I_{d[j]}$
- The next step defines the Rx's covariance matrices that will be received at each SU

$$Q_i = \sum_{j=1, j\neq i}^{d_i} \frac{P_i}{d_i} B_i^H H_{ij} A_j \tilde{V}_j \tilde{V}_j^{\dagger} A_j^H H_{ij}^{\dagger} B_j \quad (4.29)$$

The Reciprocity is the key aspect to accurate algorithms and for the $K - user$ reciprocal channel defined above, as it states that "if IA is feasible on the original IC, then it is also feasible on the reciprocal IC.

- The suppression matrices at each receiver are defined as

$$\tilde{U}_i = v_d[Q_i], \;\; d = 1, \quad \ldots \quad .d^{[k]}$$

- Setting the pre-coding matrices as reciprocals $\overleftarrow{\tilde{V}_j} and \; \overleftarrow{\tilde{U}_j}$, begin iterations
- The next step defines the receivers covariance matrices received at each receiver

$$\overleftarrow{Q_i} = \sum_{j=1, j\neq i}^{d_i} \frac{\overleftarrow{P_i}}{d_i} A_j^H \overleftarrow{H}_{ij} B_j \overleftarrow{\tilde{V}_j} \overleftarrow{\tilde{V}_j}^{\dagger} B_j^H \overleftarrow{H}_{ij}^{\dagger} G_i \quad (4.30)$$

- The reciprocal suppression matrices at each receiver are then computed as

$$\overleftarrow{\tilde{U}_i} = v_d \overleftarrow{[Q_i]}, \;\; d = 1, \quad \ldots \quad .d^{[k]}$$

- The communication channels are continuously reversed back and forth between the original and reciprocal, until convergence to zero.

The significance of this reciprocity is about two things: firstly, the SU's are only required to learn the effective channel of their desired PU. This lessens the burden of global channel

information of all available matrices. Secondly, the algorithms can be used for further analytical study of IA solutions. While IA solutions are optimal at high SNR, they are not so optimal at intermediate SNR making it impossible to obtain optimal array gain for the SUs signals.

4.6.Simulation Results and Analysis

In this section, numerical results have been provided to evaluate the performance of the ST-OIA algorithm against others such as the SU-IA-OPA. It is quite clear from the results obtained that this scheme provides improved throughput when compared with other schemes.

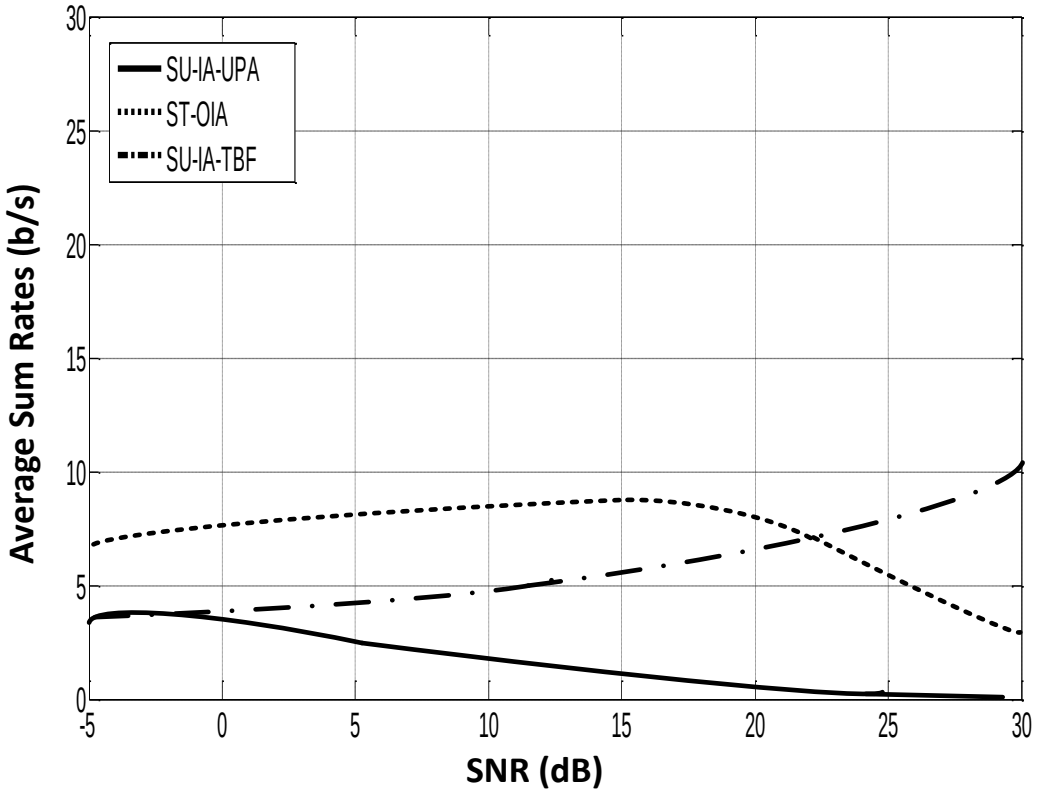

Fig. 4.4: Average Sum Rate (b/s) against SNR (dB) for a single PU link and two SUs

Monte-Carlo simulations were carried out for 2 SU pairs (Tx and Rx) and a single PU link with each node equipped with two antennas. From Fig 4.4, three separate techniques are

compared namely the legacy SU-IA-PA, the SU-MEB and of course the proposed ST-OIA. It can be seen that the SU-MEB performs best at moderate to high SNR while the SU-IA-PA performance takes a sharp drop when the SNR increases.

This could be indicative of the fact that the TOs become almost non-existent at highest SNR. However, the work in [28] shows that for practical values of SNR, there exists a non-zero number of TOs the SUs can always exploit. At intermediate to high SNR, the SU-MEB scheme performs consistently. Even at 30dB, the sum rate remains consistent and does not drop-off. The proposed scheme's (ST-OIA) performance peaks between 5dB to 15dB, but then there is a sharp drop-off as the SNR increases.

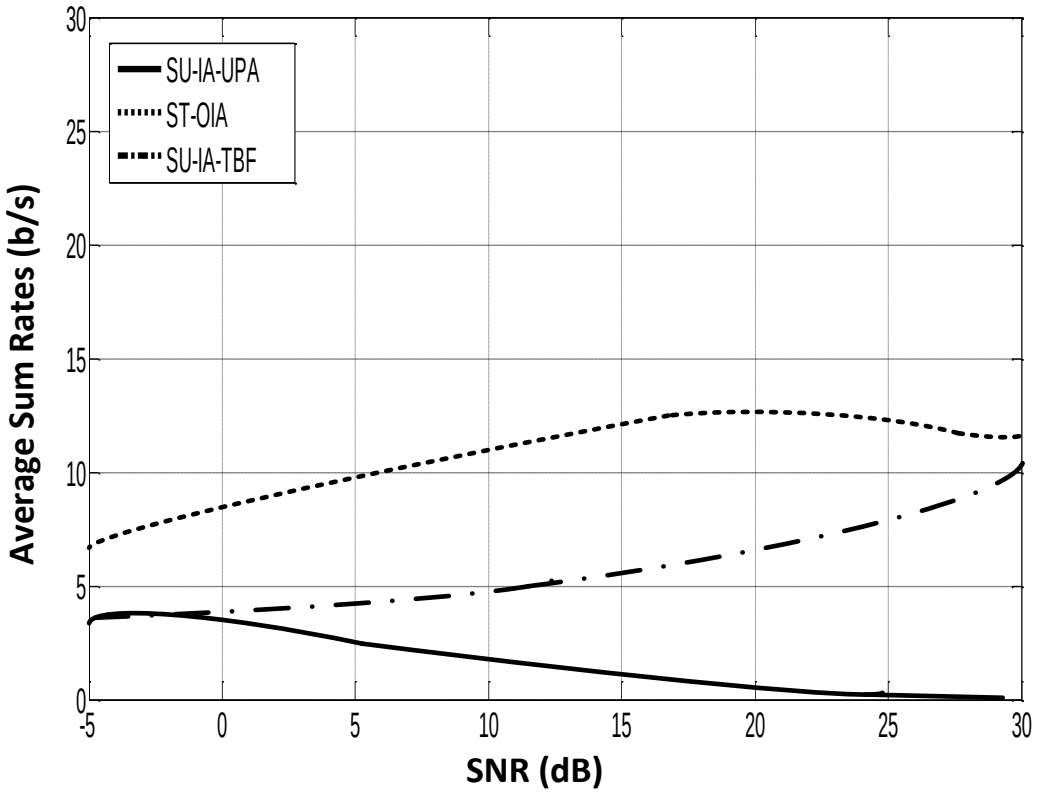

Fig. 4.5: Average Sum Rate (b/s) against SNR (dB) for a single PU link and two SUs with Reciprocity

The graph shown in fig 4.5 demonstrates the performance of employing schemes to enhance throughput. Implementing Reciprocity requires that the transmitter – receiver pair become the receive-transmitter pair. The main essence of implementing reciprocity in this work is so that the SU receivers can be setup with a threshold to sense for the unused spatial dimensions. The essence of this is setting a threshold value of SNR so that once the receiver does not attain this threshold; it ceases to communicate with the transmitter. So the SU Tx in this case becomes quiet and continues to listen for the unused dimensions. It can be seen in Fig 4.5 that this implementation has a very drastic response in terms of performance. As the SNR increases, the effect of optimizing the transmission rate of the SU is clear to see as there is a marked increase in terms of sum-rates.

4.7.Conclusion

A ST-OIA has been proposed in which SVD is performed on the PU channel matrix where a ST-WF algorithm is applied to free up some unused eigenmodes. Both PU and SU can utilize the licensed spectrum by aligning the interference from the SUs to these unused eigenmodes.

A comparative analysis between the ST-WF and other WF algorithms was carried out to show its achievable gains. Multiple SUs utilizing the benefits of cooperative spectrum sensing were used to sense the unused eigenmodes. Simulation results showed the probability of missed detection to be quite marginal with respect to theoretical values for three SUs. Finally, three separate conditions were defined and met to ensure that interference to the PU and SU receivers are perfectly aligned to the unused eigenmodes. Most significantly is that limited cooperation between the PU receiver and the multiple SUs was implemented to ensure the SUs avoided interfering with the PU-Rx. Lastly, the SU transmission rates were maximized by using the principle of reciprocity where the SU receivers can be used to transmit feedback information to the transmitters.

Simulation results showed improved performance in terms of sum rates for the three IA conditions, although there was significant performance drop with increased SNR. It was also shown that implementing feedback through reciprocity greatly increased the performance of the multiple SUs and bodes well for future work in this area.

One significant drawback of ST-WF is that its CSI requirement is based over a definite period of time that could span the whole duration of transmission, thus negating the benefits derived from the block transmission of the that ST-WF technique gives the PU. The solution to this problem and a strong consideration for future work is to assume causal knowledge of the CSI, which can then be exploited to intelligently allocate the power over the causal blocks (and hence vary the channel mutual information) to minimize the average transmitted power per block.

A significant part of this Chapter has been published in the proceedings of the 14th IEEE Wireless Communications and Networking Conference (WCNC) held in April 2016 in Doha, Qatar (http://ieeexplore.ieee.org/document/7564913/).

5. Opportunistic Interference Alignment with Space-time Coding

5.1.Introduction

This chapter's main objective continues the process of optimizing the sensing channels used in CSS. Similar to research done in [71] – [75], the work done in Chapter 4 towards has been able to establish the following key novelties. It was established that due to power limitations, the PU link makes use of a WF PA scheme to maximize its transmission over its SD's to leaves some of them unused. Secondly, the SU link can detect and take advantage of these unused SDs with a linear pre-coder that aligns the SUs transmission with the unused SDs of the PU link thereby avoiding any interference to the PU. Given the fact that a single SU is unlikely to reliably detect the presence of a PU [16], the third considers the possibility of employing multiple SU's to take advantage of CSS, where the SUs individually perform *local sensing* in order to detect the absence or presence of the unused TOs. Additionally, the ST-WF algorithm for PA of the PU link rather than the SWF algorithm used in [24], [71] – [74], which showed a slight performance advantage in terms of capacity per antenna at low to moderate SNR regimes [25], [26]. Lastly, it was also shown that the multiple SUs can make use of a TDMA mechanism so that channel reciprocity is assumed between the Tx to Rx and reverse Rx to Tx channels in order to optimize the SUs transmission rates. Based on this, the SU receivers will periodically transmit feedback through reverse channels in timeslots with channel parameters indicating a loss of fidelity or a change in the PUs transmission parameters.

The work in this chapter goes on to establish that these incremental novelties are in fact a means to an end and not the end in their own selves, by showing that incremental enhancements can still be introduced within the above mentioned novelties towards optimizing the sensing channels used in CSS. To be more specific, this chapter will focus on

the aspect of improving the detection accuracy and transmission rates of the SUs towards further optimization of CSS.

As previously shown in Chapter 4, there are three conditional statements that must be defined to ensure the functionality of ST-OIA. The SU-Tx's must not generate any interference on the PU-Rx, the SU and PU signals must be aligned to orthogonal subspaces at not only the PU receiver, but the SU receiver as well. Lastly, the multiple SUs must not impose any interference on the PU-Rx. On this last condition, simultaneously aligning all SU transmissions at the PU-Rx is always limited by availability of spatial dimensions as well as typical user loads [27]. Therefore, instead of only relying on feasibility conditions to simultaneously align sets of SUs at every PU-Rx, the work in this chapter proposes an SU selection algorithm by the FC, in which only the two SUs that are closest to the FC are aligned at each PU-Rx.

With the selection algorithm clearly defined, this chapter then goes on to explore further means of improving the detection accuracy employed by the SUs. Naturally, the success of the SUs communication in this SU model depends on the accurate availability of unused DoFs. The work in [15] proposed a fast sensing method based on GLRT that gives a more accurate outcome on the absence/presence of individual TOs, albeit with huge computational complexity. Thus to enhance accuracy of detection of TOs without the huge computational complexity associated with the GLRT, this work makes use of a double threshold ED scheme [107], [108] to enhance the detection accuracy and availability of DoF. Typically, the sensing condition states that "if the SD exceeds the water-level β value, then the SU reports unavailability of used SD. Alternatively, if it is less than β, then the SU reports availability of unused SD. However, if the detected value is between $\dot{\beta}_1$ and $\dot{\beta}_2$ (i.e. values that are slightly

above or belowβ), the SUs still report this energy value, implying that the FC receives two kinds of information from which to base its decision on. This increased range of values available to the FC leads to higher detection accuracy and thus increased DoF.

Furthermore, this research is also focused on maximizing the achievable transmission rate as well as diversity gain for the opportunistic SU links. The more legacy work of [23] and [24] use two power allocation schemes to find a covariance matrix that maximizes the achievable transmission rate for the opportunistic SU link. In was shown in [24] that the power allocation technique turns out to be a beamformer with multiple beams formed using the orthogonal eigenvectors of the correlation matrix of the estimated channel at the SU-Tx according to the WF principle. The water-level saturates the power constraints, which makes the K-user cognitive MIMO SU network equivalent to a standard IC with multiple antennas at each node.

To increase the data rate performance, parallel transmissions equipped with STBC across eigen-beams were developed in [109] – [111], which yielded a two-directional eigen-beamformer that performs better than the conventional one-directional beamformer with negligible increase in computational complexity [111], [112]. Conversely, to achieve full transmit diversity without losing sum rates, IA schemes were proposed in [113], [114] that use STBC to achieve full transmit diversity, where the STBC structure of the equivalent channels where preserved after zero-forcing the interfering users [115]. These IA schemes were shown to achieve higher diversity gain than other conventional methods [115] with only local CSI. Since the work in [116] – [119] reveals that the fundamental SU transmission is not changed by the transmit eigen-beamforming matrices, this work proposes wedding optimal precoding with STBC and IA that will achieve higher transmit diversity at the same symbol rates as the work done in [12].

The ST-WF scheme is also not without its drawbacks as was shown in [77] to be associated with a higher channel outage probability, thereby setting a lower-bound in terms of the SUs transmission rates. In order to solve this problem of maximizing the SUs rates without the need for CSI and in the presence of channel outage, this work proposes that the multiple SUs employ a DSTBC scheme that is then combined with optimal IA precoders [119], [120] that align interference at unintended Rx's thereby eliminating the need for local CSI. D-STBC encodes the transmitted information into phase differences between two consecutive symbols, where information is transmitted by first providing reference symbols which determine whether the SUs transmit or remain silent. This is then followed by linearly encoded combinations of both the original phase-shifted symbols and their conjugate. After performing zero forcing, the multiple SU-Rxs decodes the information in the current symbol by comparing its phase to the phase of the previous symbol. This scheme achieves maximum symbol rate with a much higher reliability.

It is worth noting that, although close in notion to the research done in [24], [75] and [93], this work differentiates itself in the following key aspects. Firstly, the PU's power allocation technique is based on a SVD parallel channel decomposition scheme that employs the ST-WF algorithm for the PU link to achieve better channel capacity. Secondly, this work then takes advantage of multiple SUs, similar to [75] to enhance performance by employing CSS, and proposing a double-threshold ED scheme that improves the P_d. Finally, this work proposes an IA technique that manages interference between the SUs, by proposing a full diversity technique which combines the merits of DSTBC and linear precoding, yielding a two-dimensional (2-D) beamforming solution. It was shown that this works shows better performance in terms of the SUs transmission rates.

The remainder of this chapter is organized as follows. In Section 5.2, the system model and the main assumptions required for analysis are reviewed (due to the fact that the system model for this chapter is the same as Chapter 4). In Section 5.3, a review on the comparative analysis between the MEB, SWF and ST-WF schemes is done, as well an analysis on outage probability of the ST-WF algorithm. Section 5.4 presents the opportunistic IA scheme (OIA) by presenting the sensing phase (along with the double threshold method) and the IA phase with the SU selection process. Section 5.5 presents OIA with STBC by briefly reviewing the literature before presenting the algorithms required for the STBC-beamforming-IA technique. Section 5.6 then presents the OIA with DSTBC approach that describes the steps taken towards achieving diversity and higher data rates. Section 5.7 provides an overview of simulation results as well as a performance comparison between this work and that of [23] and [24]. Finally, Section 5.8 presents the concluding remarks.

5.2.System Model and Assumptions

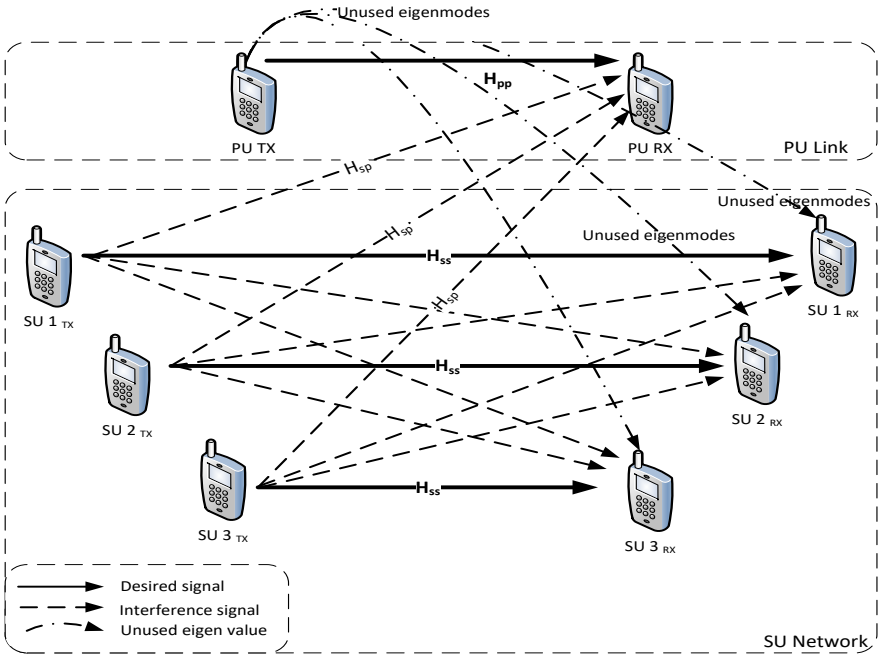

Fig. 5.1: Multiuser CR network model consisting of one PU link and multiple SUs

The system model for this work is also an overlay MIMO CR network that consists of a single PU link (PU-Tx and PU-a) and k SU-Tx/Rx pairs ($SU_1, \ldots, SU_k$) as shown in Fig. 5.1 below. All assumptions made in Chapter 4 Section 4.2 apply to the CR network in Fig. 5.1.

In the standard IA conditions, the primary and secondary received signals are represented by

$$\mathrm{Y_i} = \mathrm{H_{ii}V_i x_i} + \sum_{\mathrm{j=1}}^{\mathrm{K}} \mathrm{H_{ij}V_j x_j} + \mathrm{z_i} \tag{5.1}$$

where the coefficients of (5.1) have the same meaning as those defined in system model of Chapter 4.2., with the slight difference being that this Chapters system model will employ a 2-SU cluster with each SU having $M = N = 2$ antennas (as will be discussed in the later sections of this Chapter). It should be noted that i and j are also used as a generalization denoting each Rx and Tx pair.

5.3.PU Link Optimization

5.3.1. Review on the Numerical comparison

Referring to Chapter 4 Section 3 (4.3) on PU link optimization, the ST-W's ability to operate at low to moderate SNR regimes as well as its higher capacity performance than SWF makes it fit more appropriately for the work in this chapter.

In order to implement the ST-WF algorithm, we took a look at the original approach for WF [76], i.e. the SWF approach, which can be used to optimally allocate power to the parallel channels [26]. As described in Chapter 4 in terms of implementing the ST-WF algorithm, the PU-Tx also chooses precoding matrices as the columns of $V_{pp}(U_{pp})$ that corresponds to a non-zero power allocation that is used to maximize the rate of the PU link under power constraints such that

$$\max_{Q} E\left[log\left|I + \frac{1}{\sigma^2} H_{pp} Q {H_{pp}}^{\dagger}\right|\right] \quad subject\ to\ tr(Q) \leq P \tag{5.2}$$

For computation of the diagonal PA matrix by applying the so-called ST-WF algorithm, β can be found as follows

$$P_{\mathrm{i}} = \left(\bar{\beta} - \frac{{\sigma_i}^2}{\lambda_i}\right)^{+}; 1 \leq i \leq R_H \tag{5.3}$$

Where $\bar{\beta}$ is the mean water-level that can be solved by the equation given as

$$\sum_{l=1}^{L_p} \int_{\frac{{\sigma_i}^2}{\beta}}^{\infty} \left(\bar{\beta} - \frac{\sigma_n^2}{\lambda_i}\right) f(\lambda_i)\, d\lambda_i = \mathbf{P} \tag{5.4}$$

Where $f(\lambda_i)$ is the marginal probability density function (pdf) of the random variable(λ_i). Recalling from chapter 4 (Fig. 4.2), the average sum rate performance for a single user PU MIMO link with the ST-WF algorithm outperforms both the SWF and MEB schemes.

5.3.2. Outage Probability of ST-WF

A condition exists for the ST-WF algorithm, when SDs from PU channel matrix is not high enough to properly utilize transmission power. This can result in blockage of transmission, or more specifically channel outage. The channel outage probability defined in [121] is equivalent to the probability that the largest eigenvalue of ${H_{pp}}^{\dagger} H_{pp}$ is smaller than ${\sigma_i}^2/\beta$. Since the eigenvalues $\{\lambda_i\}_{k=1}^{M}$ of ${H_{pp}}^{\dagger} H_{pp}$ are in descending order, the channel outage probability can be expressed as

$$P_{\mathrm{i}}(\sigma^2, M) = P\left\{\lambda_i \leq \frac{\sigma^2}{\bar{\beta}}\right\} \tag{5.5}$$

The exact channel outage probability is expressed in terms of the maximal eigenvalue distribution, denoted as $\varepsilon_{max}(\lambda_i)$. If $\lambda_1 = s_h t_1$, where s_h is the shadowing random variable and t_1 is the maximal eigenvalue of ${H_{pp}}^{\dagger} H_{pp}$, the distribution of t_1 denoted as $\delta_{max}(t_1)$ and can be obtained by integrating out $t_M, t_{M-1}, \ldots . t_2$, that is,

$$\delta_{max}(t_1) = \int_0^{t_1} \ldots . \int_0^{t_{M-2}} \int_0^{t_{M-1}} K_{M^{e^{-\Sigma_i t_i}}} \times \prod_{i<j} (t_1 - t_j)^2 dt_M dt_{M-1} \ldots . dt_2 \qquad (5.6)$$

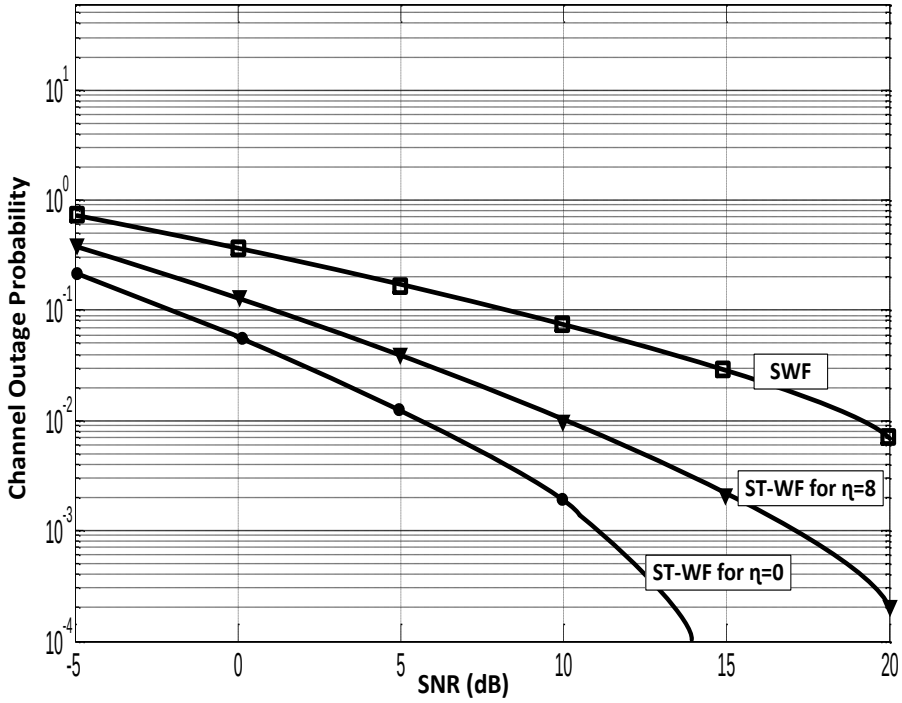

Fig. 5.2: Outage probability curves for SWF and ST-WF

Given that $\delta(t)$ was defined by [122] as the probability density function (pdf) of an instantaneous eigenvalue t, it was found in [123] that the cumulative distribution function (cdf) of λ_i is given as

$$\epsilon(\lambda_i) = \int_0^{\infty} \int_0^{\lambda/s} r(s)\delta(t)dtds \tag{5.7}$$

Differentiating (5.6) yields the pdf of λ_i given as

$$\varepsilon(\lambda_i) = \frac{10}{\rho log 10\sqrt{2\pi}} \int_0^{\bar{\beta}} \delta_{max}\left(\frac{\lambda_i}{s}\right)\frac{1}{s^2} e^{-(10log_{10}s)^2/2\rho^2} ds \tag{5.8}$$

Similarly, $\varepsilon_{max}(\lambda_i)$ can be calculated with t and $\delta(t)$ being replaced by (t_1) and $\delta_{max}(t_1)$ respectively. Thus, the channel outage probability becomes

$$P_{\text{out}}(\sigma^2, M)$$

$$= \int_0^{\frac{\sigma_i{}^2}{\bar{\beta}}} \varepsilon_{max}(\lambda_i)d\lambda$$

$$= \frac{10}{\rho log 10\sqrt{2\pi}} \int_0^{\frac{\sigma_i{}^2}{\bar{\beta}}} \int_0^{\infty} \delta_{max}\left(\frac{\lambda_i}{s}\right)\frac{1}{s^2} e^{-(10log_{10}s)^2/2\rho^2} dsd\lambda_i \tag{5.9}$$

Given the closed-form nature of the outage probability calculations, solving for $\delta(t)$ is seen to be computationally complex, and as such, only an approximated value of $\delta(t)$ will be utilized to simplify the calculation of $\bar{\beta}$.

The achievable spectral efficiencies per antenna of the two cases of SWF and ST-WF are compared by Monte Carlo simulations performed over 10^6 channel realizations.

Since we are considering practical multi-antenna systems where the channel coefficients fluctuate relatively fast, their antennas may exhibit strong correlation among fading channels, which implies that the channel's spatial correlations will typically change slowly, even when the channel coefficients fluctuate relatively fast [124]. The channel's spatial correlation is considered as a slowly varying effect similar to log-normal shadowing.

Therefore, the Rayleigh MIMO channel has variance of $1/2$ for both real and imaginary parts with a standard deviation of $\eta = 0$ for a pure Rayleigh fading scenario, and $\eta = 8$ for log-normal distribution [125].

With the average power P set to be 1, Fig. 5.2 shows the channel outage probabilities for both WF techniques for 2×2 Rayleigh channels but with and without shadowing. For $\eta = 8$, it can be seen that the SWF technique incurs a higher channel outage probability than the ST-WF technique. The case of pure Rayleigh fading for the ST-WF technique results in lower channel outage because the increase of η in log-normal shadowing conditions changes much slower than fast fading. Therefore, the distribution of the shadowing variable dominates the outage probability.

The conservative approach in terms of the number antennas (i.e. the 2×2 setup) at each SU-Tx also accounts for the outage probabilities of both cases, as was observed in [76], [77]. The general observation is that as the number of antennas increases, the channel outage probability decreases to such an extent that the outage probability for a 30×30 SU-Tx antenna set becomes zero for Rayleigh fading channels [76].

Due to the high channel outage probability, the transmission of ST-WF is similar to block transmission. For SWF, the transmission mode is continuous for every channel realization since the SU-Tx always has power to transmit. Hence ST-WF is more suitable for burst mode transmission when the channel gain distribution has a heavy tail, and SWF is preferred for continuous transmission when the channel gain distribution is close to Rayleigh or is unknown.

5.4.Opportunistic Interference Alignment

The proposed approach will be divided into two phases, the first being the sensing phase and the second being the interference alignment phase.

5.4.1. The Sensing phase

The SUs are always looking for TOs to gain access to the PU's channel [96] – [100] and will always opportunistically make use of the licensed spectrum as long as the TOs are available. This is based on the assumptions made about the system model that the PU – SU link is assumed to be operating as a MIMO broadcast (BC) channel with the PU seemingly broadcasting to many SUs, given that capacity benefits can be achieved by simultaneously transmitting to multiple users [26], [31].

At low SNR, the ST-WF algorithm allocates all power to the strongest R_H parallel channels while at high SNR, it allocates equal power to each of the R_H channels. The strongest channels are the m_1 used dimensions, while the others can be classified as the $N_1 - m_1$ unused dimensions or TOs. The SUs make independent decisions about the unused $N_1 - m_1$ dimensions.

Each SU senses the absence or presence of the unused TO such as is the case in conventional energy detection theory [4], [46], where each SU makes its local decisions by comparing its observational value with a pre-fixed threshold β, as shown in Fig. 5.3(a), and a decision is made when E_h is greater or less than the threshold value $\bar{\beta}$ under the following binary hypothesis test [22]:

$$\begin{cases} H_0;\ m_1\ eigenmode\ used\ by\ PU \\ H_1; N_1 - m_1\ eigenmode\ unused\ by\ PU \end{cases} \tag{5.10}$$

Naturally, the success of the SU communication depends on the availability of unused DoFs and as shown in the work in [74], a fast sensing method based on a generalized likelihood ratio test (GLRT) can be implemented in two phases to more accurately decide the absence of individual PU streams thereby accurately determining the availability of unused. In this chapter, a double threshold method as shown in Fig. 5.4(b) is introduced, where two thresholds are used to help the decision of the SU [107], [108].

The WF solution can be thought of as tracing out the bottom of a vessel or curve. If K units of water per sub-carrier are filled into the vessel, the depth of the water at sub-carrier n is the power allocated to that sub-carrier, and λ^{-1} is the height of the water surface of sub-carriers (which are ideally placed to be below the water level β that has been solved to satisfy the power constraint). The sub-carriers in which the bottoms of their vessels are above the water and no power is allocated to them are the unused SD. The condition for the conventional detection method states that "if the energy value E_i exceeds β, then the SU reports H_1. If E_i is less than β, SU reports H_0. However, there are some sub-carriers that are just slightly below the water level i.e. $\dot{\beta}_2$, that the normal single threshold detection classifies as used. However, the channels of these sub-carriers are actually too poor for it to be worthwhile for transmission by the PU [126], with the same applying for the reverse situation of the sub-carriers being slightly above water-level ($\dot{\beta}_1$), which are classified as unused.

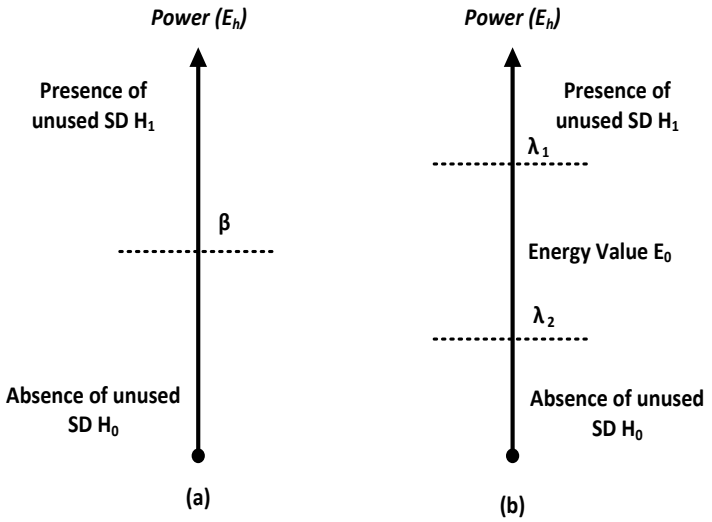

Fig. 5.3: Double detection

Therefore, the double detection technique states that if E_i is between $\dot{\beta}_1$ and $\dot{\beta}_2$, then the SU also reports this observational energy value i.e. E_i Hence, the FC receives two kinds of information; local decision and the observational value of the SU.

It is assumed that each secondary user has identical threshold values. If E_i satisfies$\dot{\beta}_1 < E_i < \dot{\beta}_2$, then the ith SU sends the measured energy value E_i to the FC. Otherwise, it reverts back to reporting its local decision L_i according to E_i, i.e. the conventional detection technique. Each SU sends a summary of its own observations to the FC in the form of P_{md}, P_f.

Let R_i denote the information that the FC receives from the i^{th} SU given by

$$R_i = \begin{cases} E_i & \dot{\beta}_1 < E_i \leq \dot{\beta}_2 \\ L_i & otherwise \end{cases} \tag{5.11}$$

and

$$L_i = \begin{cases} H_0 & 0 < E_i \leq \beta \\ H_1 & E_i > \beta \end{cases} \tag{5.12}$$

Hence the FC collects their observational values and makes an upper decision on availability of used and unused SDs. The FC then uses the hard combination fusion rule [9], [21], [46] for making the final decision based on the received information. This work utilizes probability of missed detection as one of the parameters for measuring performance.

It can be observed that the simulation results in fig. 5.5 are quite optimal yielding near perfect results when sensing ONLY for TOs.

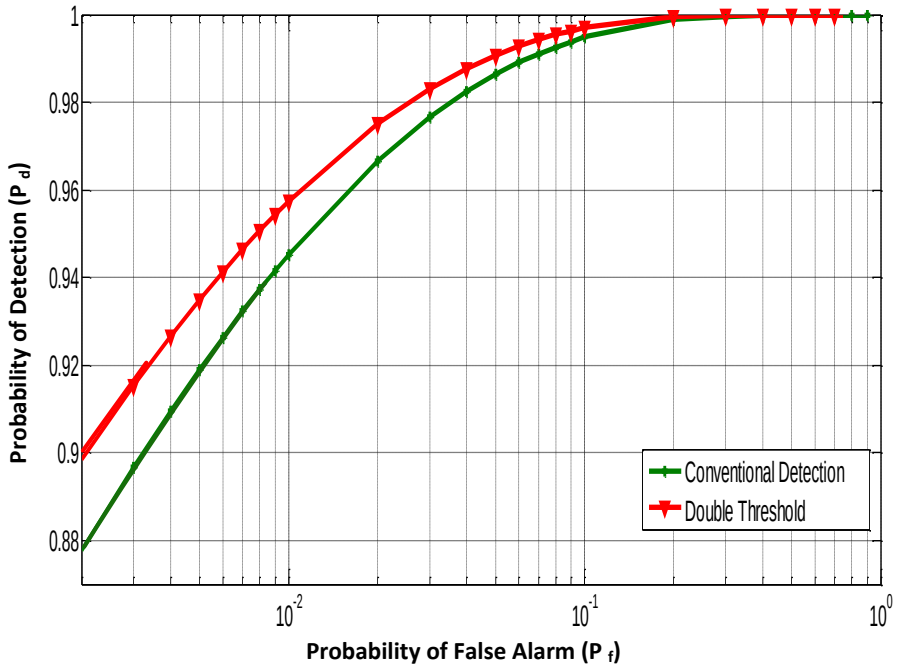

Fig. 5.4: Performance comparison of a conventional ED and a double threshold ED scheme

Fig. 5.4 illustrates that the detection probability of the proposed double threshold CSS scheme increases compared with the conventional detection scheme. Fig. 5.6 illustrates the performance variation of the P_d in relationship to SNR (dB) with multiple cognitive relays (2, 4 and 6). It can be observed that by increasing the number of SUs, P_d is increased. Additionally, the P_d increases as the SNR increases, which is consistent with performance criteria in CR networks.

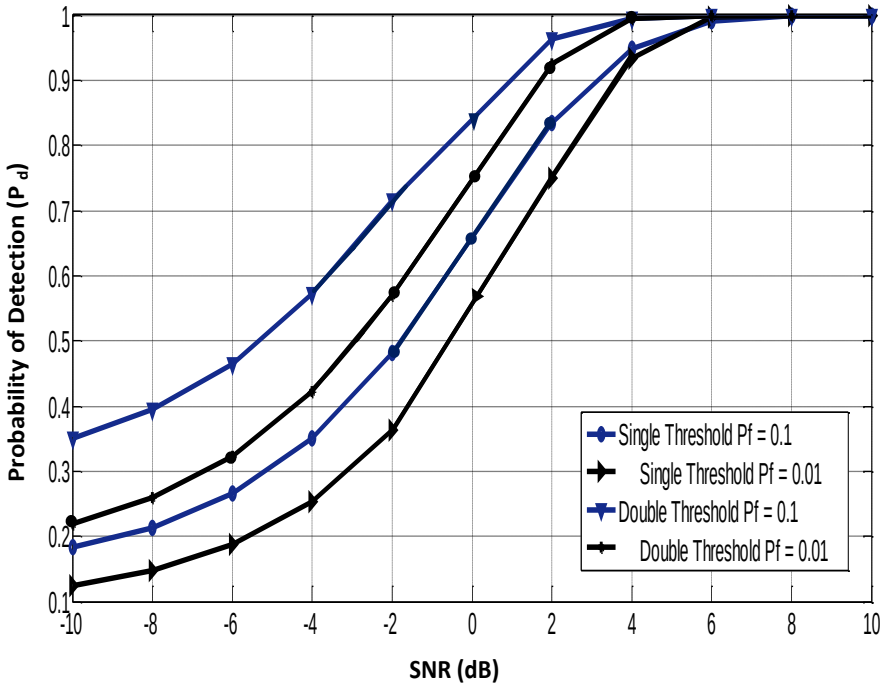

Fig. 5.5: P_d vs. SNR with P_f = 0.1 and 0.01 using a conventional ED and a double threshold ED with $R = 5$ scheme.

5.4.2. The Interference Alignment Phase

The main goal of this subsection is to derive appropriate pre- and post-coding matrices which align the SU transmissions to the $N_1 - m_1$ unused dimensions. In order to achieve that, the ST-OIA strategy was proposed in chapter 4, in which three separate conditions must be satisfied. The cognitive IA problem is formulated by defining the required conditions for IA. Given that the received signal at the ith receiver due to the jth transmitter lies in the subspace spanned by the columns of $H_{ij}V_j$, the SU-Tx's are guaranteed not to generate any interference on the PU-Rx as long as the following precoding and post-processing condition are met

$$U_{pp}^{H} H_{pj} V_j = 0_{d_p}; \quad \forall_i = 1, \ldots \ldots K \tag{5.13}$$

$$U_i^{H} H_{ip} V_{pp} = 0_{d_i}; \quad \forall_i = 1, \ldots \ldots K \tag{5.14}$$

Equation (5.13) thus guarantees the PU link achieves similar data rates as an equivalent single-tier system despite the opportunistic transmission of the SUs, while (5.14) ensures that interference from each SU-Tx is aligned at the PU-Tx, thus satisfying **the first condition** as defined in Chapter 4 (where d_i is defined as the DoF [8]).

The second condition requires that the SU and PU signals be aligned to orthogonal subspaces at not only the PU receiver, but the SU receiver as well, thus a different strategy was then used to design the SUs post-coding matrix in order to satisfy the second interference constraint. The first part of this constraint defined in (5.14) ensures that interference from each SU-Tx is aligned at the output of its corresponding unintended receivers.

$$U_i^H \boldsymbol{H_{ij}} V_j = 0_{d_p}; \quad \forall_i = 1, \ldots \ldots . K \tag{5.15}$$

$$rank\{U_i^H \boldsymbol{H_{ii}} V_i\} = d_i; \quad \forall_i = 1, \ldots \ldots . K \tag{5.16}$$

Similar to(5.13), the constraint in (5.15) guarantees that the ith SU can achieve d_i DoF. However, because this work consists of multiple SUs, **the third condition** that must be satisfied requires that ALL the SUs do not impose any interference on the PU receiver. Similar to the approach proposed in [64], [101] this work proposes to perform IA with user selection in order to optimize the performance of this third condition.

While the work done in [102] – [105] rely strictly on the feasibility conditions of IA [49], [50] to ensure multiple SUs are aligned along the PU null spaces, the number of SUs that can actually be aligned at the PUs null spaces is generally limited by the spatial dimensions available for IA based on the number of antennas at the PU-Rx. Therefore simultaneously aligning all SUs at the PU-Rx is not always feasible for typical user loads. Instead of

attempting to align the set of SUs at every PU, this work proposes an efficient clustering strategy for the SU selection.

5.4.3. The SU Clustering

The objective of this clustering strategy is to gather SUs with similar locations i.e. the SUs that are closest to the FC are aligned at each PU-Rx, into the same cluster. Its operation is similar to [128], but without making clear distinctions between cluster heads and users. Typically, the SUs are elected by the FC in a centralized way. In order to select appropriate SUs, the FC collects information from each SU node such as the distance from FC and the SUs received signal power from PU. Based on the information gathered, the FC elects the SUs that will form a cluster according to a given election algorithm and broadcasts the election to all nodes. The message broadcasted contains not only the node ID of elected SU but also the information of time synchronization, resource allocation and the maximum number of permitted access nodes in one cluster. The number of nodes in a cluster is limited to avoid too many nodes crowding in one cluster. Let Δ denote the average distance from nodes to FC, where the selected SUs are expected to be located at minimal Δ away from FC. The SU election algorithm is described as follows:

(I).Initialization: Calculate Δ of all SUs from the FC and place nodes in ascending order of Δ in a queue. Choose $2k$ nodes with the shortest Δ in the queue as a set of candidate SUs to form clusters denoted as C_i.

(II).Randomly assign K nodes as SU set from C_i where $\mathsf{C}_i = \{i_1, \cdots, i_k\}$ and initialize $\bar{m} = \{\bar{m}_1, \cdots, \bar{m}_k\}$, where $\bar{m}_k = \vec{m}_{ik}$

(III).Allocate each node into the cluster, where

$$k = \arg \min_{1 \le k \le K} (|\vec{m}_i - \bar{m}_k|), i\ 1, 2 \quad (5.17)$$

Where $\bar{m}_i$ denotes the observation vector for each given SU node i. For each cluster, update $\bar{m}_k$ by averaging $\overrightarrow{m}$ of all nodes in cluster *k*. Similarly, update the node ID of each selected SU as

$$i_k = \arg \min_{i \in C_{can}} (|\vec{m}_i - \bar{m}_k|) \quad (5.18)$$

And then *return to Initialization.* Else, *GOTO Step IV*.

(IV). Restore all node IDs of selected SUs $i_k, k = 1 \cdots K$ where i_k denotes the node ID of each SU *and K* is the number of cluster obtained.

The number of SUs aligned at each PU-Rx cannot exceed $n = 2$, which is introduced to control the maximum number of elements of each set. It should be noted that limiting the selection of SUs to a bare minimum can negate the benefits of multi-user diversity. However, our selection scheme will be justified in section 5.5 of this chapter.

5.4.4. Feasibility conditions of IA

This section discusses the feasibility of the proposed method as well as the conditions for perfect IA. The conditions for which the system is proper are first determined by establishing that the number of variables to be determined is greater than or equal to the number of equations in the IA system. In order to find the number of equations, we reformulate the IA conditions in [128] as the follows:

$$d_i \le min\left\{M_i - \left(\sum_{j=1}^{K_p} d_j\right), N_i - \left(\sum_{j=1}^{K_p} d_j\right)\right\} \quad (5.19)$$

Our model looks to design a cluster of SUs based on geographical proximity as discussed in section 5.4.3 above, and for the sake of simplicity, we limit our initial design to two SUs per cluster with each SU having two Tx/Rx antennas, and as is generally well known from the Bezout's theorem that generic polynomial systems are solvable if and only if the number of equations does not exceed the number of variables [128]. As such, signal space IA problems can either be proper or improper [63]. Thus, from the Theorem of Proper Characterization as described in Chapter 4 (subsection 4.4.3), "a symmetric system $(M \times N, d)^K$ is proper if and only if

$$N_v \geq N_e \Rightarrow M + N - (K+1)d \geq 0 \tag{5.20}$$

5.5.Opportunistic Interference Alignment with Space-time Coding

5.5.1. Background

In [12], a source covariance matrix was chosen in which the SU-Tx can allocate power to maximize its achievable rate. This was achieved by using UPA and OPA schemes. In the UPA case, the opportunistic SU-Tx does not perform any optimization on its transmit power, but rather uniformly spreads its total power among the previously identified TOs, which saturates the transmit power constraint [12]. The OPA scheme, on the other hand takes on a WF solution with an $Nd_i \times L_2$ SVD matrix such that the OP can be rewritten as

$$\max_{P_i} \log_2 \left| I_{d_i} + \frac{1}{\sigma_i^2} H_{ii} U_i^H P_i V_i H_{ii}^H U_i \right.$$

$$s.t.(P_i) \geq Trace(V_i^H P_i V_i) \leq P_i \tag{5.21}$$

Given that the SVD of the matrix $U_i^H H_{ii} V_i$ is given as $\tilde{V}_i^H \Sigma_i \tilde{U}_i$, where the columns of $\tilde{U}_i$ and $\tilde{V}_i$ contain the singular vectors and Σ_i is the $Nd_i \times L_2$ diagonal matrix containing the

corresponding singular values $\{\gamma_i\}$. The optimal solution is thus given as $\tilde{V}_i^H \tilde{P}_i \, \tilde{U}_i = P_i$. The diagonal matrix $\tilde{P}_i$ is used to represent the OPA solution and the optimal values of its diagonal elements translates into the WF solution

$$\tilde{P}_i = \left(\bar{\beta}_i - \frac{{\sigma_i}^2}{{\gamma_i}^2} \right)^+ \tag{5.22}$$

where $\bar{\beta}_i$ is the lagrangian multiplier chosen to satisfy (5.21). The optimal SU precoder described above turns out to be a generalized beamformer formed using the eigenvectors matrices of the optimized channel at the SU-Tx, which could be used to enhance throughput as shown in the work done in [75], where even after the SUs use a covariance matrix to maximize their throughput, a TBF power-allocation strategy is proposed to improve both the spectral and power efficiency of the SUs. The TBF scheme is an effective tool for saving SU-Tx power and improving spectrum efficiency in poor channel conditions. With this scheme, the SUs transmit pilot signals at the start of each transmission block which are used by each SU-Rx to estimate their own channel matrix (local CSI). This is then fed back as M_k bits (which denotes the SU-Tx antenna index) to the corresponding SU-Tx as long as the largest eigenvalue of the channel matrix is greater than a pre-specified threshold level λ_{TH}. The selected SU-Tx puts all its power on the antenna corresponding to the feedback index when $\lambda_{k,max} > \lambda_{TH}$; otherwise it remains silent.

If the receiver can acquire the CSI as reliably as shown in [75] or when partial CSI is available at the transmitter, coherent detection along with orthogonal space–time block coding (STBC) [84], [110], [111] can be employed to increase data rate leading to the so-called two-directional (2D) eigen-beamformer (which consists of parallel transmissions equipped with STBC across optimally loaded eigen-beams). With minimal variation in

computational complexity compared with traditional one-directional (1D) beamforming, 2D beamforming was shown to achieve better performance [110] – [113].

In addition to network throughput, reliability in terms of diversity gain is another aspect of performance measurement for the SUs. When channels experience fading, the SNR level at the Rx becomes low and is usually dominated by outage events. As a result, techniques such as Alamouti codes and STBC in point-to-point MIMO channels [113] have been proposed to explore the spatial diversity gain. Recently, the work in [113] presented the scenario where a trade-off between symbol-rate, diversity, and IA was possible in a multi-user network, thus motivating the work in [114], [115]. Leaning on Alamouti's property of improving the diversity of double-antenna systems [116], the work in [113], [114] proposed a new IA scheme that uses Alamouti codes to achieve full transmit diversity without losing rate, i.e., a diversity gain of two, at the same symbol-rate from node-to-node. The Tx's in this proposed scheme only require CSI from themselves to both Rx's instead of global channel information as assumed in [10].

It is clear that the scope of the literature on wedding optimal precoding/eigen-beamforming with orthogonal STBC to improve throughput does not delve into the full process of IA i.e. zero forcing (ZF) at the multiple Rx's. The scope of the literature on the latter i.e. achieving higher diversity gain on, does incorporate STBC with beamforming where ZF is used to decouple symbols at the interfering users, but obviously without optimal precoding. As such, this work found an opportunity to propose an IA scheme where each Tx needs only channel information from itself to both Rx's that can achieve the same symbol-rate as the scheme in [10] but with a higher diversity gain. Given the fact that Alamouti codes achieve full transmit spatial diversity in point-to-point MIMO systems [116], this work incorporates Alamouti codes in the design of optimal precoding matrices, the product of which is a 2D eigen-

beamformer without rate reduction. Since the equivalent channels are linearly independent, ZF is conducted at each Rx to cancel interference and separate useful symbols to obtain symbol-by-symbol decoding.

5.5.2. STBC BEAMFORMING IA PROCESS

The initial approach considered a two-user IC as shown in Fig. 5.7 where H_1, G_1, H_2, G_2 are used to denote the 2×2 channel matrices where the channel matrices H_1 and G_1 are perfectly known at SU-Rx 1, and H_2 and G_2 are known at SU-Rx 2 and each of the entries are i.i.d. Gaussian distributed. It is also assumed that the channels are block fading (or constant), i.e., all channels keep unchanged during transmission. Two double antenna Tx's send symbols to two double antenna Rx's where the desired signals at SU-Rx 1 are only from SU-Tx 1 while the interference at SU-Rx 1 only comes from SU-Tx 2 [113]. Each of the two Tx's have independent symbols, generated from modulators with fixed BPSK constellation for each of the two Rx's.

At a given symbol period, two signals are simultaneously transmitted from the SU-Tx antennas, denoted as s_{ij}.

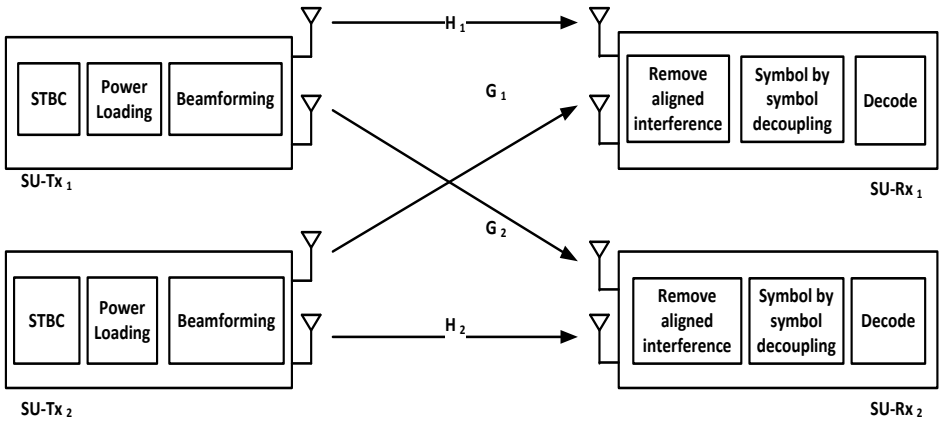

Fig. 5.6: STBC process

At the next symbol period, two complex conjugate signals are then transmitted from the two antennas of the SU, denoted as s_{ij}^{*}. The superscript in s_{ij}^{k} denotes the index of symbol and the first subscript i denotes the index of the transmitter and j the index of receiver.

SU-Tx i linearly combines four symbols s_{ij}^{k} and generates a block code X_i. The equivalent transmitted vectors can be expressed as

$$X_1 = V_{11}\begin{bmatrix} s_1^{11} & s_2^{11} \\ -s_2^{11*} & s_1^{11*} \end{bmatrix} + V_{12}\begin{bmatrix} s_1^{12} & s_2^{12} \\ -s_2^{12*} & s_1^{12*} \end{bmatrix} \tag{5.23}$$

$$X_2 = V_{21}\begin{bmatrix} s_1^{21} & s_2^{21} \\ -s_2^{21*} & s_1^{21*} \end{bmatrix} + V_{22}\begin{bmatrix} s_1^{22} & s_2^{22} \\ -s_2^{22*} & s_1^{22*} \end{bmatrix} \tag{5.24}$$

where V_{ij} denotes the beamforming matrix from Tx j to Rx i. The symbols s_{ij}^{1} intended for SU-Rx 1 become interference for SU-Rx 2, and $\bar{v}_{11}$ aligns them with SU-Rx 2. The decompositions in (4.18) and (4.19) for the precoding and post-processing matrices of the SUs can be modified due to the presence of the PU link to get the following equations

$$U_i^H H_{ij} D_{pl} \tilde{V}_j = 0_{d_i \times d_j} \quad \forall_{i,j} = 1, \ldots\ldots K, i \neq j \tag{5.25}$$

$$rank\{\tilde{U}_i^H H_{ii} D_{pl} V_i\} = d_i \quad \forall_i = 1, \ldots\ldots K \tag{5.26}$$

The modified equations in (5.25) and (5.26)represent a standard IA problem with the variables $\{V_i\}_{i=1}^{K}$ and $\{U_i\}_{i=1}^{K}$. Given that $V_i = \in \mathbb{C}^{(M_i - d_0)\times d_i}$ and $U_i = \in \mathbb{C}^{(N_i - d_0)\times d_i}$ as being the beamforming matrices at the ith SU-Tx and SU-Rx, (5.25) ensures that all the interfering signals at ith SU-Rx lie in the subspace orthogonal to $\tilde{U}_j$, while (5.26) assures that the signal subspace $H_{ij} D_{pl} \tilde{V}_j$, has dimension d_k and is linearly independent of the interference subspace. The constant D_{pl} is a diagonal matrix which contains power loading

coefficients. By exploiting the knowledge of the covariance matrix, the power loading coefficients will be derived based on the SER values. From [12], the SNR of the covariance matrix P_i for a fixed channel realization can be found as follows:

$$\gamma = \sum_{\mu=1}^{N_t} \varphi_\mu \left|h_\mu\right|^2 \frac{E_s}{N_0} \tag{5.27}$$

where N_t denotes the independent eigen value channels, h_μ is the Rayleigh distribution of the μth sub-channels, φ_μ denotes the μth eigenvalue of $U_i^H H_{ii} V_i$ that is non-negative: and $\varphi_\mu \left|h_\mu\right|^2 E_s/N_0$denoting the μth sub-channel's SNR [110].

This implies that we can approximately compute the SER using [110]

$$P_{SER} = \frac{1}{\pi} \int_0^{\frac{(M-1)\pi}{M}} \prod_{\mu}^{N_t} I_\mu \left(\frac{\varphi_\mu E_s}{N_0}, g_{BPSK}, \theta \right) d\theta \tag{5.28}$$

where $g_{BPSK} = sin^2 \frac{\pi}{\mathcal{M}}$, $I_\mu(x, g, \theta) = \mathcal{M}$ is the moment generating function of the probability density function of the Rayleigh distribution. The power loading coefficients contained in the diagonal matrix D_{pl} based on the approximate SER values are shown to also come very close to the actual SER values at low SNR

$$P_{SER} = \frac{(M-1)}{M} \frac{1}{\prod_{\mu=1}^{N_t} \left[1 + \frac{g_{BPSK} \lambda_Q E_s D^2{}_{pl}}{2N_0}\right]} \tag{5.29}$$

where λ_Q is the eigenvalue of the channel covariance matrix Q. To select power loading coefficients, we now formulate the following optimization problem:

$$\max_{D} \sum_{\mu=1}^{N_t} \log\left[1 + \frac{g_{PSK}\lambda_Q E_s {D^2}_{pl}}{2N_0}\right]$$

$$subject\ to \sum_{\mu=1}^{N_t} {D^2}_{pl} = 1 \tag{5.30}$$

Using the Lagrange multiplier method, we can find power loading coefficients as follows:

$${D^2}_{pl} = \frac{1}{\bar{N}_t} + \frac{N_0}{g_{PSK}E_s}\left(\frac{1}{\bar{N}_t}\sum_{\mu=1}^{\bar{N}_t}\frac{1}{\lambda_{Qj}} - \frac{1}{\lambda_{Qi}}\right) \tag{5.31}$$

where $\bar{N}_t (0 < \bar{N}_t < N_t)$ is the number of beamformers that transmit signals, given the transmitted power budget E_s. Each Tx sends two symbols to one Rx. The transmitted block codes are designed as follows:

$$X_1 = \sqrt{\frac{\rho}{\mu}}\left(\begin{bmatrix} s_1^{11} & s_2^{11} \\ -s_2^{11*} & s_1^{11*} \end{bmatrix} D_{pl} V_{11} + \begin{bmatrix} s_1^{12} & s_2^{12} \\ -s_2^{12*} & s_1^{12*} \end{bmatrix} D_{pl} V_{12}\right) \tag{5.32}$$

$$X_2 = \sqrt{\frac{\rho}{\mu}}\left(\begin{bmatrix} s_1^{21} & s_2^{21} \\ -s_2^{21*} & s_1^{21*} \end{bmatrix} D_{pl} V_{21} + \begin{bmatrix} s_1^{22} & s_2^{22} \\ -s_2^{22*} & s_1^{22*} \end{bmatrix} D_{pl} V_{22}\right) \tag{5.33}$$

The coefficients ρ and μ are the average SNR and the normalization factor at each SU-Rx respectively that are introduced to ensure average energy of the coded symbols are unitary across all the antennas.

Each symbol is sent using Alamouti codes and each transmitter sends linear combinations of both the original symbol and their conjugate. To this end, X_1 is transmitted along the eigenvectors of the channel correlation matrix with power loaded on each eigenvector.

Recalling that the received $T \times 2$ signal matrix at Rx i can be represented as

$$Y_1 = X_1 H + X_2 G + W_1, \;\; Y_2 = X_1 A + X_2 B + W_2 \tag{5.34}$$

where W_j denotes the $T \times 2$ additive white Gaussian noise (AWGN) matrix at Rx j, therefore

$$Y_1 = \sqrt{\frac{\rho}{\mu}} \begin{bmatrix} s_1^{11} & s_2^{11} \\ -s_2^{11*} & s_1^{11*} \end{bmatrix} D_{pl} V_{11} \boldsymbol{H_1} + \sqrt{\frac{\rho}{\mu}} \begin{bmatrix} s_1^{22} & s_2^{22} \\ -s_2^{22*} & s_1^{22*} \end{bmatrix} D_{pl} V_{21} \boldsymbol{G_1} + W_1 \tag{5.35}$$

$$Y_2 = \sqrt{\frac{\rho}{\mu}} \begin{bmatrix} s_1^{21} & s_2^{21} \\ -s_2^{21*} & s_1^{21*} \end{bmatrix} D_{pl} V_{12} \boldsymbol{H_2} + \sqrt{\frac{\rho}{\mu}} \begin{bmatrix} s_1^{12} & s_2^{12} \\ -s_2^{12*} & s_1^{12*} \end{bmatrix} D_{pl} V_{22} \boldsymbol{G_2} + W_2 \tag{5.36}$$

Both the second terms in (5.35) and (5.36) represent interference, which then makes it clear to see how the post-processing filters of (5.25) and (5.26) align symbols s_{ij}^{22} and s_{ij}^{22*} at SU-Rx 1, while s_{ij}^{12} and s_{ij}^{12*} are aligned at SU-Rx 2.

After completing IA at both SU-Rx's, the individual symbols can be decoded using symbol-by-symbol decoding. As mentioned earlier, the Alamouti structure ensures the corresponding definite channel matrices $\bar{H}_1, \bar{G}_1, \bar{H}_2, \bar{G}_2$ at the SU-Rx retain the same structure due to the completeness of its multiplication and addition properties [116].

Therefore, s_{ij}^{11} can be decoded with the following equation:

$$s_{ij}^{11} = \arg\max_{s} \sum_{j}^{k=1} \bar{h}_k^* y_k s, \qquad k = 1,2 \tag{5.37}$$

Equation (5.37) therefore applies to the remaining symbols at SU-Rx 1 and SU-Rx 2 that result in four separate procedures for symbol-by-symbol decoding to recover the desired symbols.

5.6.Opportunistic Interference Alignment with Differential-STBC

This research endeavor, along with the other work described in [110], [116] require some form of CSI at the SU-Rx. However, channel estimation becomes difficult or requires too many training symbols, especially when the channel is rapidly changing in a mobile environment. In such cases, space–time modulation and differential space–time modulation [53], [130] are well motivated because they bypass CSI acquisition at the SU-Rx.

As such, this work considers differential space–time modulation based on orthogonal STBC, *without* partial CSI at the SU-Tx for independent, i.i.d. fading channels. One of the advantages of MIMO systems is their ability to exhibit strong correlation in the presence of fading due to multiple Tx antennas. This implies that the channel's spatial correlations in fast fading channels will still fluctuate slowly [55], [130]. Thus, while there is no knowledge of CSI in differential space–time transmission, the channel's spatial correlations can easily be estimated at the SU-Rx due to slower fluctuation and be fed back to the SU-Tx. Similar to [116], the differential modulation based on orthogonal STBC is also much easier to construct and leads to low-complexity symbol-by-symbol decoding. Given its inherent advantages, this work will consider incorporating D-STBC into the STBC beamforming solution described in 5.5.2. The following sections will look at how the DSTBC-beamforming-IA (DSTBC-BF-IA) solution can be used to save the SU-Tx power in rapidly changing channel conditions and improve the spectrum efficiency.

The schemes used in differential modulation encode the transmitted information into phase differences between two consecutive symbols i.e. the Tx first provides a set of symbols that contain no information but only serve as reference symbols that contain no information, but only serve as reference symbols for differential encoding. These reference symbols generate consecutive phase-shifted information carrying symbols, which are recovered at the Rx by

comparing the phase differences between the received symbols [101]. As an example, consider a PSK modulated symbols sequence $s(t)$ that is transmitted such that under ideal Nyquist signaling conditions the received samples can be represented by: $r(t) = s(t)h(t) + z(t)$, Where $h(t)$ represents the path gain at the t_{th} time interval and $z(t)$ denotes the corresponding noise. If the phase of $h(t)$ fluctuates rapidly and randomly with respect to t, it is impractical to estimate the channel from transitions in the carrier phase. However, if $h(t)$ fluctuates slowly enough with minimal degree of randomness such that it can be estimated over at least two consecutive symbol intervals, then phase transitions can be used to estimate the channel and thus recover the information symbols.

The spectral efficiency gain of ST-WF is typically associated with a higher channel outage probability, which sets a lower-bound on optimizing the SUs transmission rates. It is therefore necessary to find a solution that not only helps with optimizing transmission rates, but also encourages the SUs to use their power more efficiently. Thus similar to work done in [75], where the SU-Rx depends on pilot signals transmitted at the start of each transmission to estimate its own channel matrix (local CSI) and determine whether the SU-Tx remain silent or transmit, this work considers using DSTBC, but *without* local CSI at SU-Tx's for independent, identically distributed (i.i.d.) fading channels. This solution states that if the channel is approximately constant for a time at least two symbol periods without any outage i.e. within 3 dB of the coherent demodulation in Gaussian channels, then the SUs transmit. Otherwise, the SUs remain silent.

5.6.1. Differential Encoding

Extensions of differential schemes have been considered to provide simple differential encoding and decoding algorithms to either MIMO or virtual MIMO systems [49]. The key to

generating these codes depends on computing a set of coefficient vectors (R_1, R_2) and mapping a block of information bits into the coefficient vector sets.

In order to implement D-STBC for the SUs, signal transmissions begins by sending a reference codeword matrix C_0 which consists of an arbitrary pair of symbols c_1 and c_2 at time t_1 from the two SU-Tx's, followed by the related pair of symbols $-c_2^*$ and c_1^* at time t_2 that provide the receiver with a known *frame of reference* for facilitating the D-STBC process. Where the channel has a phase response that is approximately constant from one symbol period to the next defined by a threshold τ_{th}, the SU-Rx is able to decode the information in the current symbol.

Where the channel has a phase response that fluctuates from one symbol period to the next and the SU-Rx is not able to decode current symbol by comparing its phase to the phase of the previous symbol defined by a threshold τ_{th}, the SU-Rx feeds back M_{th} bits (denoting the phase index) to the corresponding SU-Tx's. For this case, the SU-Tx's puts all its power in the corresponding feedback index when $\tau_{th} > M_{th}$, implying they are free to transmit, otherwise they remain silent; thereby use their power more efficiently.

The SUs encode the data sequence in a differential manner so that the signals to be transmitted are subsequently represented as linear overlays of those times at t_1 and t_2, thus generating s_{2t-1}, s_{2t} and $-s_{2t}^*, s_{2t-1}^*$ from the two SU-Txs at times $2t-1$ and $2t$. With information bits $2m$ at the encoder used to select two complex coefficients (R_1, R_2), the modulated symbols for the next two transmissions are given as $s_{2t+1}^k, s_{2t+2}^k = R_1(s_{2t-1}^k, s_{2t}^k) + R_2(-s_{2t}^{k*}, s_{2t-1}^{k*})$. The transmitter therefore sends s_{2t+1}^k and s_{2t+2}^k at time $2t+1$ from antenna one and two, and sends $-s_{2t+2}^{k*}$ and s_{2t+1}^{k*} at time $2t+2$ from antennas one and two respectively.

This process is mapped into the coefficient vector sets and inductively repeated until the end of the frame, the mapping process computing the transmitted symbols for different combinations of decision statistics until the end of the transmission.

Specifically, the information matrix s_{ij}^{k} is transmitted according to its matrix structure defined in (5.37), first collected in an $N \times N$ STBC matrix comprising the linear combinations of both original symbol and their conjugate as follows

$$s_{ij} = \sqrt{\frac{\rho}{\mu}} \sum_{p=1}^{p} \left(s_{ij}^{k} + j s_{ij}^{k*} \right) \tag{5.38}$$

It follows that the $N \times N$ D-STBC matrix C_0 can be written as follows

$$C_0 = s_{ij}^{k} C_{k-1}, \quad i > 0 \tag{5.39}$$

where the codeword matrix also has the following structure

$$C_{k(i,j)} = \begin{bmatrix} c_1^{ij} & c_2^{ij} \\ -c_2^{ij*} & c_1^{ij*} \end{bmatrix} \tag{5.40}$$

Similar to the STBC solution, C_0 will be transmitted along the eigenvectors of the correlation matrix with power loaded on each channel eigenvector. As such, the transmitted signal at the ith block can be expressed as:

$$X_i = \sum_{K=i,j}^{K} \sqrt{\frac{\rho}{\mu}} C_0 V_{ij} D_{pl} \tag{5.41}$$

where D_{pl} contains power loading coefficients. Due to the unitary property of the codeword matrix $C_{k(i,j)}$ and the works in [116], [130] the SU-Tx power remains unchanged, implying

that the fundamental differential transmission equation is not changed by the power loaded eigen-beamforming matrices.

Similar to the STBC-Beamforming solution, the SER is also used to derive power loading coefficients using $(5.29) - (5.31)$. Using the Lagrange multiplier method, we can find power loading coefficients as follows [37]:

$$D^2{}_{pl} = \frac{1}{\bar{N}_t} + \frac{2N_0}{g_{PSK}E_s}\left(\frac{1}{\bar{N}_t}\sum_{\mu=1}^{\bar{N}_t}\frac{1}{\lambda_{Qj}} - \frac{1}{\lambda_{Qi}}\right) \tag{5.42}$$

Equation (5.42) above is similar to [33] for *coherent* STBC except for a factor 2 in the second term, which is used to compensate for the 3 dB discrepancy between the P_{SER} for D-STBC and its counterpart in coherent STBC [130].

5.6.2. Differential Decoding

The first step towards differential decoding entails removing the aligned interference. Given that the equivalent channels spanned by the useful signals have Alamouti structure, and since the equivalent channels for interference I_1 and I_2 are constant, the aligned interference $I1$ and $I2$ can simply be cancelled.

From(5.35) and (5.36), $I_1 = \sqrt{\frac{\rho}{\mu}}\begin{bmatrix} s_1^{22} & s_2^{22} \\ -s_2^{22*} & s_1^{22*} \end{bmatrix} D_{pl}V_{21}G_1$ and

$$I_2 = \sqrt{\frac{\rho}{\mu}}\begin{bmatrix} s_1^{12} & s_2^{12} \\ -s_2^{12*} & s_1^{12*} \end{bmatrix} D_{pl}V_{22}G_2$$

For clarity, we first consider a single Rx antenna. The received data are processed by computing the differential phases between any two consecutive symbols.

The following parameters are defined as follows

$Y_k =$ Received signal at time , $W_k =$ Noise sample at time t, $H_i, H_j =$ Fading coefficients from the two SU-Tx to the SU-Rx antenna, which also has the following structure

$$H = \begin{pmatrix} h_1 & h_2^* \\ h_2 & -h_1^* \end{pmatrix}$$

and

$$W_{2t-1} = (n_{2t-1}, n_{2t}^*)$$
$$W_{2t} = (n_{2t}, -n_{2t-1}^*)$$

The signal received is given in vector form by the following equations

$$Y_k = \sum_{k=i,j}^{K} \sqrt{\frac{\rho}{\mu}} C_0 V_{ij} D_{pl} H_{ij} + W_{ij} \tag{5.43}$$

The received signal matrix Y_k is measured at the SU-Rx, while the codeword matrix C_k, the radio channel transfer matrix H_{ij} and the noise W_{ij} are totally unknown for the SU-Rx. The decoding process is performed by multiplying the Rx signal matrix Y_k by the Hermitian of the previous receive signal matrix Y_{k-1}; which is given as follows

$$\begin{aligned} D_k &= Y_k \cdot Y_{k-1}^* \\ &= \left(C_k H_{ij} + W_{ij}\right) \cdot \left(C_{k-1} H_{ij-1} + W_{ij-1}\right)^* \\ &= C_k H_{ij} H_{ij-1}^* C_{k-1}^* + noise \end{aligned} \tag{5.44}$$

where D_k denotes the demodulation matrix. Assuming that $H_{ij} \approx H_{ij-1}$ *i.e.* the channel remains fixed over two successive code blocks:

$$H_{ij}H_{ij-1}^{*}$$

$$= \left(\left|h_{1,ij}\right|^2 + \left|h_{2,ij}\right|^2\right).I_2 \tag{5.45}$$

Therefore, D_k can be written as:

$$D_k = \left(\left|h_{1,ij}\right|^2 + \left|h_{2,ij}\right|^2\right)S_{ij} + W_{ij} \tag{5.46}$$

Where $D_k = Y_k \cdot Y_{k-1}^{*}$ has the same structure as the information matrix S_{ij} and the codeword matrix C_k such that:

$$D_k = \begin{pmatrix} d_{1,k} & d_{2,k} \\ -d_{2,k}^{*} & d_{1,k}^{*} \end{pmatrix}$$

It can be seen from (50) that D_k is proportional to S_{ij} and that the real valued scaling factor given as $\left(\left|h_{1,k}\right|^2 + \left|h_{2,k}\right|^2\right)$ is unknown at the SU-Rx, making it impossible for the SU-Rx to estimate the absolute Tx power. However, the relative phase and amplitude of the coefficients of S_{ij} can be recovered.

Therefore, the information symbols can be estimated according to (5.47) and (5.48) below, directly from the demodulation matrix D_k and then processed by a maximum likelihood demodulation technique, which chooses the closest coefficient vector to the decision statistics [53]:

$$\hat{s}_{1,ij} = \frac{d_{1,k}}{\sqrt{\left|d_{1,k}\right|^2 + \left|d_{2,k}\right|^2}} \tag{5.47}$$

$$\hat{s}_{2,ij} = \frac{d_{2,k}}{\sqrt{\left|d_{1,k}\right|^2 + \left|d_{2,k}\right|^2}} \tag{5.48}$$

5.7.Simulation Results and Analysis

In this section, numerical results have been provided to evaluate the performance of the OIA-STBC algorithm against the SU-IA-OPA and SU-IA-TBF algorithms. It is quite clear from the results obtained that this scheme provides improved throughput when compared with other schemes.

The performance curves of conventional STBC with coherent detection are shown to be parallel to those of the DSTBC schemes, indicating that the DSTBC schemes also achieve full transmit diversity due to the orthogonal designs. Traditionally, the one drawback of the differential scheme is that it is almost always 3 dB worse than the respective STBC with coherent detection since it does not require any CSI. The inherent requirement of perfect CSI by the coherent STBC scheme introduces channel estimation errors as well as additional power consumed by training symbols, particularly in this work that employs optimal power-loading, making it inapplicable to fast fading channels. DSTBC on the other hand does not require CSI at the SU-Rx, making it well suited to perform well in fast fading channels.

In our simulations, both coherent STBC and DSTBC use BPSK, where the channel is both fixed and independent over a pair of successive blocks in each run (i.e. channel variation is negligible in two consecutive blocks) making our simulations valid for fast fading channels. As stated earlier, practical multi-antennas systems may exhibit strong correlation among fading channels, which implies that the channel's spatial correlations will typically change slowly, even when the channel coefficients fluctuate relatively fast, which is a requirement common to all differential schemes.

The SER performance curves of coherent STBC and DSTBC with beamforming with two Tx antennas and both one and two RX antennas are evaluated by simulations as shown in Fig. 5.7 below.

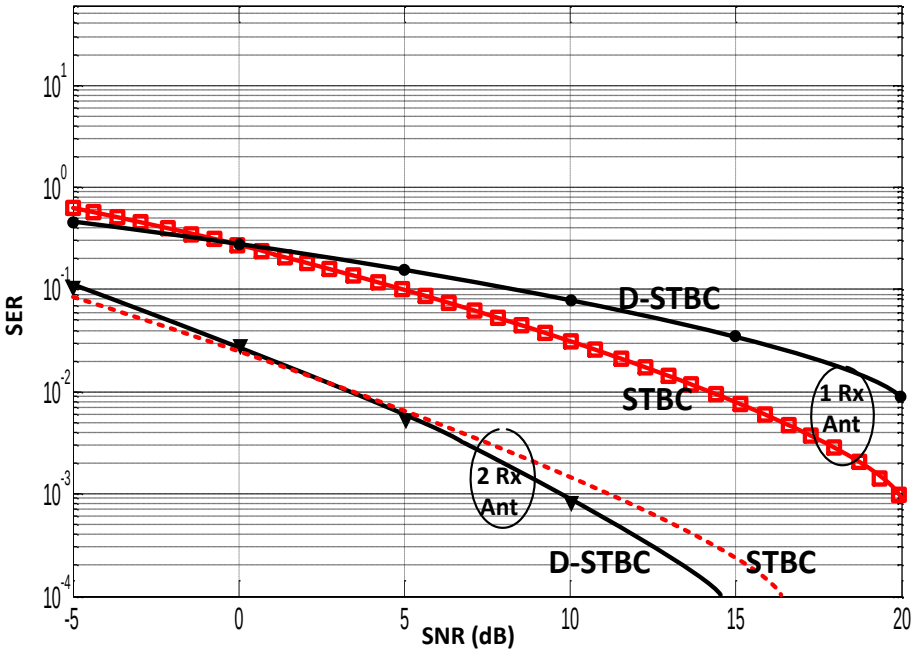

Fig. 5.7: SER Curves for coherent STBC and DSTBC-beamforming schemes

If we take into account the channel estimation error and the transmitted power consumed by training, coherent STBC with two Rx antennas shows better performance than with one Rx antenna. On the other hand, we see that for one Rx antenna, the proposed DSTBC-beamforming scheme initially outperforms the coherent STBC at very low SNR since DSTBC does not require CSI at the Rx. With two Rx antennas, the DSTBC-beamforming scheme eventually shows better performance than coherent STBC with an increasing margin as the SNR was increased. Therefore, our results demonstrate that in highly correlated channels, the proposed DSTBC modulation scheme has better or comparable error probability performance to coherent STBC, proving the point that the training symbols used in coherent STBC incur a significant loss in data rate. This is a clear demonstration that combining

DSTBC with optimally loaded beamforming offers higher data rates. The downside of this work is the significant difference of the diversity order between STBC and DSTBC. This discrepancy could most likely be attributed to DSTBC having no prior knowledge of CSI. The analysis of the performance curves presented in Fig. 5.8 and Fig. 5.9 provide further insight into the improved data rates of the DSTBC-beamforming scheme.

Monte-Carlo simulations were carried out for 2 SU pairs (Tx and Rx) and a single PU link with each node equipped with two antennas. As shown in Fig. 5.8, three separate techniques are compared namely the legacy SU-IA-PA [12], the SU-IA-TBF [22] and of course the proposed STBC-BF-IA scheme.

For the SU-IA-PA scheme, it is observed that at low and high SNR for the PU link, the performances of both the uniform PA and optimal PA are unsatisfactory and almost identical, even when the SU-Tx spreads its power amongst all the available TOs or performs optimal PA which translates into a WF solution. This poor outcome is most probably due to transmission power of the PU-Tx being at lower and higher ends of the transmit power spectrum, thus not leaving any unused SDs. Indeed, in that case, we are faced with the conventional CR system in which SUs can only utilize the PUs frequency band in an opportunistic manner to avoid imposing the interference on the PU i.e. when the PU is idle. At intermediate SNR values however, significant data rates for the IA-OPA and IA-UPA approaches are achieved by the SUs.

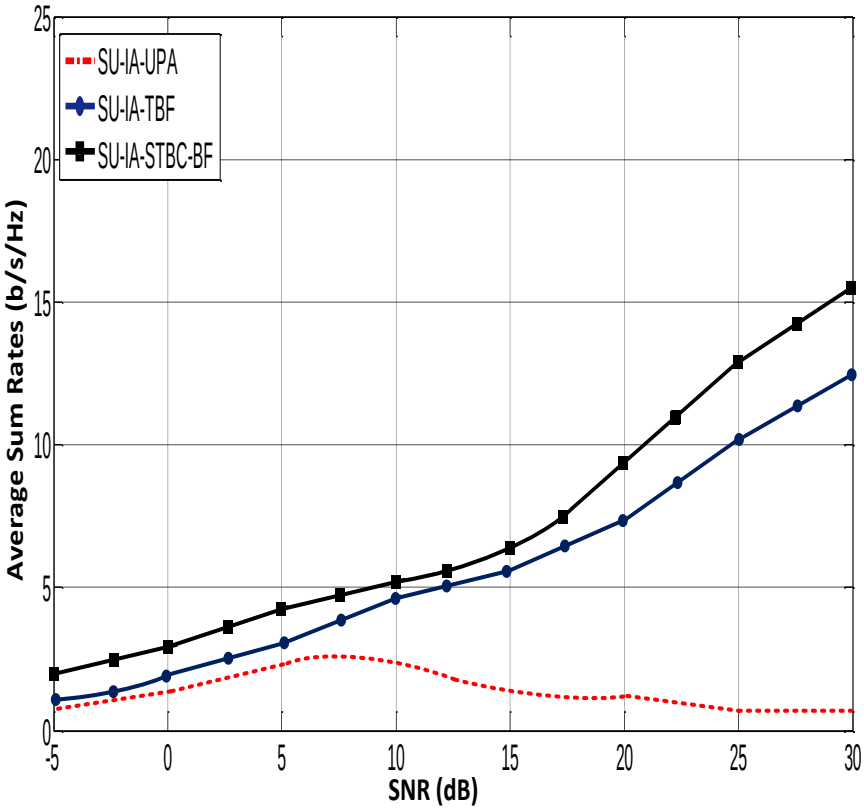

Fig. 5.8: Average Sum Rate (b/s) against SNR (dB) for two SUs

For the TBF scheme shown in Fig. 5.8, while the discrepancy in performance of the PU link optimization using the MEB technique is very little in comparison to the ST-WF algorithms (see Fig. 4.2), the throughput performance the of SUs on the other hand, increases exponentially at high SNR values when compared to the SU-IA-OPA scheme at almost no cost to the PU. The improved performance of the SUs sum rates can be attributed to two things: Firstly, the MEB algorithm ensures that at least one of the PUs eigenmode will always be available to convey the SU's data. Secondly, the SUs with the poor channel condition stay silent as per TBF to cooperate with the other SU links to enhance the performance of the network through controlling the interference. It could also be suggested that as the number of candidate SUs increases, the average sum rate also increases. It should be noted that the observations are all predicated on the fact that the achievable rates of the SUs have to be

computed using the following equation: $R_{su}(P, H_i) = logdet(I_{d_i} + \frac{1}{\sigma^2} P_i H_{ii}^H H_{ii})$ for all $i \in j$. From Fig. 5.8, the proposed STBC-BF solution clearly performs better than the TBF solution even with the TBF solution seemingly enjoying the advantage of increased number of candidate SUs and its efficient SU rate optimization scheme that is applied after threshold beamforming to help keep the sum rates above a prespecified threshold level. This improved performance is initially founded on the fact that the SU selection scheme limits the number of SUs in a cluster, which was otherwise not the case in other works such as the [22]. While an increased number of SUs can improve detection accuracy, it could also be an additional source of interference to the PU transmission. Helped by the double detection scheme, the SUs are therefore almost assured free TOs that they could align their transmission with. Secondly, the increased sum rates of this scheme is a direct manifestation of employing coherent STBC with beamforming and optimal power loading to improve reliability in terms of diversity gain without much discrepancy in terms of computational complexity.

The graph shown in fig. 5.9 demonstrates the performance comparison between SU-IA-STBC and SU-IA-DSTBC where the channel's spatial correlations are considered to have a slowly varying effect similar to shadowing.

Both the DSTBC and the STBC technique are seen to significantly outperform the SU-IA-UPA technique because implementing 2D eigen-beamforming minimizes the error probability and outperforms 1D beamforming especially at moderate to high SNR. This is indicative of the fact that for the SU-IA-UPA scheme, the TOs become almost non-existent at highest SNR. However, this work shows that for practical values of SNR, there are a non-zero number of TOs the SUs can always exploit. At intermediate to high SNR, the SU-IA-

DSTBC scheme performs consistently better than the SU-IA-STBC scheme. Even at 30dB, the sum rate remains consistent and does not drop-off.

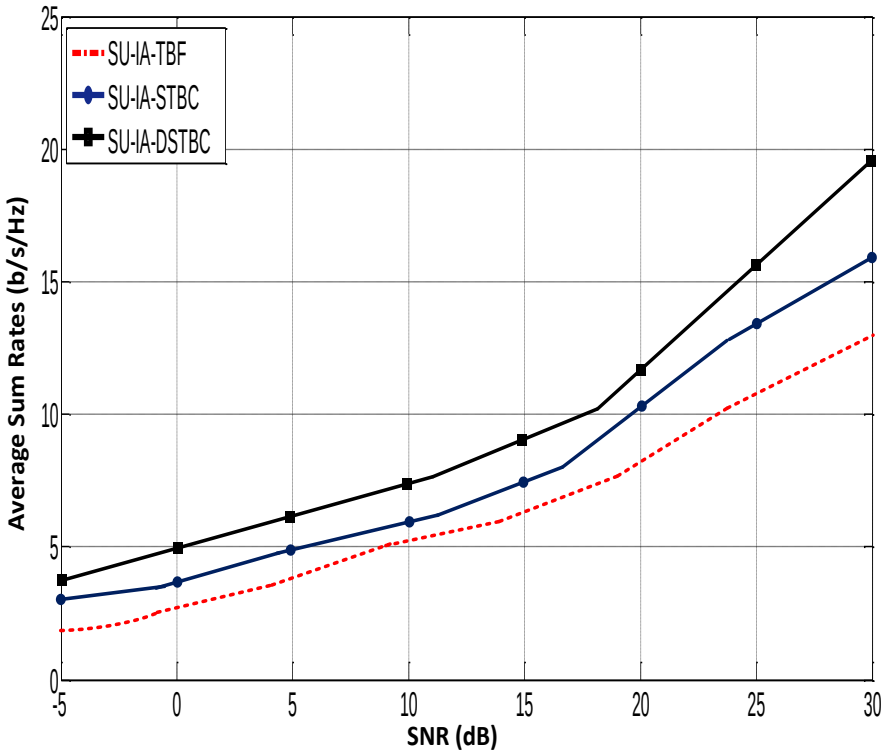

Fig. 5.9: Average Sum Rate (b/s) against SNR (dB) for two SUs

The graph shown in fig. 5.9 demonstrates the performance differential between the SU-IA-TBF against the SU-IA-DSTBC schemes. It has been shown that even though the ST-WF PA scheme provides efficient performance for the SUs only in the intermediate SNRs, this work combines the benefits of double ED as well as the SU-IA-STBC algorithm to release even more eigenmodes, thus achieving higher data rate performance than the SU-IA-TBF algorithm. The essential drawback of the MEB algorithm used in TBF is that the PU-Tx puts all its power on the antenna corresponding to the largest eigenmode of its singular allocated channel matrix H_{00}. This makes the MEB scheme less dynamic than ST-WF and more susceptible to lower data rates.

It can also be seen in Fig. 5.9 that the data rate performance of the SU-IA-DSTBC is higher than that of the SU-IA-DSTBC schemes, owing to the fact that the threshold function of the DSTBC scheme is an effective tool for saving the PUs transmit power due to the WPA's channel outage conditions (see Fig. 5.2). The consequence of saving the SUs transmit power can be seen in Fig. 5.9, where the sum rate performance of the SU-IA-DSTBC curve increases even further especially at moderate to high SNR, when compared with the SU-IA-STBC curve. Also, with two SU-Rx antennas, the DSTBC-beamforming scheme shows better SER performance than coherent STBC with an increasing margin as the SNR was increased, demonstrating that in highly correlated channels, training symbols used in coherent STBC incur a significant loss in data rate. Hence, its deficit in performance compared to the SU-IA-DSTBC modulation scheme.

5.8.Conclusion

An opportunistic interference alignment (OIA) scheme has been proposed that is based on the literature described in [11] – [23]. However, this work differentiates itself in a number of key areas to achieve significantly higher data rate performance. Firstly, the SVD that is performed `1Both PU and SU can utilize the licensed spectrum by aligning the interference from the SUs to these unused eigenmodes. The ST-WF achieves higher capacity per antenna than SWF, and even though ST-WF has a higher channel outage probability than that of SWF, its transmission is similar to block transmission, which makes this scheme operate in conditions more suited to CR networks.

Secondly, to further enhance accuracy of detection of TOs, this work makes use of a double threshold energy detection (ED) scheme where, the FC receives two kinds of information from which to base its decision on. This increased range of values available to the FC leads to higher detection accuracy and thus increased number of TOs.

Thirdly, to increase the SUs sum rate performance, a new IA scheme equipped with STBC across eigen-beams were combined to yield a two-directional eigen-beamformer that performs better than the conventional one-directional beamformer with negligible increase in computational complexity. The incremental gains in performance achieved from the ST-WF and double ED detection schemes coupled with a careful SU selection scheme that always ensures a $2Tx \times 2Rx$ for the SUs are combined with the SU-IA-STBC scheme to give higher data rates. Lastly, the new IA scheme was used to achieve full transmit diversity without losing sum rates by wedding optimal precoding with orthogonal DSTBC, where the DSTBC structure of the equivalent channels where preserved after zero-forcing the interfering users. Since the fundamental SU transmission is not changed by the transmit eigen-beamforming matrices, these IA schemes were shown to achieve higher diversity gain than other conventional methods.

A significant portion of this chapter has been submitted to IEEE Transactions of Cognitive Communications.

6. Conclusion and Future Work

6.1.Conclusion

The rapid advancement in research, design and deployment of wireless systems has been largely instigated by the massive demand for wireless applications. Users of wireless applications are more dependent on real-time data rate transmission and mobile broadband communication, prompting the need for 'high quality of service' in the principal design objective of wireless technologies. There are however two main phenomenon inherent in wireless technology that have so far hindered the realization of high quality of service in wireless communications namely fading and interference. Fading occurs when the transmitted signal is affected by objects in the wireless environment thereby causing deficiency in the quality of the received signal, which leads to the phenomenon of interference, which constructively amplifies or destroys the signal.

One of such technologies that has recently emerged and is at the forefront of enhancing high quality of service in wireless communications is CR, a technology which attempts to optimize underutilization of the wireless spectrum. However, CR is also hampered by the two phenomena mentioned earlier, with fading occurring mostly on the reporting channels when the SUs are reporting presence/absence of the PUs. The latter phenomenon occurs on the sensing channels when the SUs are in the process of sensing for spectrum holes.

It is on this note that this thesis set out to investigate novel and practical solutions towards improving the performance of cognitive radio. By considering a number of secondary users with single antennas grouped to form a virtual MIMO array, diversity techniques namely spatial diversity was considered to combat the detrimental effects of fading on the reporting channels of cognitive radio. This thesis thus presented a differential space-time block coding

cooperative sensing scheme in order to improve performance of non-ideal reporting channels under deep fading conditions. Firstly, it was shown through simulation results that implementing DSTBC in CR follows the same pattern in terms of BER performance (with approximately 3dB loss), proving that it can also achieve full transmit diversity. Secondly, it was again shown through simulation results that despite not having prior knowledge of the reporting channels, DSTBC reporting with varying fusion rules *(OR/AND/MRC/EGC)* outperformed typical non-DSTBC reporting under the same conditions for various number of CR clusters. In terms of managing interference between the PU and SUs on the sensing channels, IA has recently been employed for CR in the manner of direct or indirect SS. Of particular interest in this thesis is indirect SS, where the SUs are compelled to sense for the PUs unused eigenmodes. By performing optimal power allocation on the PUs link using WF techniques, some of the PUs spatial dimensions are left unused for the SUs to align their transmission with. This curbs the possibility of there being harmful interference between the PU and SUs transmission. This thesis explores two key areas of performance namely the PU's power allocation algorithms as well as the secondary user's transmission rates.

For the former, this thesis deploys ST-WF algorithms which tend to have increased performance gains per antenna. As for the latter, the conditional statements that make it possible for the SUs to avoid interfering with the pu transmission converts the cognitive IA solution into an unconstrained one where the SUs can operate in complete oblivion to the PU. The principle of reciprocity was applied for the SU network to optimize their transmission rates. This principle was founded on the basis that if the DoF allocation is feasible on the original interference network, then IA on the reciprocal interference network is simply achieved by choosing the Tx filters and Rx filters on the reciprocal channel as the Rx filters and the Tx filters of the original channel. It was shown through simulation results that

implementing feedback through reciprocity greatly increased the performance of the multiple SUs.

Given the fact that spatial diversity has gained the widest attention because of the simplicity of implementation and the feasibility of deployment, it was considered for the unconstrained secondary user's network. In spatial diversity, multiple antennas are deployed to produce multiple independent fading paths for the transmitted information signals and because it is unlikely that the multiple independent paths will experience identical fading events, the advantages of spatial diversity are clear to see. Therefore, this research combined DSTBC with capacity benefits if interference alignment to linearly scale up the transmission rates of SUs. It was seen through simulation results that the data rate performance of this technique is higher than other more conventional schemes, owing to the fact that the threshold function of the diversity technique is an effective tool for saving the PUs transmit power, the consequence of which the sum rate performance increases even further especially at moderate to high SNR.

6.2.Future Work

6.2.1. Cooperative Spectrum Sensing with DSTBC Reporting

The design of DSTBC has generally led to other diversity schemes such as orthogonal frequency division multiplexing (DSTBC-OFDM) schemes and distributed space-frequency coding (DSFC) schemes. DSTBC-OFDM schemes are able to exhibit maximum spatial and temporal gain at the expense of frequency diversity and inherent processing delay. To exploit the achievable frequency diversity and counteract the processing delay, DSFC transmits information symbols across multiple sub-carriers within a single OFDM block. Further comparative analysis on these schemes shows that while DSTBC-OFDM is insensitive to high delay spread, it is highly susceptible to Doppler frequency. This limits the application of

the scheme to slow fading channels. On the other hand, DSFC is more robust to fast fading channels such that the scheme exhibits maximum frequency and spatial diversity when utilized in fast fading environments. The outlined benefit of DSFC over DSTBC-OFDM makes it an attractive proposition for improving non-ideal reporting channels.

6.2.2. Opportunistic Interference Alignment with Space-time Coding

Relative to the applications of interference alignment in this thesis, the IC setting with three or more users presents a fresh challenge in that each signal needs to satisfy more than one alignment condition, thus creating a chain of alignment conditions that could make the problem can quickly appear infeasible. This integration of 3 or more users with the already discussed diversity techniques poses a new research question and could be considered further in future works.

References

[1] M. C. Chuah and Q. Zhang, (2009). Design and Performance of 3G Wireless Networks and Wireless LANS. Springer.

[2] M. H. Rehmani and Y. Faheem, (2014). Cognitive Radio Sensor Networks: Applications, Architectures, and Challenges. USA: IGI Publishing.

[3] A. Osseiran, J. F. Monserrat, and W. Mohr, (2011). Mobile and Wireless Communications for IMT-advanced and Beyond. Wiley.

[4] A.Medeisis and Oliver Holland, (2014). Cognitive Radio Policy and Regulation, Springer.

[5] E. Hossain, D. Niyato and Z. Han, (2009). Dynamic Spectrum Access and Management in Cognitive Radio Networks. Cambridge Press.

[6] X. Chen, H.H. Chen and W. Meng, "Cooperative Communications for Cognitive Radio Networks – From Theory to Applications", *IEEE Communications Surveys & Tutorials*, Vol. 16, no. 3, pp. 1180 – 1192, March 2014.

[7] M. J. Marcus, "Spectrum Policy for Radio Spectrum Access", *Proceedings of the IEEE*, Vol. 100, pp. 1685 – 1691, May 13th, 2012.

[8] A. Khattab, D. Perkins and M. Bayoumi, (2013). Cognitive Radio Networks From Theory to Practice. Springer.

[9] J. Mitola and G. Q. Maguire, "Cognitive Radio: Making Software Radios More Personal," *IEEE Personal Communications*, Vol. 6, no. 4, pp. 13 – 18, Aug. 1999.

[10] “Cognitive Radio: Brain-Empowered Wireless Communications”, *IEEE Journal on Selected Areas in Communications*, Vol. 23, no. 2, pp. 201 – 220, Feb. 2005

[11] T. Yucek and H. Arslan, “A Survey of Spectrum Sensing Algorithms for Cognitive Radio Applications”, *IEEE Communications Surveys & Tutorials*, Vol.11, no. 1, pp. 116 – 130, March 2009.

[12] P. Kolodzy, et al., “Next generation communications: Kickoff meeting”, *Proceedings of the Defense Advanced Research Projects Agency (DARPA)*, 2001.

[13] S. Haykin, D. J. Thomson, and J. H. Reed, “Spectrum Sensing for Cognitive Radio,” *Proceedings of the IEEE*, Vol. 97, no. 5, pp. 849 – 877, May 2010.

[14] Y. Zeng, Y.-C. Liang, A. T. Hoang, and R. Zhang, “A Review on Spectrum Sensing techniques for Cognitive Radio: Challenges and Solutions,” *EURASIP Journal on Advanced Signal Processing*, Vol. 2010, no. 1, Article Number: 381465, pp. 1 – 15, 2010.

[15] Y. Liang, K. Chen, G. Yeli and P. Mahonen, “Cognitive Radio Networking and Communications: An Overview”, *IEEE Transactions on Vehicular Technology*, Vol. 60, no. 7, September 2011.

[16] Y. He and S. Dey, “Throughput Maximization in Cognitive Radio under Peak Interference Constraints with Limited Feedback,” *IEEE Transactions on Vehicular Technology*, Vol. 61, no. 3, pp. 1287 – 1305, March 2012.

[17] S.A. Jafar, (2011) Interference Alignment - A New Look at Signal Dimensions in a Communication Network, USA: Now Publishers.

[18] O. El-Ayach, S.W. Peters and R.W. Heath, "The Practical Challenges of Interference Alignment", *IEEE Wireless Communications,* Vol. 20, no. 1, pp. 35 – 42, February 2013

[19] S. A. Jafar and S. Shamai, "Degrees of Freedom Region of the MIMO X Channel," *IEEE Transactions on Information Theory*, Vol. 54, no. 1, pp. 151–170, Jan. 2008.

[20] S. Jafar and M. Fakhereddin, "Degrees of Freedom for the MIMO Interference Channel", *IEEE Transactions on Information Theory*, Vol. 53, no. 7, pp. 2637–2642, Jul. 2007.

[21] A.M. Wyglinski, M. Nekovee and Y.T. Hou, (2010) Cognitive Radio Communications and Networks Principles and Practice, USA Elsevier

[22] T. Qu, Q. Zhao, H. Yin and F. R. Yu, "Interference Alignment for Overlay Cognitive Radio Based on Game Theory", *Proceedings of 14th IEEE International Conference on Communication Technology (ICCT)*, Chengu, China, pp. 67 – 72, Nov. 9 – 11, 2012.

[23] S.M. Perlaza, M. Debbah, S. Lasaulce and J.-M. Chaufray, "Opportunistic interference alignment in MIMO interference channels", *IEEE 19th International Symposium on Personal, Indoor and Mobile Radio Communications (PIMRC)*, pp. 1-5, Sep. 2008

[24] S.M. Perlaza, N. Fawaz, S. Lasaulce and M.Debbah, "From Spectrum Pooling to Space Pooling: Opportunistic Interference Alignment in MIMO Cognitive Network", *IEEE Transactions on Signal Processing*, Vol. 58, no. 7, March 2010.

[25] B. Wang and K. J. R. Liu, "Advances in Cognitive Radio Networks: A Survey," *IEEE Journal on Selected Topics on Signal Processing*, Vol. 5, no. 1, pp. 5 – 23. Feb. 2011.

[26] S. Chaudhari, J. Lunden, V. Koivunen, and H. V. Poor, “Cooperative Sensing with Imperfect Reporting Channels: Hard Decision or Soft Decision?” *IEEE Transaction on Signal Processing*, Vol. 60, no. 1, pp. 18 – 28, Jan. 2012.

[27] X. Gui, G. Kang, and P. Zhang, “Linear Precoding Design in Multi-User Cognitive MIMO systems with Cooperative Feedback,” *IEEE Communications Letters*, Vol. 16, no. 10, pp. 1580 – 1583, Oct. 2012.

[28] D. T. Ngo and T, Le-Ngoc, “Distributed Resource Allocation for Cognitive Radio Networks with Spectrum-sharing Constraints,” *IEEE Transactions on Vehicular Technolgy*, Vol. 60, no. 7, pp. 3436 – 3449, Sep. 2011.

[29] S. Ganesan, M. Sellathurai, and T. Ratnarajah, “Opportunistic Interference Projection in Cognitive MIMO Radio with Multiuser Diversity,” *Proceedings of IEEE New Frontiers in Dynamic Spectrum*, pp. 1 – 6, Apr. 2010.

[30] K. B. Letaief and W. Zhang. “Cooperative Communications for Cognitive Radio Networks” *Proceedings of the IEEE*, Vol. 97, no. 5, pp. 878 – 893, May 2009.

[31] I. F. Akyildiz, F. L. Brandon and R. Balakrishnan, “Cooperative Spectrum Sensing in Cognitive Radio Networks: A Survey”, *In Journal of Physical Communications*, vol 4, Issue 1, pp. 40 – 62, March 2011.

[32] J. Lee, H. Wang, J. G. Andrew, and D. Hong, “Outage Probability of Cognitive Relay Networks with Interference Constraints,” *IEEE Transactions on Wireless Communications*, Vol. 10, no. 2, pp. 390 – 395, Sep. 2011.

[33] J. Ma, G. Li, B.H. Juang, "Signal Processing in Cognitive Radio", *Proceedings of the IEEE,* Vol. 97, no. 5, pp. 805 – 823, 2009.

[34] T. Yucek, H. Arslan, "A Survey of Spectrum Sensing Algorithms for Cognitive Radio Applications", *IEEE Communications Surveys Tutorials*, Vol. 11, no. 1, pp. 116 – 130, 2009.

[35] X. Gui, G. Kang, and P. Zhang, "Linear Precoding Design in Multi-user Cognitive MIMO Systems with Cooperative Feedback," *IEEE Communications Letters*, Vol. 16, no. 10, pp. 1580 – 1583, Oct. 2012.

[36] H. Urkowitz, "Energy Detection of Unknown Deterministic Signals," *Proceedings of the IEEE,* Vol. 55, no. 4, pp. 523–531, 1967.

[37] F.F. Digham, M.-S. Alouini, M.K. Simon, "On the Energy Detection of Unknown Signals over Fading Channels", *IEEE Transactions on Communications,* Vol. 55, no. 1, pp. 21 – 24, 2007.

[38] V. I. Kostylev, "Energy Detection of a Signal with Random Amplitude", *Proceedings of IEEE International Conference on Communications (ICC),* pp. 1606 – 1610, New York, May 2002.

[39] A. Ghasemi and E. Sousa, "Opportunistic Spectrum Access in Fading Channels through Collaborative Sensing," *Journal of Communications,* Vol. 2, no. 2, p. 71, 2007.

[40] G. Ganesan and L. Ye, "Cooperative Spectrum Sensing in Cognitive Radio, Part II: Multiuser Networks," *IEEE Transactions on Wireless Communications,* Vol. 6, no. 6, pp. 2214 – 2222, 2007.

[41] I. Gradshteyn, I. Ryzhik, A. Jeffrey, and D. Zwillinger, (2007). *Table of Integrals, Series and Products*. Academic press.

[42] J. Unnikrishnan, V.V. Veeravalli, "Cooperative Sensing for Primary Detection in Cognitive Radio", *IEEE Journal of Selected Topics in Signal Processing*, Vol. 2, no. 1, pp. 18 – 27, 2008.

[43] N. Noorshams, M. Malboubi and A. Bahai, "Centralized and Decentralized Cooperative Spectrum Sensing in Cognitive Radio Networks: A Novel Approach", *Proceedings of IEEE Eleventh International Workshop on Signal Processing Advances in Wireless Communications (SPAWC)*, June 2010.

[44] N. Ahmed, D. Hadaller, and S. Keshav, "GUESS: Gossiping Updates for Efficient Spectrum Sensing," *Proceedings of International Workshop on Decentralized Resource Sharing in Mobile Computing and Networking*, pp. 12–17, California, USA, 2006.

[45] A. Ghasemi and E. Sousa, "Collaborative Spectrum Sensing for Opportunistic Access in Fading Environments," *Proceedings of IEEE International Symposium on New Frontiers in Dynamic Spectrum Access Networks*, Baltimore, pp. 131–136, USA, Nov. 2005.

[46] M. Gandetto and C. Regazzoni, "Spectrum Sensing: A Distributed Approach for Cognitive Terminals," *IEEE Journal on Selected Areas in Communications*, Vol. 25, no. 3, pp. 546–557, April 2007.

[47] W. Zhang, R. Mallik, K. Letaief, "Optimization of Cooperative Spectrum Sensing with Energy Detection in Cognitive Radio Networks", *IEEE Transactions on Wireless Communications*, Vol. 8, no. 12, pp. 5761 – 5766, 2009.

[48] E. Peh, Y.-C. Liang, Y.L. Guan, Y. Zeng, Optimization of cooperative sensing in cognitive radio networks: a sensing-throughput tradeoff view, IEEE Transactions on Vehicular Technology 58 (9) (2009) 5294–5299.

[49] A. Malady, C. da Silva, "Clustering Methods for Distributed Spectrum Sensing in Cognitive Radio Systems", *Proceedings of IEEE Military Communications Conference (MILCOM)*, San Diego, USA, pp. 1 – 5, 2008.

[50] J. Park, E. Kim and K. Kim, "Large-Signal Robustness of the Chair-Varshney Fusion Rule under Generalized Gaussian Noises", *IEEE Sensors Journal*, Vol. 10, no. 9, Sept. 2010.

[51] W. Han, J. Li, Z. Li, J. Si, and Y. Zhang, "Efficient Soft Decision Fusion Rule in Cooperative Spectrum Sensing," IEEE Transactions on Signal Processing , vol. 61, pp. 1931 – 1943, 2013.

[52] N. Thanh and I. Koo, "Evidence-Theory-Based Cooperative Spectrum Sensing With Efficient Quantization Method in Cognitive Radio", *IEEE Transactions on Vehicular Technology*, Vol. 60, no. 1, pp. 185 – 195, Jan. 2011.

[53] S. Jana, K. Zeng and P. Mohapatra, "Trusted Collaborative Spectrum Sensing for Mobile Cognitive Radio Networks", *Proceedings of IEEE International Conference on Computer Communications (INFOCOM)*, Orlando, Florida, March, 2012.

[54] M. A. Ali, S. A. Motahari, and A. K. Khandani. "Communication over MIMO X Channels: Interference Alignment, Decomposition, and Performance Analysis", *IEEE Transactions on Information Theory*, 2008.

[55] J. Andrews, “Interference Cancellation for Cellular Systems: A Contemporary Overview”, *IEEE Wireless Communications,* 2005.

[56] V. Cadambe and S. Jafar, “Interference Alignment and the Degrees of Freedom of the K user Interference Channel,” *IEEE Transactions on Information Theory,* Vol. 54, no. 8, pp. 3425–3441, August 2008.

[57] O.E. Ayach and R.W. Heath, “Interference Alignment with Analog Channel State Feedback’, *IEEE Transactions on Wireless Communications,* Vol. 11, no. 2, pp. 626 – 636, 2012.

[58] M. Maddah-Ali, A. Motahari, and A. Khandani, “Signaling over MIMO Multibase Systems - Combination of Multi-access and Broadcast Schemes,” *Proceedings of ISIT,* pp. 2104–2108, July 2006.

[59] T. Qu, N. Zhao, H. Yin and F. R. Yu, “Interference Alignment for Overlay Cognitive Radio Based on Game Theory”, *Proceedings of 14th IEEE International Conference on Communication Technology (ICCT),* Chengu, China, pp. 67 – 72, Nov. 9 – 11, 2012.

[60] Q. Zhao and B.M. Sadler, “A Survey of Dynamic Spectrum Access,” *IEEE Signal Processing Magazine,* Vol. 24, no. 3, pp. 79 – 89, May 2007.

[61] B. Nosrat-Makouei, J. G. Andrews, and R. W. Heath, Jr., “User Arrival in MIMO Interference Alignment Networks,” *IEEE Transactions on Wireless Communications,* Vol. 11, no. 2, pp. 842–851, July 2012.

[62] S.W. Peters and R.W. Heath, “Interference Alignment via Alternating Minimization,” *IEEE International Conference on Acoustics, Speech and Signal Processing, 2009. (ICASSP 2009)*, pp. 2445 – 2448, April 2009.

[63] K. Gomadam, V. Cadambe and S. Jafar, “A Distributed Numerical Approach to Interference Alignment and Applications to Wireless Interference Networks”, *IEEE Transactions on Information Theory*, Vol. 57, no. 6, pp. 3309 – 3322, 2011.

[64] H. Du, T. Ratnarajah, H. Zhou and Y.C. Liang, “Interference Alignment for Peer-to-Peer Underlay MIMO Cognitive Radio Network”, *Proceedings of 45th Asilomar Conference on Signals, Systems and Computers,* pp. 349 – 353, Nov. 2011.

[65] H. Zhou and T. Ratnarajah, “A Novel Interference Draining Scheme for Cognitive Radio based on Interference Alignment”, *IEEE Symposium on New Frontiers in Dynamic Spectrum*, pp. 1 – 6, April 2010.

[66] F. Rezaei and Aliakbar Tadaion, “Sum-Rate Improvement in Cognitive Radio through Interference Alignment”, *IEEE Transactions on Vehicular Technology,* Vol. 65, no. 1, pp. 145 – 154, Jan. 2016

[67] K. R. Kumar and F. Xue, “An Iterative Algorithm for Joint Signal and Interference Alignment”, *Proceedings of IEEE ISIT*, pp. 2293–2297, June 2010.

[68] S. Ma, H. Q. Du, T. Ratnarajah and L. Dong, “Robust Joint Signal and Interference Alignment in Cognitive Radio Networks with Ellipsoidal Channel State Information Uncertainties”, *IET Communications,* Vol. 7, No. 13, Sep. 2013.

[69] S. Boyd, L. El Ghaoui, E. Feron and V. Balakrishnan, (1994). “Linear Matrix Inequalities in System and Control Theory”.

[70] A. Goldsmith, S. A. Jafar, N. Jindal, and S. Vishwanath, “Capacity Limits of MIMO Channels,” *IEEE Journal on Selected Area in Communications*, Vol. 21, no. 5, pp. 684 – 702, Jun. 2003.

[71] K. Gomadam, V. Cadambe, and S. Jafar, “Approaching the Capacity of Wireless Networks through Distributed Interference Alignment”, *IEEE Global Telecommunications Conference* (IEEE GLOBECOM), New Orleans, Dec. 2008.

[72] J. Tang, S. Lambotharan and S. Pomeroy, “Interference Cancellation and Alignment Techniques for Multiple-input and Multiple-output Cognitive Relay Networks”, *IET Signal Processing*, Vol. 7, no. 3, pp. 188 – 200, May 2013.

[73] L. Sboui, H, Ghazzai, Z. Rezki and M. S. Alouini, “Achievable Rate of Spectrum Sharing Cognitive Radio Multiple-Antenna Channels”, *IEEE Transactions on Wireless Communications*, Vol. 14, no. 9, pp. 4847 – 4856, Sept. 2015.

[74] A. Alizadeh, H. R. Bahrami, M. Maleki and S. Sastry, “Spatial Sensing and Cognitive Radio Communication in the Presence of a *K*-User Interference Primary Network”, *IEEE Journal on Selected Areas in Communications*, Vol. 33, no. 5, pp. 741 – 754, May 2015.

[75] S. Mosleh, J. Abouei and M. R. Aghabozorgi, “Distributed Opportunistic Interference Alignment Using Threshold-Based Beamforming in MIMO Overlay Cognitive Radio”, *IEEE Transactions on Vehicular Technology*, Vol. 63, No. 8, pp. 3783 – 3793, Oct. 2014.

[76] Z. Shen, R. W. Heath Jr., J. G. Andrews and B. L. Evans, “Space-Time Water-Filling for Composite MIMO Fading Channels”, *EURASIP Journal on Wireless Communications and Networking*, Vol. 2006, no. 6, Pages 1–8, May 2006.

[77] Z. Shen, J. Heath, J. Andrews and B. Evans, “Comparison of Space-time Water-filling and Spatial Water-filling for MIMO Fading Channels”, *in Proceedings of IEEE Global Communications Conference, Exhibition and Industry Forum (GLOBECOM)*, Vol. 1, pp. 431 – 435, Dallas, TX, Dec. 2004.

[78] X. Zhou, J. Ma, G. Li, Y. Kwon, A. Soong, “Probability-based Combination for Cooperative Spectrum Sensing”, *IEEE Transactions on Communications* Vol. 58, no. 2, pp. 463 – 466, 2010.

[79] J. Wei and X. Zhang, “Energy-efficient Distributed Spectrum Sensing for Wireless Cognitive Radio Networks”, *INFOCOM IEEE Conference on Computer Communications Workshops*, pp. 1 – 6, 2010.

[80] W. Zhang and K. B. Letaief, “Cooperative Spectrum Sensing with Transmit and Relay Diversity in Cognitive Radio Networks” *IEEE Transactions on Wireless Communications*, vol. 7, no. 12, Dec. 2008

[81] L. Wang, Z. Q. Bai, et al. “Cooperative Spectrum Sensing with Different Sensing Duration in Cognitive Radio Systems,” *IEEE International Conference on Communication Technology*，Jinan, pp. 259–263, September 2011.

[82] X. Liang, Z. Bai, L. Wang and K. Kwak, "Dynamically clustering based Cooperative spectrum sensing with STBC scheme", *Fourth International Conference on Ubiquitous and Future Networks, Phuket*, pp. 227-231, July 2012.

[83] Wang, B., Bai, Z., Xu, Y., Gong, P and Kwak, K. “A Robust STBC Based Dynamical Clustering Cooperative Spectrum Sensing Scheme in CR Systems” *in IEEE Fifth International Conference on Ubiquitous and Future Networks,* pp 553 – 557, July 2013.

[84] V. Tarokh, and H. Jafarkhani, “A Differential Detection Scheme for Transmit Diversity,” *IEEE Journals on Selected Areas in Communications,* pp. 1169–1174, July 2000

[85] B. Hughes, “Differential space-time modulation,” *IEEE Transactions on Information Theory,* Vol. 46, pp. 2567–2578, Nov. 2000

[86] Z. Chen and W. Yen “Differential Space-time Block Coding Based Cooperative Spectrum Sensing over Fading Environments in Cognitive Radio Sensor Networks” *In Journal of Information and Computational Science,* vol 9, Issue 15, pp 4599 – 4606, 2012.

[87] F. K. Jondral, B Cognitive radio: A communications engineering view,[IEEE Wireless Commun., vol. 14, pp. 28–33, Aug. 2007.

[88] A. N. Mody, S. R. Blatt, et al, “Recent advances in cognitive communications”, IEEE Commun. Mag., vol. 45, pp. 54–61, Oct. 2007.

[89] B. Le, T. W. Rondeau, and C. W. Bostian, Cognitive radio realities, Wireless Commun. Mobile Comput., vol. 7, no. 9, pp. 1037–1048, Nov. 2007.

[90] A. Nosratinia, T. E. Hunter, and A. Hedayat, “Cooperative communciation in wireless Networks”, IEEE Commun. Mag., vol. 42, pp. 74–80, Oct. 2004.

[91] A.M. Wyglinski, M. Nekovee and Y.T. Hou, (2010) Cognitive Radio Communications and Networks Principles and Practice, USA Elsevier.

[92] S. Alamouti, “A Simple Transmit Diversity Technique for Wireless Communications”, *IEEE Journal on Selected Areas in Communications*, Vol.16, pp. 1451–1458, August 1998.

[93] H. Jafarkhani and V. Tarokh "Multiple Transmit Antenna Differential Detection from Generalized Orthogonal Designs". *IEEE Transactions on Information Theory*, Vol. 47, No. 6, pp. 2626–2631, September 2001.

[94] S. Atapattu, C. Tellambura and H. J. Jiang, “Energy detection Based Cooperative Spectrum Sensing in Cognitive Radio Networks”, *IEEE Trans. on Signal Processing*, Vol. 10, Issue 4, pp. 1232-1242, April, 2011.

[95] Teguig, D., Scheers, B. and Le Nir, V. “Data fusion schemes for cooperative spectrum sensing in cognitive radio networks” *in IEEE Communications and Information Systems Conference (MCC)*, pp. 1 – 7, 2012.

[96] N. Devroye, P. Mitran, and V. Tarokh, “Achievable rates in cognitive radio channels,” *IEEE Trans. Inf. Theory*, vol. 52, no. 5, pp. 1813–1827, May 2006.

[97] B. Koo and D. Park, “Interference Alignment with Cooperative Primary Receiver in Cognitive Networks” *IEEE Communications Letters*, Vol. 16, Issue 7, pp. 1072-1075, July 2012.

[98] B. Guler and A. Yener, “Selective Interference Alignment for MIMO Cognitive Femtocell Networks”, *IEEE Journal on Selected Areas in Communications*, Vol. 32, Issue 3, pp. 439-450, March 2014.

[99] Z. Shen, J. Heath, J. Andrews, and B. Evans, “Comparison of Space-time Water-filling and Spatial Water-filling for MIMO Fading Channels”, *IEEE Global Telecommun. Conf.*, vol. 1, Dallas, TX, Dec. 2004.

[100] C. G. Tsinos and K. Berberidis, “Blind Opportunistic Interference Alignment in MIMO Cognitive Radio Systems”, *IEEE Journal on Emerging and Selected Topics in Circuits and Systems”,* Vol. 3, Issue 4, pp. 626-639, Dec. 2013.

[101] Y. Abdulkadir, O. Simpson, N. Nwanekezie and Y. Sun, “A Differential Space-Time Coding Scheme for Cooperative Spectrum Sensing in Cognitive Radio Networks”, *IEEE 26th International Symposium on Personal, Indoor and Mobile Radio Communications (PIMRC),* pp. 1386-1391, Hong Kong, Aug - Sep. 2015.

[102] M. Amir, A. El-Keyi, and M. Nafie, “Constrained Interference Alignment and the Spatial Degrees of Freedom of MIMO Cognitive Networks,” *IEEE Trans. Inf. Theory*, vol. 57, no. 5, pp. 2994–3004, May 2011.

[103] H. J. Yang, W. Y. Shin, B. C. Jung and A. Paulraj, “Opportunistic Interference Alignment for MIMO Interfering Multiple-Access Channels”, *IEEE Transactions on Wireless Communications*, Vol. 12, No. 5, pp. 2180 – 2192, May 2013.

[104] F. Rezaei and A. Tadaion, “Interference Alignment in Cognitive Radio Networks”, *IET Communications*, Vol. 8, No. 10, pp. 1769 – 1777, July 3 2014.

[105] M. Hasani-Baferani, J. Abouei and Z. Zeinalpour-Yazdi, “Interference Alignment in Overlay Cognitive Radio Femtocell Networks”, *IET Communications*, Vol. 10, No. 11, pp. 1401 – 1410, July 2016.

[106] S. Gesualdo, D. P. Palomar and S. Barbarossa, "The MIMO Iterative Waterfilling Algorithm", *IEEE Transactions on Signal Processing",* vol. 57, no. 5, pp 1917 – 1935, May 2009.

[107] O. Simpson, Y. Abdulkadir, Y. Sun and B. Chi, "Relay-Based Cooperative Spectrum Sensing with Improved Energy Detection in Cognitive Radio", *10th International Conference on Broadband and Wireless Computing, Communications and Applications (BWCCA)*, Nov. 2015.

[108] S. S. Kalamkar and A. Banerjee, "Improved Double Threshold Energy Detection for Cooperative Spectrum Sensing in Cognitive Radio", *Defence Science Journal*, Vol. 63, No. 1, pp. 34 – 40, Jan. 2013.

[109] G. Jöngren, M. Skoglund and B. Ottersten, "Combining Beamforming and Orthogonal Space–Time Block Coding", *IEEE Transactions on Information Theory*, Vol. 48, No. 3, pp. 611 – 627, July 2003.

[110] S. Zhou and G. B. Giannakis, "Optimal Transmitter Eigen-Beamforming and Space–Time Block Coding Based on Channel Correlations", *IEEE Transactions on Information Theory*, Vol. 49, No. 7, pp. 1673 – 1689, July 2003.

[111] M.R. Bhatnagar and A. Hjørungnes, "Linear Precoding of STBC over Correlated Ricean MIMO Channels", *IEEE Transactions on Wireless Communications*, Vol. 9, No. 6, pp. 1832 – 1836, June 2010.

[112] A. Abdel-Samad, T. N. Davidson and A. B. Gershman, "Robust Transmit Eigen Beamforming Based on Imperfect Channel State Information", *IEEE Transactions on Signal Processing*, Vol. 54, No. 5, pp. 1596 – 1608, June 2010.

[113] L. Shi, W. Zhang and X. G. Xia, "On Designs of Full Diversity Space-Time Block Codes for Two-User MIMO Interference Channels", *IEEE Transactions on Wireless Communications,* Vol. 11, No. 11, pp. 4184 – 4191, Nov. 2012.

[114] L. Li and H. Jafarkhani, "Maximum-Rate Transmission With Improved Diversity Gain for Interference Networks", *IEEE Transactions on Information Theory,* Vol. 59, No. 9, pp. 5313 – 5330, Sep. 2013.

[115] A. Naguib, N. Seshadri, and A. Calderbank, "Applications of Space-time Block Codes and Interference Suppression for High Capacity and High Data Rate Wireless Systems," in *Proceedings of Asilomar Conference,* Pacific Grove, CA, Oct. 1998.

[116] S. Alamouti, "A Simple Transmitter Diversity scheme for Wireless Communications", *IEEE Journal on Selected Areas in Communications*, Vol. 16, No. 8, pp. 1451 – 1458, Oct. 1998.

[117] X. Cai and G. B. Giannakis, "Differential Space–Time Modulation With Eigen-Beamforming for Correlated MIMO Fading Channels", *IEEE Transactions on Signal Processing*, Vol. 54, No. 4, pp. 1279 – 1288, April 2006.

[118] M.R. Bhatnagar, A. Hjørungnes and L. Song, "Precoded Differential Orthogonal Space-Time Modulation Over Correlated Ricean MIMO Channels", *IEEE Journal of Selected Topics in Signal Processing,* Vol. 2, No. 2, pp. 124 – 134, Feb. 2011.

[119] F. Li and H. Jafarkhani, "Space-time Processing for X Channel using Precoders," *IEEE Transactions on Signal Processing*, Vol. 60, No. 4, pp. 1849 – 1861, April 2011.

[120] X. Cai and G. B. Giannakis, “Differential Space–Time Modulation With Eigen-Beamforming for Correlated MIMO Fading Channels”, *IEEE Transactions on Signal Processing*, Vol. 54, No. 4, pp. 1279 – 1288, April 2006.

[121] F. T. Alotaibi and J. A. Chambers, “Outage Probability of Cooperative Cognitive Networks Based on Distributed Orthogonal Space–Time Block Codes”, *IEEE Transactions on Vehicular Technology*, Vol. 61, No. 8, pp. 3759 – 3765, Oct. 2011.

[122] I. E. Telatar, “Capacity of Multi-antenna Gaussian Channels,” *European Transactions on Telecommunications*, Vol. 10, No. 6, pp. 585 – 595, Nov. 1999.

[123] D. Tse and P. Viswanath, *Fundamentals of Wireless Communication*. Cambridge, U.K.: Cambridge Univ. Press, 2005.

[124] X. Guo *and* X.G. Xia, “On Full Diversity Space–Time Block Codes With Partial Interference Cancellation Group Decoding”, *IEEE Transactions on Information Theory*, Vol. 55, No. 10, pp. 4366 – 4385, Oct. 2009.

[125] G. L. StÄuber, *Principles of Mobile Communication*, 2nd Edition, Kluwer Academic Publishers, 2001.

[126] D. P. Palomar and J. R. Fonollosa, “Practical Algorithms for a Family of Water-filling Solutions”, *IEEE Transactions on Signal Processing*, Vol. 53, No. 2, pp. 686 – 695, Feb. 2005.

[127] S. Zhang, Q. Zhou, C. Kai, and W. Zhang, “Full Diversity Physical-layer Network Coding in two-way Relay Channels with Multiple Antennas,” *IEEE Transactions on Wireless Communications*

[128] C. M. Yetis, G, Tiangao, S. A. Jafar and A. H. Kayran, “On Feasibility of Interference Alignment in MIMO Interference Networks”, *IEEE Transactions on Signal Processing*, Vol. 58, Issue 9, pp. 4771 – 4782, Aug. 2010.

[129] C. Guo, T. Peng, S. Xu, H. Wang and W. Wang, “Cooperative Spectrum Sensing with Cluster-Based Architecture in Cognitive Radio Networks”, in Proceedings of IEEE 69th Vehicular Technology Conference (VTC), pp. 1 – 5, April 2009.

[130] H. Jafarkhani and V. Tarokh, “Multiple Transmit Antenna Differential detection from Generalized Orthogonal Designs,” *IEEE Transactions on Information Theory*, Vol. 47, No. 6, pp. 2626 – 2631, Sep. 2001.